



**HAL**  
open science

# Bio-sourced alternatives to diglycidyl ether of bisphenol A in epoxy–amine thermosets

Romain Tavernier, Mona Semsarilar, Sylvain Caillol

► **To cite this version:**

Romain Tavernier, Mona Semsarilar, Sylvain Caillol. Bio-sourced alternatives to diglycidyl ether of bisphenol A in epoxy–amine thermosets. *Green materials*, 2024, 12 (3), pp.121-167. 10.1680/jgrma.23.00027 . hal-04222577

**HAL Id: hal-04222577**

<https://hal.umontpellier.fr/hal-04222577v1>

Submitted on 29 Sep 2023

**HAL** is a multi-disciplinary open access archive for the deposit and dissemination of scientific research documents, whether they are published or not. The documents may come from teaching and research institutions in France or abroad, or from public or private research centers.

L'archive ouverte pluridisciplinaire **HAL**, est destinée au dépôt et à la diffusion de documents scientifiques de niveau recherche, publiés ou non, émanant des établissements d'enseignement et de recherche français ou étrangers, des laboratoires publics ou privés.

1  
2  
3  
4  
5  
6  
7  
8  
9  
10  
11  
12  
13  
14  
15  
16  
17  
18  
19  
20  
21  
22  
23  
24  
25  
26  
27  
28  
29  
30  
31  
32  
33  
34  
35  
36  
37

# Biosourced alternatives to diglycidylether of bisphenol A in epoxy-amine thermosets: a focus on materials properties and endocrine activity

**Romain Tavernier, Dr.**  
Associate Prof., Univ Lyon, CNRS, Université Claude Bernard Lyon 1, INSA Lyon, Université Jean Monnet, UMR 5223, Ingénierie des matériaux Polymères, Villeurbanne, France, 0000-0001-8186-9557

**Mona Semsarilar, Dr.**  
CNRS Researcher, IEM, Univ Montpellier, CNRS, ENSCM, Montpellier, France, 0000-0002-1544-1824

**Sylvain Caillol, Dr.**  
CNRS Researcher, ICGM, Univ Montpellier, CNRS, ENSCM, Montpellier, France, 0000-0003-3106-5547

**\* Mona Semsarilar, Dr.**  
Institut Européen des Membranes, 300 Av Prof Emile Jeanbrau, 34090, mona.semsarilar@umontpellier.fr, +33(0)467149122

**\* Sylvain Caillol, Dr.**  
Institut Charles Gerhardt, 240 Av Prof Emile Jeanbrau, 34296, sylvain.caillol@enscm.fr, +33(0)448792007

## Abstract

Since 1940s, bisphenol A (BPA) has been used in plastic industry reaching production of 10 million tons in 2022. More than 30 % of the produced BPA is used in the production of epoxy resins. Decades of research has now provided enough evidence that (BPA) has endocrine disrupting activity. Hence, it is an urgent matter to replace the use of BPA in production of epoxy resins. In the past years, considerable effort have been put into finding alternatives to the toxic BPA. However, the diglycidylether bisphenol A (DGEBA) does not only exhibits high polymerization reactivity, but the presence of aromatic rings confers interesting thermos-mechanical resistance to epoxy networks therefrom. Hence, this properties are also expected from potential alternatives to BPA. In this review, first the elements leading to toxicity of BPA is explained and then a thorough account of possible bio-sourced aromatic alternatives to BPA are gathered. The reported synthetic routes to each of these alternatives and their toxicity are described. Also, their use in synthesis of epoxy resins and how the new alternatives influence the mechanical properties are discussed. This is a concise summary of the structure-property and structure-toxicity relationship for possible bio-sourced substitutes of BPA in synthesis of epoxy resins.

<

38  
39  
40  
41  
42  
43  
44  
45  
46  
47  
48  
49  
50  
51  
52  
53  
54  
55  
56  
57  
58  
59  
60  
61  
62  
63  
64  
65  
66  
67  
68  
69  
70  
71  
72  
73  
74  
75  
76  
77  
78  
79  
80  
81  
82  
83  
84  
85  
86  
87  
88  
89  
90  
91  
92  
93  
94

## Introduction

Epoxy thermosetting resins are an important class of plastics that are used in a wide range of fields such as paints, coatings, composites, electronics, adhesives, construction, wind turbines, etc. The global epoxy resin market size is estimated to worth 11.26 billion dollars by 2026, and it was valued at 7.6 billion dollars in 2019.<sup>1</sup> The main application segments of epoxies are paints and coatings, for over 40 % of the total market. The most used epoxy monomer is diglycidylether of bisphenol A (DGEBA), followed by diglycidylether of bisphenol F (DGEBF). The majority of epoxy resins are derived from fossil resources.

The shift toward the use of bioresources for polymer synthesis could be a major move in the reduction of fossil carbon dissemination into the environment. For example, in the field of packaging, more than 80 billion kg are annually produced and originate from fossil resources.<sup>2</sup> A recent analysis of patent literature shows that there is a growing interest in sustainability in industry. More specifically, the use of bioresources for the production of chemicals, process optimisation that minimize waste or emissions are some of the main source of innovations.<sup>3</sup> In addition with tackling the global challenges for a more sustainable use and production of plastics, the use of bioresources is also a source of innovation, thanks to the diversity of monomer design from naturally available building blocks.<sup>4</sup>

Polymer scientists have long been working on biobased epoxy monomers for synthesis of epoxy networks. The use of biobased starting materials is an effective way to reduce the carbon footprint, and it allows to valorise organic wastes, as well as investigating new structures for thermosetting epoxies. The use of biobased materials in itself does not specifically prevent the use of toxic or hazardous compounds, but following the green chemistry principles usually includes the seek for low impacts either on the environment than on health. Epoxy monomers can be obtained from the oxidation of unsaturated compounds (epoxidation of carbon-carbon double bonds), or via the addition of a glycidyl moiety, for example using epichlorohydrin. When converting a double bond to an epoxide moiety, the reaction does not imply the introduction of carbon into the monomer, it is usually carbon neutral (considering only the atoms introduced, and ignoring any use of solvent, catalyst or waste generation). However, the introduction of a glycidyl moiety will involve the addition of carbon into the monomer. But this step does not necessarily involve the introduction of fossil carbon, since commercially available biobased epichlorohydrin can be utilized to target 100 % biobased epoxy monomers. For example, the synthesis of DGEBA using petrosourced BPA and biobased epichlorohydrin will lead to nearly 30 % of carbon originating from renewable resources. Several manufacturers are already selling epoxy formulations that contain a high biobased carbon percentage.<sup>5</sup> Academic scientists however have conceived a wider range of epoxy monomers obtained from biobased compounds, and several reviews have already focused on these monomers. For instance, in 2014, Auvergne *et al.* published an important review on biobased thermosetting epoxy resins, which covered the whole available literature on biobased epoxy monomers.<sup>6</sup> Since then, other groups also worked on gathering new data from literature, either for a general purpose<sup>7-11</sup>, or for specific applications such as aerospace industry.<sup>12</sup> With a focus on specific starting materials, such as furanics or aromatics, other reviews have gathered valuable information on reported structures. Ng *et al.* focused their work on aromatic compounds<sup>13</sup>, Wan *et al.* worked on phenols<sup>14</sup>, Caillol *et al.* on eugenol<sup>15</sup>, while a very recent paper by Eid *et al.* highlights the progress made in furanic monomers.<sup>16,17</sup> The use of specific biomass types for synthesis of monomers is also investigated, and especially aromatic-containing biomass such as lignin is an important area of research.<sup>18-21</sup> Since BPA is not only used as an epoxy precursor, some work of interest on the generation of potential for substitutes for any application can feed the research on thermosetting epoxy resins, for instance, Liguori *et al.* provided a very complete overview of potential substitutes, focusing on their synthesis.<sup>22</sup> Synthetic tools to obtain functional monomers from biobased furans and phenols have also been reviewed recently by Decostanzi *et al.*<sup>23</sup> Finally, it is worth mentioning that in the case of epoxy-amine networks, it is also important to consider the origin of the amine, and especially, the availability of biobased amine is still low.<sup>24,25</sup>

In this review, available structures that could replace bisphenol A, or more specifically, DGEBA in the synthesis of epoxy-amine resins are summarized. For this purpose, the initial focus would be on potentially biosourced compounds, and then on phenolic or furanic derivatives, that would be the most relevant structures to replace DGEBA in the synthesis of thermosets. For each compound, the thermoset properties using amine hardeners are discussed and compared with the same network obtained using DGEBA. Further, the available data on their endocrine disruption are compared with the know hazards of BPA.

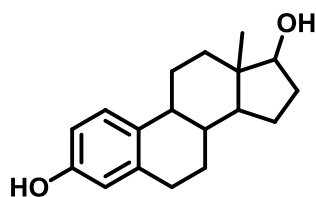
BPA is used as a monomer in the synthesis of polycarbonate thermoplastics and as monomer precursor in epoxy resins.<sup>26</sup> Thus, environmental BPA contamination mainly comes from leaching from the polymers under specific conditions, depending on the stability of the material. For example, the release of BPA from polycarbonates occurs due to hydrolysis under acidic conditions and upon heating.<sup>27</sup> Similarly, BPA is released from epoxy resins when

95 heated above 100 °C (often during sterilization step).<sup>28,29,30</sup> BPA contamination has also been detected from dental  
96 sealants,<sup>31</sup> in house dust and air,<sup>32</sup> as well as in textile.<sup>33</sup>

## 97 Endocrine activity assays

98

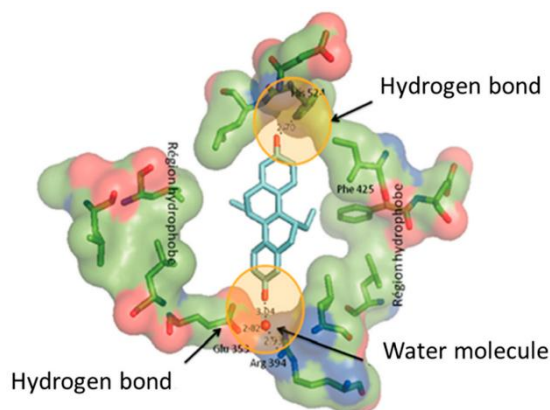
99 The toxicity of BPA is due to its similar activity to 17 $\beta$ -oestradiol hormone, a human oestrogen  $\alpha$  receptor.<sup>34</sup> This  
100 activity is due to the chemical structure of BPA mimicking 17 $\beta$ -oestradiol (Figure 1). Several factors control this  
101 similar activity. First is the presence of the two hydroxyl groups ensuring the efficient interaction between the  
102 receptor and the potential agonist. The second factor is the size of the receptor and the compound. In order to have a  
103 binding inside the receptor's binding site, the compound has to fit inside the receptor pocket. The size of the  
104 receptor pocket is 440 Å, while the size of 17 $\beta$ -oestradiol is 245 Å, allowing an adequate fitting. Apart from these  
105 factors the distance between the hydroxyl groups as well as the hydrophobic nature of the middle part of the  
106 molecule (for example, the two methyl units in BPA) also influence the interactions between the compound and the  
107 receptor (Figure 2).<sup>35,36</sup>  
108



109

110

Figure 1 - Chemical structure of 17 $\beta$ -oestradiol



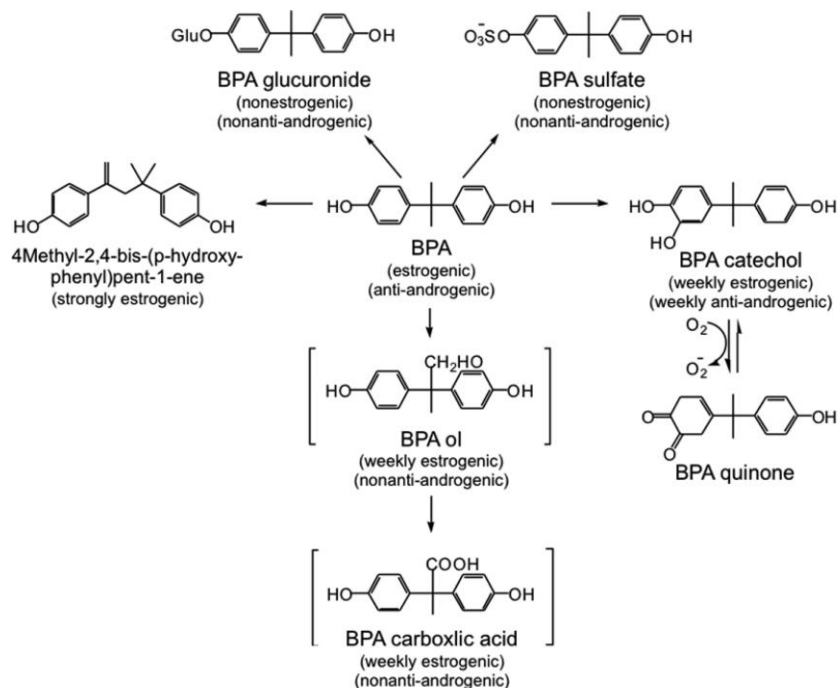
111

112

Figure 2 - X-ray structure of the pocket of ER $\alpha$ , reproduced from Ng et al.<sup>13</sup>

113

114 evaluation of endocrine disruption is not only due to the oestrogen receptor  $\alpha$ ,<sup>34</sup> but also to other biochemical  
115 mechanisms that have influence on the oestrogen binding.<sup>37</sup> The entire steroid metabolism have an effect on the  
116 oestrogen binding, since oestradiol belongs to the class of steroids. Hence, any effect on the steroid metabolism  
117 could have an effect on the binding in ER $\alpha$ .<sup>38</sup>  
118



119

120

Figure 3 - Postulated metabolic pathway of Bisphenol A, reproduced from Chen et al.<sup>39</sup>

121

Usually, regarding *in vitro* or *in vivo* bioassays, the compound activity is compared with the activity of the natural hormone, in order to determine a coefficient of activity. In addition, as a control, the activity of the tested compound is also compared to the vehicle, which is the vector used to drive the compound to the receptor. For instance, the vehicle is the solvent in which the compound is solubilised for *in vitro* testing, or the type of food in which the compound is included for *in vivo* experiments.

126

127

128

129

130

131

132

133

134

135

136

137

138

139

140

141

142

143

144

145

146

147

148

149

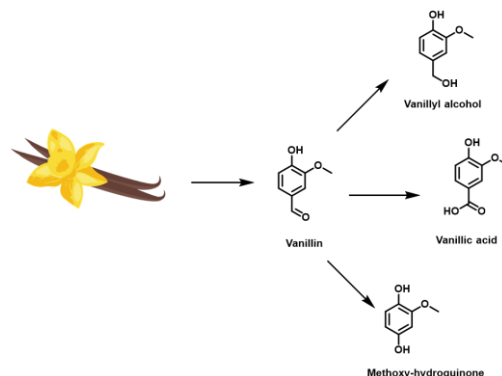
150

151

<b>Abbreviation</b>	<b>Full term</b>
<b>17βE2 / E2</b>	Human oestradiol
<b>AR</b>	Androgen receptor
<b>DMA</b>	Dynamic mechanical analysis
<b>DSC</b>	Differential scanning calorimetry
<b>DTG</b>	Derivative thermogravimetric analysis
<b>E'</b>	Young's modulus
<b>EA</b>	Oestrogen affinity
<b>EC<sub>50</sub></b>	Lower concentration efficacy
<b>ED</b>	Endocrine Disruptor
<b>EEW</b>	Epoxy equivalent weight
<b>EFSA</b>	European Food and Safety Authority
<b>Erα / hERα</b>	Human oestrogen receptor alpha
<b>HRC</b>	Heat release capacity
<b>LOI</b>	Limiting oxygen index
<b>mCPBA</b>	<i>meta</i> -chloroperbenzoic acid
<b>PXR</b>	Steroid receptor
<b>REE</b>	Relative oestrogen efficacy
<b>% RME2</b>	Normalized EA
<b>SVHC</b>	Substance of very high concern
<b>T<sub>α</sub></b>	Alpha transition temperature
<b>T<sub>d5%</sub></b>	Temperature of 5 % degradation
<b>T<sub>g</sub></b>	Glass transition temperature
<b>TGA</b>	Thermogravimetric analysis
<b>TMA</b>	Thermomechanical analysis
<b>TRβ</b>	Thyroid receptor beta

Name(s)	Abbreviation(s)	Structure
4,4'-methylenedianiline or 4,4'- diaminodiphenylmethane	DDM (or MDA)	
Amicure	PACM	
isophorone diamine	IPDA	
4,4'-diaminodiphenylsulfone	44DDS	
3,3'-diaminodiphenylsulfone	33DDS	
dicyandiamide	DICY	
triethylenetetramine	TETA	
diethylenetriamine	DETA	
decanediamine	DA10	
difurfurylamine A	DIFFA	
Jeffamine D400 or D230	D400/D230	
hexamethylenediamine	HMDA	
Polyetheramine EDR-148	EDR-148	
Polyetheramine EDR-192	EDR-192	
diethyltoluenediamine	Epikure W	
methylenedifurfuryldiamine	DFDA	
ethylidenedifurfuryldiamine	DFDA-Me	

159 Phenols  
 160  
 161 I. Vanillin

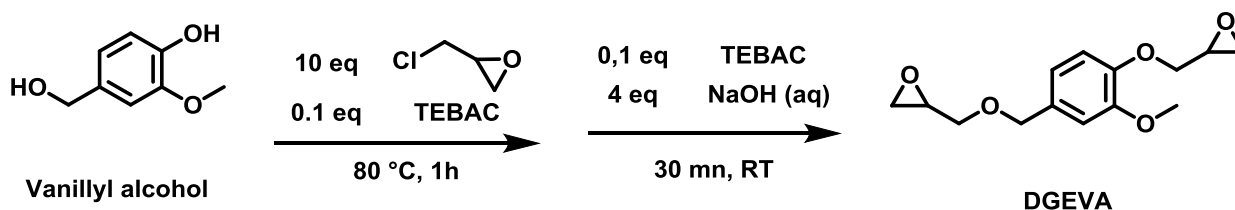


162  
 163 Figure 4 - Chemical structure of vanillin and some simple vanillin derivatives used as epoxy monomer  
 164 precursors

165 Vanillin (Figure 4) is a natural monophenol, bearing a methoxy moiety and an aldehyde. It is one of the main  
 166 components of natural vanilla aroma, and it has been produced on a large scale from fossil resources mainly for food  
 167 industry. Vanillin is also synthesized from bioresources on an industrial scale.<sup>40</sup> As a food additive, its toxicological  
 168 profile is thus positive, and it has led researcher to study different chemical modification of the compound for the  
 169 synthesis of epoxy monomers.<sup>41</sup> Vanillin derivatives has been widely used in the literature for the synthesis of epoxy  
 170 monomers.

171 Vanillin in itself does not seem to have an impact on the endocrine system. A recent article by Ji *et al.* has evaluated  
 172 the activity of vanillin on different receptors, such as ER $\alpha$ , androgen receptor, thyroid receptor and retinoic X  
 173 receptor  $\beta$ .<sup>42</sup> Vanillin did not show any activity against these receptors, for all the concentrations tested.

174  
 175 1. Vanillyl alcohol  
 176



177  
 178 Figure 5 – Synthesis procedure for DGEVA by Fache *et al.*<sup>41</sup>

179 Vanillyl alcohol (VA) is a vanillin derivative that can be obtained from the reduction of the aldehyde. VA is  
 180 commercially available since it is used as a flavouring.<sup>43</sup> This aromatic compound contains a methoxy moiety, a  
 181 phenolic hydroxyl and a primary alcohol, the two latter being the reactive sites for glycidylation. Diglycidylether of  
 182 vanillyl alcohol (DGEVA, Figure 5) has been synthesized first by Fache *et al.* as part of a series of monomers  
 183 obtained from vanillin.<sup>41</sup> Since then, several groups used DGEVA in order to elaborate thermosets, with different  
 184 hardeners, and some thermomechanical properties are reported in

185  
 186 Table 1. Fache *et al.* studied the curing behaviour of DGEVA with IPDA, and they obtained lower  $T_g$  (97 °C) than  
 187 with DGEBA (166 °C).<sup>44</sup> This can be explained by the fact that there is less aromatics in DGEVA compared to  
 188 DGEBA, and that DGEVA contains a methylene, that can induce more mobility of the chains. The calculated  
 189 crosslink density is also lower for DGEVA (0.7 mmol·m<sup>-3</sup> vs 1.4 mmol·m<sup>-3</sup> for DGEBA). Degradation under  
 190 nitrogen is a one step process for both DGEBA and DGEVA-IPDA thermosets, and the DTG peak corresponding to  
 191 the degradation happens for both materials around 360 °C, but DGEVA produces more char yield (19 % vs 10 % for  
 192 DGEBA).  
 193



Table 1 - Thermomechanical properties of DGEVA cured with different amines, from the literature

Amine Hardener	$T_g$ or $T_\alpha$ (°C)		$E'_{\text{glassy}}$ (GPa)		$T_{d5\%}$ (°C)		Char yield (%)	
	DGEBA	DGEVA	DGEBA	DGEVA	DGEBA	DGEVA	DGEBA	DGEVA
IPDA	166	97	-	-	-	-	10	19
PACM	190	100	-	-	-	-	2	7
DICY	146	93	-	-	342	289	13	23
DDM	154	111 / 124	2.3	2.8	-	-	-	-
TETA	142	71 & 109*	4	3.7	-	-	-	16
DETA	100	90	2	3.5	305	247	8	7
44DDS	238	108	-	-	-	-	14	7
DFDA	109	81	2.4	3.7	330	304	23	46

196 \* two relaxations are observed by DMA

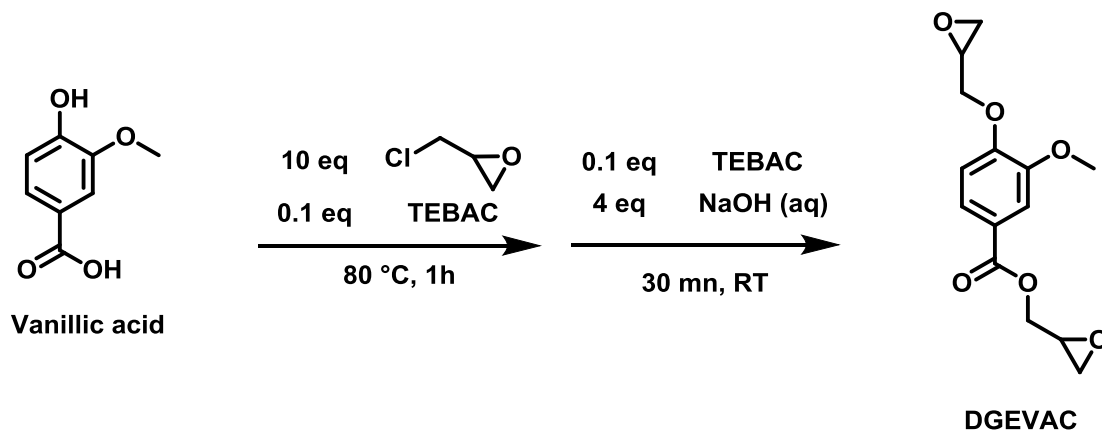
197 Hernandez *et al.* used a dicyclohexyl diamine (Amicure), with DGEVA and other vanillin-based epoxides.<sup>45</sup> The  
 198 thermosets were compared with DGEBA and DGEBF. DGEVA thermoset displays a  $T_g$  around 100 °C, compared to  
 199 the DGEBA system (190 °C). The glass transition temperature of DGEVA cured with IPDA and PACM is thus very  
 200 close, which is not surprising considering the two amines are based on cyclohexyl moieties, however, the storage  
 201 moduli are higher for DGEVA and DGEBA cured with PACM than with IPDA. Finally, the degradation of  
 202 DGEVA-PACM occurs at a lower temperature than with DGEBA, under nitrogen. The char yield is higher for  
 203 DGEVA thermoset (7 %) than for DGEBA (2 %), following the same trend than DGEVA-IPDA.

204 Ng *et al.* used DGEVA with dicyandiamide (DICY) for the elaboration of coatings.<sup>46</sup> They used oligo-DGEBA and  
 205 pure DGEBA for comparison. The cure temperature of the neat mixture of amine and epoxide is 220 °C for both  
 206 DGEBA types and 210 °C for DGEVA, which are very close. Glass transition temperatures determined for DGEBA  
 207 material are 146 °C and 93 °C for DGEVA, which is following the same trend than discussed before. The  $T_{d5\%}$  under  
 208 nitrogen is 342 °C for DGEBA, and 289 °C for DGEVA, which is slightly lower. However, the char yield is higher  
 209 for DGEVA (23 %) than for DGEBA (13 %). The adhesion properties of the corresponding coatings performed well  
 210 with or without adhesion promoter, with an ISO 2409 classification of 0 or 1 on a 5-scale (the lower the value, the  
 211 higher is the adhesion). Reinforcement of a glass plate was also evaluated by measuring the break strength, and it is  
 212 higher for DGEVA formulation than for pure DGEBA, but very similar to oligomerized DGEBA.

213 Tian *et al.* used DGEVA with the addition of an eugenol-based diepoxide for the elaboration of shape-memory  
 214 polymers.<sup>47</sup> They used DDM as the curing agent. They obtained  $T_g$ s between 111 and 124 °C (respectively from  
 215 DSC and DMA as  $\tan \delta$  peak), as compared to DGEBA/DDM system that reaches 154 °C (from  $\tan \delta$  in the work of  
 216 Wan *et al.*<sup>48</sup>). The storage modulus at 25-30 °C is 2.8 GPa for DGEVA thermoset, that is higher than for DGEBA-  
 217 DDM material (2.3 GPa). In overall, formulation with the eugenol-based monomers have shown effective shape  
 218 memory properties, especially using DGEVA as a hard segment, for the induction of phase separation, as evidenced  
 219 by AFM.

220 Wang *et al.* prepared epoxy composites using DGEVA/TETA as the matrix and lignin-containing cellulose nano-  
 221 fibres. They obtained for the neat resin two exothermic signals, with maxima at 113 °C and 167 °C. The two peaks  
 222 are attributed respectively to the reaction of primary and secondary amines. In the DGEBA/TETA system, only one  
 223 peak is observed for stoichiometric compositions, with a maximum at 98 °C.<sup>49,50</sup> This two-stage curing behaviour  
 224 could be attributed to diffusion differences between DGEBA et DGEVA systems, since stoichiometric ratios were  
 225 applied with DGEVA. A study of TETA/DGEVA ratios *vs*  $T_g$  of materials should be of interest. Mechanical  
 226 properties of cured DGEVA were reported, especially using DMA. Two relaxations were found for DGEVA, with  
 227  $T_\alpha$  of 71 °C and 109 °C, revealing an inhomogeneous network, probably due to two types of crosslinking brought by  
 228 the amine containing both primary and secondary NH. The storage modulus at 30 °C was found to be 3.7 GPa.  
 229 DGEBA cured with TETA presents also two  $\tan \delta$  peaks, but with a maximum contribution of the second peak,  
 230 which maximum is 142 °C, and the storage modulus at 40 °C is around 4 GPa.<sup>49</sup> Degradation behaviour of  
 231 DGEVA/TETA has been investigated under nitrogen, and a two-step degradation pathway was found, with a  
 232 maximum of degradation at 309 °C and a char yield of 16 %. The DGEBA system presents a single-stage

233 degradation with a DTG peak at 372 °C, which shows a better thermal stability.<sup>51</sup> Char yield was not reported for  
234 this material, but is believed to be lower than for DGEVA according to the trend observed.  
235 Gnanasekar *et al.* synthesized a phosphorylated epoxy monomer using vanillin as the precursor.<sup>52</sup> In order to assess  
236 the effect of the phosphorylation, they also used DGEVA as a phosphorus-free control. The study was also focused  
237 on the use of polyurethane as a toughening agent in the synthesis of epoxy thermosets. DGEVA and the  
238 phosphorylated monomer were cured with DETA. DGEVA/DETA properties could then be compared with  
239 DGEBA. DMA tests showed a glassy modulus at 30 °C for DGEVA/DETA to be around 3.5 GPa, compared to 2  
240 GPa for the DGEBA network as reported in the literature.<sup>53</sup> The  $\tan \delta$  peak of the DGEVA/DETA network appears  
241 around 90 °C, which is slightly lower than that of DGEBA (100 °C). Thermal stability under nitrogen was also  
242 assessed. The  $T_{d5\%}$  of DGEVA/DETA was 247 °C and char yield at 600 °C is 7 %, compared to DGEBA/DETA  
243 with a  $T_{d5\%}$  of 305 °C and a char yield of 8 %. The lower thermal stability could be attributed to the presence of the  
244 methoxy moiety, consistently with the other reports from literature. However, the lower char yield is unexpected  
245 compare to the other DGEVA networks. However, it is worth mentioning that the low char yield was expected due  
246 to the aliphatic structure of the hardener.  
247 In a different work, Gnanasekar *et al.* used phosphorylated vanillin-based epoxy monomer, with modified graphene  
248 oxide as the filler.<sup>54</sup> They also used DGEVA as a phosphorus-free control. The authors report the use of 4,4'-DDS as  
249 the hardener, without describing the curing procedure. They determined the glass transition temperature of  
250 DGEBA/44DDS using DSC at 108 °C. As a comparison, DGEBA/44DDS network has a  $T_g$  of 238 °C.<sup>55</sup> Thermal  
251 stability under nitrogen was also assessed, and the DGEVA/44DDS showed a  $T_{d10\%}$  of 251 °C, which is lower than  
252  $T_{d5\%}$  for DGEBA/44DDS thermosets reported (> 300 °C). Char yield at 600 °C was 7 %, which is lower than when  
253 DGEBA is used (approx. 14 %). The global lower performances of DGEVA cured with 44DDS can be attributed to  
254 the lower aromatic density, and the presence of a methylene moiety in the structure of the epoxy monomer.  
255 Mauck *et al.* used a diamine based on furfurylamine with DGEVA in order to get epoxy thermosets.<sup>56</sup> The  
256 methylenedifurfurylamine (DFDA) was used to harden several epoxy monomers derived from biophenols. The  
257 authors determined the EEW of their synthesized DGEVA at 133 g·eq<sup>-1</sup>, slightly lower than the DGEBA used for  
258 comparison (190 g·eq<sup>-1</sup>). Thermomechanical properties were evaluated for cured networks. DMA showed that the  
259 DGEVA/DFDA has a  $T_g$  of 81 °C compared to 109 °C for DGEBA/DFDA network. The Young's modulus at 25 °C  
260 is 3.7 GPa for DGEVA compared to 2.4 GPa for DGEBA. It is consistent with all other articles discussed herein,  
261 DGEVA giving lower  $T_g$  values and higher stiffness. As expected, the crosslinking density is higher for DGEVA,  
262 which is composed on one aromatic ring compared to DGEBA, respectively 3.82 mmol·m<sup>-3</sup> vs 2.62 mmol·m<sup>-3</sup>.  
263 Regarding thermal stability under inert atmosphere (Ar), DGEVA thermoset degrades earlier than DGEBA, as  
264 shown by the  $T_{d5\%}$ , namely 304 °C for DGEVA/DFDA compared to 330 °C for DGEBA/DFDA. However, char  
265 yield at 600 °C is higher with DGEVA (42 % vs 23 % for DGEBA).  
266 Mora *et al.* synthesized new aromatic-containing amines and cured DGEVA and DGEBA for comparisons.<sup>57</sup> They  
267 reported lower thermal stability for all DGEVA-based thermosets ( $T_{d5\%}$ ) but higher char yields. Glass transitions  
268 temperatures and  $T_g$  were also lowered with DGEVA compared to DGEBA. They also reported the synthesis of  
269 nearly full vanillin-based epoxy networks, using an aminated DGEVA as the curing agent with DGEVA, and with  
270 DGEBA for comparison.<sup>58</sup> This resulted in lower decomposition temperatures as well as  $T_g / T_d$  but higher char yield  
271 for DGEVA. As demonstrated by Noè *et al.*, DGEVA could also be used in photopolymerisation process. However,  
272 in such case conversion gets limited by a fast vitrification of the forming coating.<sup>59</sup> Epoxy thermosets based on  
273 DGEVA could also be used in manufacturing of composites with cellulose nano-fibres as the filler<sup>60</sup> as well as glass  
274 coatings for food contact material.<sup>46</sup>  
275



277

278

Figure 6 - Reaction scheme for the synthesis of DGEVAC according to Fache *et al.*<sup>41</sup>

279

280

281

282

283

284

285

286

287

288

289

290

291

292

293

294

295

296

297

298

299

300

301

302

303

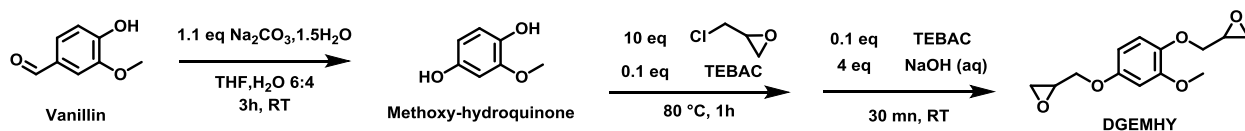
304

Vanillic acid is the oxidized form of vanillin, where the aldehyde is transformed into a carboxylic acid. This compound gives the flavour of natural vanilla, and is also an artificial flavouring. Diglycidylether of vanillic acid (DGEVAC, Figure 6) is a diepoxy readily obtained from the reaction between vanillic acid and epichlorohydrin. The nucleophilic substitution of the phenolate and the carboxylate can occur at the same time.<sup>41</sup> Another way to obtain this compound is the one pot allylation of the same moieties, followed by epoxidation *via* the use of *m*CPBA, or through an enzymatic process.<sup>61</sup>

Fache *et al.* cured DGEVAC with IPDA, and they obtained a glass transition temperature of 152 °C and a  $T_g$  of 166 °C, these values are slightly lower compared to those reported for DGEBA-IPDA ( $T_g$  of 166 °C and  $T_g$  of 182 °C).<sup>44</sup> The presence of the ester linkage on the aromatic ring could bring rigidity, compared to the above-mentioned DGEVA that contains a methylene instead. It is noteworthy that the  $T_g$  values are very close, even if the epoxy monomers have very different structure (two aromatic rings for DGEBA compared to only one for DGEBA). Usually, the  $T_g$  value increases linearly with the number of aromatic rings in the monomer. It can be observed that rigid structures like ester linkages can be as effective as aromatic density to improve the  $T_g$  of the epoxy thermosets. This behaviour is not correlated to the crosslinking density that has been calculated to be 1.4 mmol·m<sup>-3</sup> for both DGEVAC and DGEBA materials. In addition, the storage modulus of DGEVAC thermoset was measured at 2.1 GPa, as compared to 1.9 GPa for DGEVA. Thermal stability under nitrogen is however lower for DGEVAC compared to DGEBA. DGEVAC/IPDA degrades in two step, measured at 315 and 370 °C compared to the unique decomposition temperature of DGEVA system, with a peak at 360 °C. This two-step degradation behaviour can be attributed to the earlier rupture of the ester bond. The char yield of DGEVAC thermoset follows the trend observed with DGEVA, since it is higher than for DGEBA (14 % for DGEVAC and 10 % for DGEBA).

No more investigation has been performed on epoxy-amine thermosets with DGEVAC. However, there are examples on the epoxy-anhydride thermosets, such as the use of methylhexahydrophthalic anhydride and the hydrolytic degradation.<sup>62,63</sup> DGEVAC has also been used with nadic methyl anhydride as the curing agent.<sup>64</sup>

### 3. Methoxy-hydroquinone



305

306

307

Figure 7 - Reaction scheme for the synthesis of DGEMHY starting from vanillin according to Fache *et al.*<sup>41</sup>

308

309

310

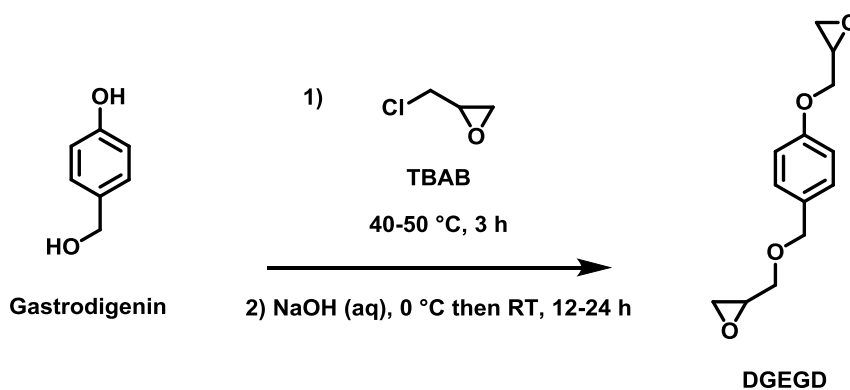
311

312

Methoxyhydroquinone is a commercially available compound, but it can also be obtained from the Dakin oxidation of vanillin, using sodium percarbonate as the oxidizing agent. The aldehyde from vanillin is oxidized into a phenol in mild conditions. The diglycidylether of methoxyhydroquinone (DGEMHY) can be obtained through the glycidylation of both phenolic moieties (Figure 7). It was first prepared by Fache *et al.*<sup>41</sup> and the curing reaction with IPDA was extensively studied.<sup>44</sup>  $T_g$  and  $T_g$  values of 132 °C and 154 °C were reported. DGEBA with the same

313 curing agent gave higher transition temperatures. The calculated crosslinking density was similar to the DGEBA  
 314 system ( $1.4 \text{ mmol}\cdot\text{m}^{-3}$ ) and in the DGEMHY system ( $1.3 \text{ mmol}\cdot\text{m}^{-3}$ ). The degradation of the thermoset under  
 315 nitrogen atmosphere resulted in a single step weight loss with a peak at  $338 \text{ }^\circ\text{C}$ , lower than in the case of DGEBA  
 316 ( $360 \text{ }^\circ\text{C}$ ). However, the char yield obtained was  $20 \%$  at  $600 \text{ }^\circ\text{C}$  compared to  $10 \%$  with DGEBA.  
 317 Curing of DGEMHY has also been performed with other amines: DA10 is decanediamine, an aliphatic biobased  
 318 amine obtained from castor oil, vanillylamine is a vanillin-derived amine and BFAA is bisfurfurylamine A, a  
 319 potentially biobased diamine.<sup>65</sup> DGEMHY cured with the biobased amines shows lower  $T_g$  values than DGEBA-  
 320 based thermosets. The aliphatic amine DA10 gave a  $T_g$  of  $74 \text{ }^\circ\text{C}$  with DGEMHY ( $98 \text{ }^\circ\text{C}$  with DGEBA),  
 321 vanillylamine gave nearly the same  $T_g$  with DGEMHY ( $64 \text{ }^\circ\text{C}$ ) and DGEBA ( $67^\circ\text{C}$ ) and BFAA lead to a  $T_g$  of  $111$   
 322  $^\circ\text{C}$  with DGEBA and  $85^\circ\text{C}$  with DGEMHY. The aromatic content seems to be the most influential contributor to the  
 323  $T_g$  values of these epoxy thermosets, leading to higher values with DGEBA. The higher decrease regarding DA10  
 324 and BFAA with DGEMHY could be due to the presence of the methylene moieties in both amine and epoxy  
 325 monomers. The lower  $T_g$  values were obtained for DGEBA and DGEMHY cured with vanillylamine, which could  
 326 be due to the lower functionality of the amine.  
 327 The commercially available DGEBA mainly contains two epoxide moieties, (or as oligomers) with different epoxide  
 328 contents and chain lengths. DGEMHY has been also studied in its oligomerized form.<sup>66</sup> Fache and co-workers  
 329 performed a catalytic oligomerization by using triphenylbutylphosphonium bromide, using methoxyhydroquinone  
 330 with an excess of DGEMHY. Then, the crosslinking of the oligomers was obtained using IPDA as the hardener. A  
 331 decrease in the  $T_g$  and  $T_\alpha$  of the cured samples were observed with the increase of the repeating units. This is due to  
 332 the higher chain length between two crosslinking nodes. However, the effect of the chain length was counter  
 333 balanced by the higher aromatic density in the oligomers, which rather limited the increase of the  $T_g$  and  $T_\alpha$  values.  
 334

#### 335 4. Gastrodigenin



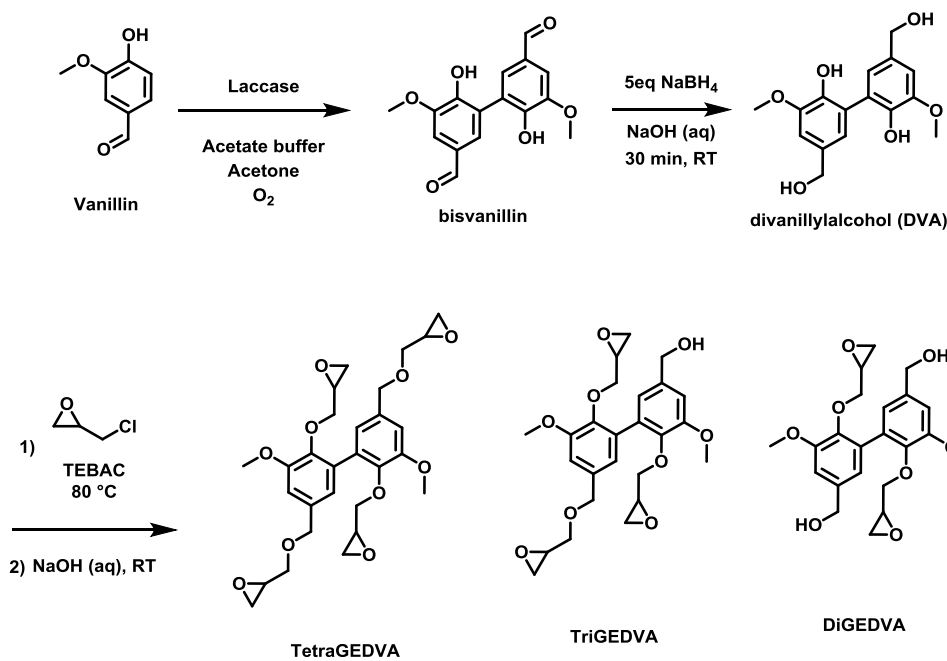
338 Figure 8 - Synthesis of DGEGD by Hernandez *et al.*<sup>45</sup>

339 Gastrodigenin is a monophenolic compound that can be found in *Gastrodia elata*, a flower from the Orchidaceae  
 340 family. This compound is one of the main active ingredients of this plant, and has shown some analgesic effects.<sup>67</sup>  
 341 The structure of this molecule consist in a phenol bearing a methylenol in para position. The glycidylation of this  
 342 compound leads to a diepoxy monomer, as shown in Figure 8. Hernandez *et al.* prepared DGEGD monomer with an  
 343 EEW of  $119 \text{ g}\cdot\text{eq}^{-1}$  and used PACM as the hardener.<sup>45</sup> Dynamic mechanical analysis of the DGEGD revealed a  $T_\alpha$  of  
 344  $132 \text{ }^\circ\text{C}$ , which is lower than with DGEBA ( $158 \text{ }^\circ\text{C}$ ). The storage modulus of the DGEGD thermoset at  $25 \text{ }^\circ\text{C}$  is  
 345  $2.29 \text{ GPa}$ , which is very close to DGEBA ( $2.37 \text{ GPa}$ ). Regarding thermal stability under nitrogen, the DGEGD  
 346 networks degrades earlier than DGEBA. More specifically, the  $T_{d5\%}$  of DGEGD/PACM is  $337 \text{ }^\circ\text{C}$ , and  
 347 DGEBA/PACM is  $379 \text{ }^\circ\text{C}$ . This may be due to the presence of the methylene in DGEGD, which could induce a  
 348 lower thermal stability. However, char yield is lower with DGEBA ( $2 \%$  at  $650 \text{ }^\circ\text{C}$ ) compared to  $4 \%$  with DGEGD.  
 349 Mauck *et al.* have used DFDA as hardener.<sup>56</sup> With this furan-based diamine, they obtained a  $T_\alpha$  of  $84 \text{ }^\circ\text{C}$  for  
 350 DGEGD/DFDA compared to  $109 \text{ }^\circ\text{C}$  with DGEBA. The storage moduli however are close, namely  $2.29 \text{ GPa}$  for  
 351 DGEGD and  $2.44 \text{ GPa}$  for DGEBA. It has to be noted that the crosslinking density for DGEGD/DFDA is  $4.97$   
 352 compared to  $2.62$  for DGEBA/DFDA. It may be due to the lower molecular weight of DGEGD compared to  
 353 DGEBA. The presence of a methylene and a single aromatic ring in gastrodigenin, may explain the lower  $T_g$  but due  
 354 to the higher crosslinking density, a comparable storage modulus. The thermal stability under argon reveals an  
 355 earlier degradation of DGEGD/DFDA with a  $T_{d5\%}$  of  $297 \text{ }^\circ\text{C}$  compared to  $330 \text{ }^\circ\text{C}$  with DGEBA. However, the char  
 356 yield in those systems is higher with DGEGD ( $40 \%$  at  $600 \text{ }^\circ\text{C}$ ) compared to DGEBA ( $23 \%$ ). Gastrodigenin has

357 been identified as a bisphenol F (BPF) metabolite. BPF has a well-known endocrine activity. In the work of Fic et  
358 al., gatrodigenin has been evaluated among other compounds, but has shown no deleterious activity.<sup>68</sup> The  
359 XenoScreen XL YES/YAS assay used in this report is a yeast based in vitro method to assess the activity of  
360 compounds both on the ER $\alpha$  receptor and the human androgen receptor.  
361

## 362 5. Bisvanillyls

363



364

365 Figure 9 - Synthesis of bisvanillyl based epoxy monomers according to Savonnet *et al.*<sup>69</sup>

366 The oxidative coupling of phenolics by enzymatic processes leads to the formation of diphenolic compounds that  
367 can help access to difunctional aromatic monomers.<sup>70</sup> The coupling of vanillin, and the reduction of the aldehyde  
368 moieties lead to a bisaromatic compound bearing two phenolic hydroxyls and two hydroxymethyl moieties. Thus, a  
369 tetra-functional epoxy monomer can be afforded after glycidylation. Savonnet *et al.* performed the synthesis of  
370 tetrafunctional monomer, but also obtained tri and difunctional monomers, by adjusting the ratios of epichlorohydrin  
371 in the glycidylation reaction of divanillylalcohol (Figure 9).<sup>69</sup> Purification allowed the study of these different  
372 monomers, especially upon curing with IPDA.

373 The three monomers are DiGEDVA (diglycidylether of divanillylalcohol), where the two hydroxymethyl moieties are  
374 reacted with epichlorohydrin, TriGEDVA with one phenolic moiety reacted, and then the TetraGEDVA, fully  
375 reacted. Interestingly, the viscosity at 40 °C shows that the tetrafunctional monomer has the lower viscosity.  
376 TetraGEDVA has a viscosity of 2 Pa·s, compared to DGEBA with 1 Pa·s. The TriGEDVA has a viscosity of 60  
377 Pa·s, and the DiGEDVA has a viscosity of 1300 Pa·s. This increase in viscosity is due to the number of free  
378 hydroxyl groups (1 for TriGEDVA and 2 for DiGEDVA). Free phenols or hydroxyls can provide hydrogen bonding  
379 to the system, and thus increase the viscosity or the crystallinity.

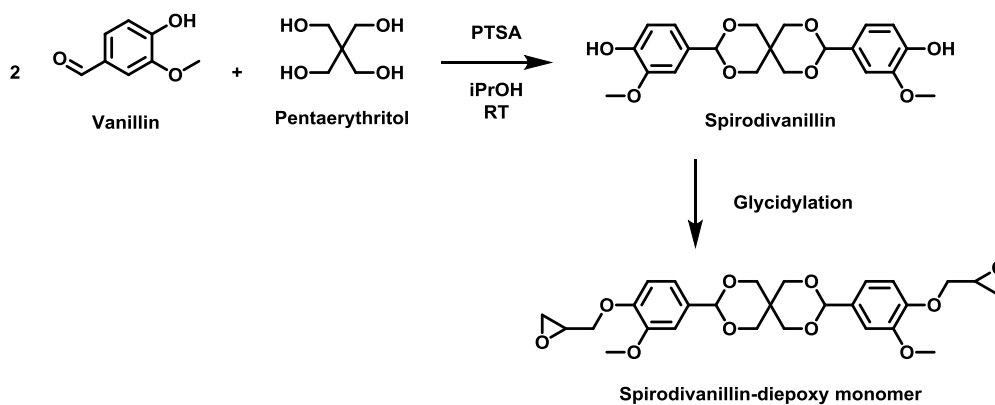
380 The crosslinked networks with IPDA give different  $T_g$  values, DiGEDVA has the lowest one at 138 °C, TriGEDVA  
381 intermediate one at 163 °C and TetraGEDVA the higher one at 198 °C. The functionality of the epoxy monomer can  
382 help to tune the  $T_g$ , especially because DGEBA gives usually a high  $T_g$ , such as 152 °C with IPDA, as studied by the  
383 authors. DMA was also performed, and properties such as the  $\alpha$  transition temperatures, the Young's moduli and the  
384 crosslinking densities were measured. The  $T_\alpha$  followed indeed the same trend than  $T_g$  measured by DSC. The  
385 GEDVA epoxy monomers have  $T_\alpha$ s of respectively 140, 177 and 200 °C with increasing functionality, as compared  
386 with DGEBA/IPDA with a  $T_\alpha$  of 155 °C. In overall, the Young's moduli on the glassy state are higher than for  
387 DGEBA, in the range 1.9-2.4 GPa, with the higher for TriGEDVA. On the rubbery state, higher moduli are also  
388 measured for the GEDVAs, ranging between 35 and 210 MPa, with values increasing from mono to tetrafunctional.  
389 Interestingly, DGEBA/IPDA give a modulus 35 MPa, similar to DiGEDVA. Crosslinking densities are similar  
390 between DGEBA and DiGEDVA networks (namely 9.2 and 9.5 kmol·m<sup>-3</sup>). For the higher functionalities,  
391 crosslinking density increases accordingly, with 25 kmol·m<sup>-3</sup> for TriGEDVA and 49 kmol·m<sup>-3</sup> for TetraGEDVA.

392 The higher crosslinking densities of tri and tetra epoxy monomers mainly explain the higher mechanical properties  
 393 observed. Tensile tests performed revealed that GEDVA monomers lead to higher Young's moduli, with increasing  
 394 value when functionality also increases. However, elongation at break is lower in all cases than the DGEBA  
 395 network. The rigidity of the monomers with a single carbon-carbon bond attaching the two aromatic rings seems to  
 396 be detrimental to the elasticity of the network. Thus, DGEBA/IPDA displays an elongation at break of 6.3 %  
 397 whereas DGEVAS network are between 3.3 and 4.7 %.

398 The thermal stability under air and under inert atmosphere showed that degradation of GEDVA networks happens at  
 399 lower temperature than with DGEBA. The presence of the methoxy moieties usually leads to lower degradation  
 400 temperatures. The  $T_{d5\%}$  is similar for all networks under air and under nitrogen, in the range 273-292 °C for  
 401 GEDVAs and around 330 °C for DGEBA. There is no residue at 600 °C under air for all the networks. Under inert  
 402 atmosphere, the char yield at 700 °C is around 10 % for DGEBA/IPDA, whereas it increases for GEDVAS. Tri and  
 403 TetraGEDVA have a char yield around 30 % whereas it is 40 % for DiGEDVA. This is simply explained by the free  
 404 hydroxymethyl moieties in DiGEDVA. It is known that hydroxymethyl moieties can undergo a novolac-type  
 405 condensation that could possibly happen during the degradation of the network, finally increasing the char  
 406 formation.

407 It is worth mentioning that a bio-based amine was also prepared from the difunctional vanillin derivative, and it was  
 408 used as the hardener in fully vanillin-based epoxy-amine thermosets.<sup>71</sup> This amine was also used to crosslink  
 409 DGEBA, and quite elevated  $T_g$  was obtained (176 °C), however lower than DGEVA/44DDS (204 °C).

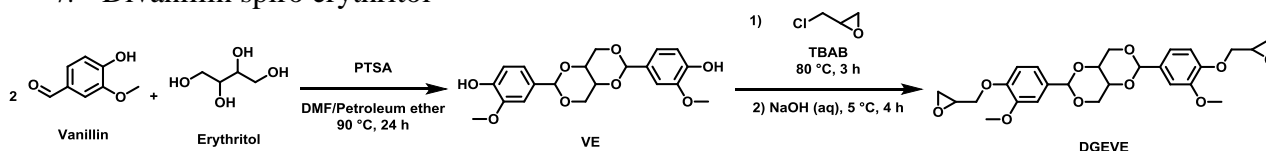
## 410 411 412 6. Spiro-divanillin



414 Figure 10 - Synthesis of spirodivanillin according to Mankar *et al.*<sup>72</sup> Glycidylation conditions were not  
 415 reported.

416 Vanillin and other aromatic aldehydes derivatives were also used in order to synthesize rigid structures using a  
 417 spiroacetal linker, based on pentaerythritol, a tetra-hydroxyl compound (Figure 10).<sup>72</sup> Different bisphenolic  
 418 structures were synthesized by Ochi *et al.* in order to analyse the contribution of methoxy moieties in epoxy  
 419 thermosets using mechanical and dielectric analyses.<sup>73,74</sup> The monomers cured with DDM show slightly less  
 420 crosslinking densities than DGEBA, and present alpha transitions very close to the DGEBA-DDM system (around  
 421 160 °C). The presence of methoxy moieties have shown to improve impact strength of the materials. However, no  
 422 more study has been reported in the literature about degradation behaviour or other properties.

## 423 424 7. Divanillin spiro erythritol

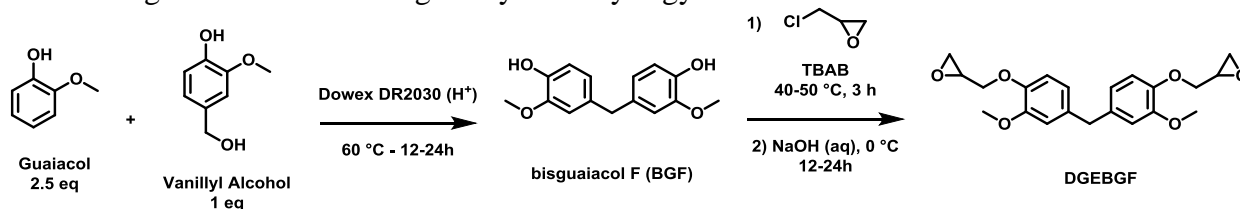


426 427 Figure 11 - Synthesis of DGEVE from vanillin and erythritol, according to Yuan *et al.*<sup>75</sup>

428

429 A bisphenol based on vanillin and the sugar substitute erythritol was synthesized by Yuan *et al.*<sup>75</sup> The glycidylation  
 430 leads to a diepoxy monomer (DGEVE, Figure 11), which was then cured with DDS and compared with DGEBA-  
 431 based thermoset. The high melting temperature of the monomer (245 °C), led the team to heat the formulation at  
 432 250 °C prior to a curing step at 180 °C, but the DGEBA-based mixture had the same curing scheme for comparison.  
 433 Dynamic mechanical analysis revealed an alpha transition temperature of 184 °C which is close to the  
 434 DGEBA/DDS formulation (208 °C). This high transition temperatures reveals a very rigid behaviour of the spiro  
 435 acetal containing monomer. The rubbery plateau is lower for the newly synthesized monomer (11 MPa for the  
 436 DGEVE monomer and 23 MPa for DGEBA). However, on the glassy plateau, from the published curves, we can  
 437 observe that the modulus at 0 °C is about 1.5 GPa for DGEBA epoxy, compared to 3 GPa for the methoxy-  
 438 containing network. The degradation behaviour showed that methoxy-containing material degrades at lower  
 439 temperature than DGEBA. For instance, under inert atmosphere, the  $T_{d5\%}$  of DGEBA/DDS is 394 °C whereas it is  
 440 343 °C for the DGEVE/DDS network. The char yield is higher with the methoxy-containing network since it nearly  
 441 triples (34.4 % for DGEVE vs 11.7 % for DGEBA, at 700 °C).  
 442 Tensile strength measurements were also performed on both networks. It can be remarked that DGEBA/DDS has a  
 443 higher elongation at break (7.1 %) than DGEVE/DDS (3.1 %). However, the tensile modulus is higher for DGEVE  
 444 (3.3 GPa) than for DGEBA network (1.8 GPa). The tensile strength is similar (71-83 MPa). The DGEVE monomer  
 445 gives a higher hardness to the system, due to the rigid spiro acetal structure. However, the lower elongation at break  
 446 shows a higher brittleness of the network.  
 447 Degradation in aqueous conditions have also been monitored. Indeed, the linker based on acetal moieties can be  
 448 easily cleaved in acidic conditions. Epoxy film samples were immersed in a mixture of polar organic solvent and  
 449 water with different mineral acids. Then the time was measured to the point where no observable material was  
 450 remained. Hydrochloric acid showed the lowest degradation time compared to sulphuric and phosphoric acid.  
 451 Regarding the organic co-solvent it was observed that degradation was accelerated when the most polar solvent was  
 452 used. Degradation time was between 55 and 160 minutes depending on the organic solvent used with 0.1 M HCl at  
 453 50 °C. Degradation was also monitored by NMR spectroscopy, and it was observed that the degradation occurred  
 454 through acidic cleavage of the acetal moiety, leading to regeneration of the aldehyde. The aging of the epoxy resin  
 455 was also studied using a Xenon test chamber, at a temperature of 60 °C and a humidity of 95 %. Under such  
 456 conditions the  $T_g$  of the material did not change significantly after 15 days.

## 458 8. Bisguaiacol F and other guaiacyls and syringyls



460 Figure 12 - Synthetic scheme of DGEBF synthesis according to Hernandez *et al.*<sup>45</sup>

461  
 462 Coupling of phenolics is an interesting way to access bisphenolic compounds, with a structure close to BPA.<sup>23</sup> The  
 463 properties of their epoxide derivatives are expected to be close to DGEBA. Hernandez *et al.* prepared a bisphenol  
 464 from vanillyl alcohol and guaiacol, another lignin derivative (Figure 12).<sup>45</sup> Reaction was conducted in acidic  
 465 medium, and purification by column chromatography afforded the desired isomer. After glycidylation, the EEW was  
 466 determined to be 193 g·eq<sup>-1</sup>, a value close to the DGEBA used for comparison (190 g·eq<sup>-1</sup>). The bisguaiacol was  
 467 cured with PACM, and compared with DGEBA/PACM system. Dynamic mechanical analysis was performed on the  
 468 networks, and it was observed that DGEBGF gave the higher  $E'$  (3.35 GPa) compared to DGEBA (2.37 GPa).  
 469 However, the  $\tan \delta$  of the DGEBA network displayed a peak maximum at 158 °C, whereas DGEBGF displayed a  
 470 peak at 111 °C. DSC confirmed the trend with a measured  $T_g$  of 149 °C for DGEBA network and 104 °C for  
 471 DGEBGF. It was observed that the presence of the methoxy moieties in DGEBGF gave higher loss modulus on the  
 472 glassy plateau, but that the packing of the network was less efficient due to the same methoxy moieties. This could  
 473 explain both the higher loss modulus and the lower  $T_g$  in comparison with DGEBA, which does not bear any  
 474 methoxy. Degradation under nitrogen atmosphere revealed that the DGEBA network started to degrade at a higher  
 475 temperature than DGEBGF, however the char yield was lower (2.3 % compared to 5.6 % for DGEBGF). The  
 476 bisguaiacol-based epoxy showed the same trend than all the other vanillin-based monomers, resulting in lower  $T_g$   
 477 but higher thermal stabilities.

478

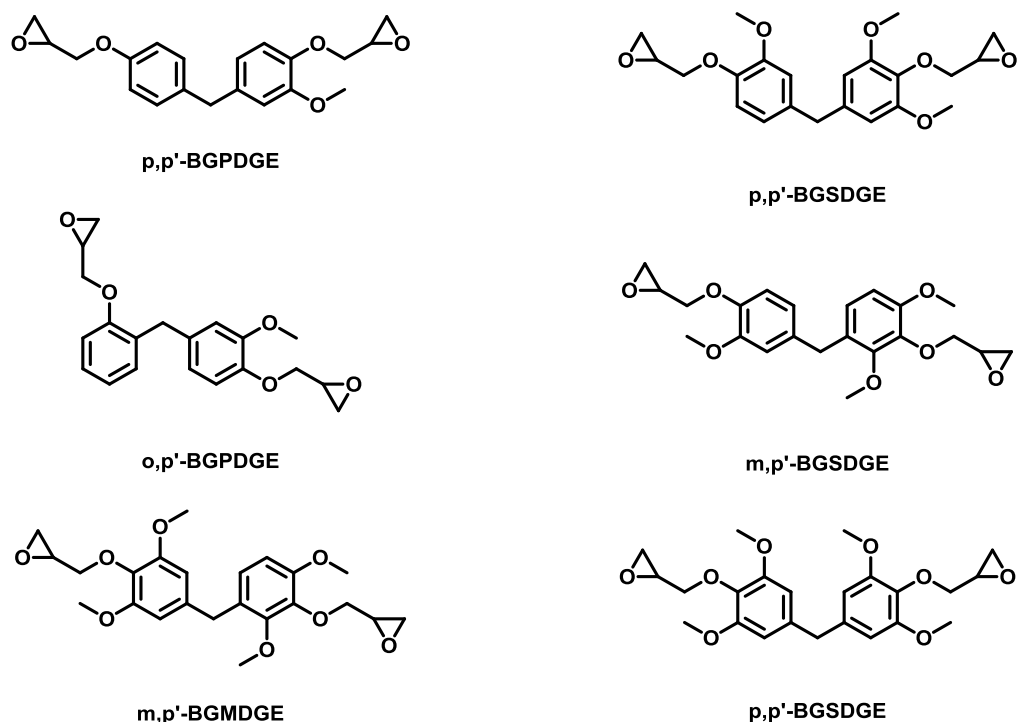


Figure 13 - Bisphenolic epoxy monomers synthesized by Nicastro *et al.*<sup>76</sup>

479

480

481

482 In a more recent paper, Nicastro *et al.* synthesized several bisphenols based on vanillic alcohol or syringyl alcohol,  
 483 condensed with other phenols,<sup>76</sup> using a similar protocol than Hernandez *et al.*<sup>45</sup> The condensation on the aromatic  
 484 ring could happen at different position (ortho, meta, para), depending on the phenol, and the authors obtained  
 485 mixtures, some of them were purified to obtain pure isomers. Thermomechanical properties evaluated by DMA of  
 486 the pure isomers and the glycidylated mixtures of isomers (shown in Figure 13) are summarized in Table 2. All the  
 487 thermosets were prepared using MDA as the hardener. All the thermosets displayed alpha transition temperatures  
 488 lower than the DGEBA/MDA system, but it should be noted that most of the prepared monomers have higher EEW  
 489 than DGEBA. A higher oligomerization degree could lower the crosslinking density. It has also been shown that at  
 490 the rubbery state, the storage modulus decreased as the number of methoxy moieties increased.  
 491

492

Table 2 - Thermomechanical properties of epoxy thermosets from bisphenols and MDA

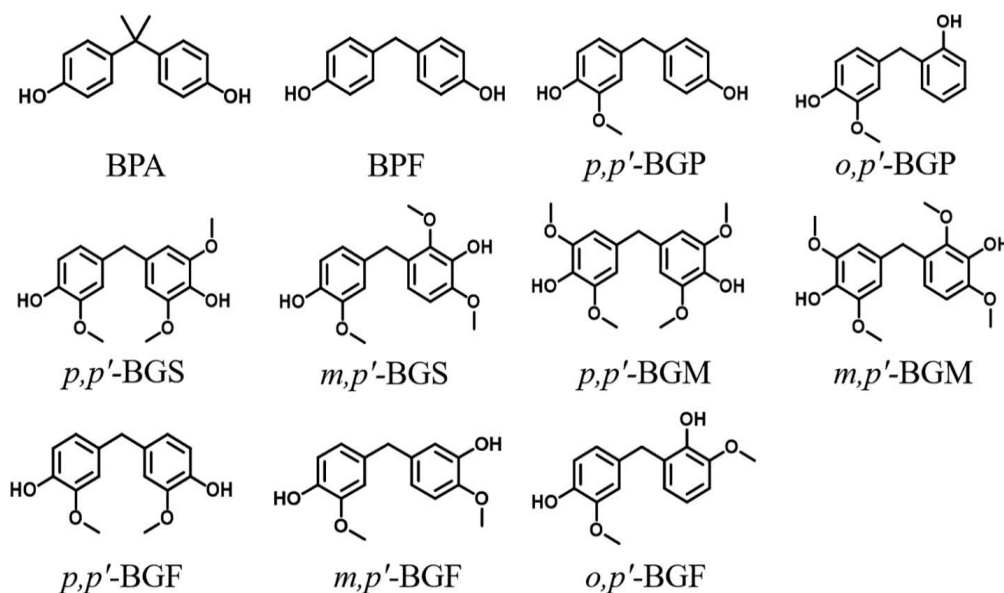
Epoxy monomer	$E'_{30}$ (GPa)	$E'_{200}$ (MPa)	$T_{\alpha}$ (°C)
p,p'-BGPDGE	2.5	46	151
o,p'-BGPDGE	2.8	22	141
p,p'-BGSDGE	2.7	33	134
m,p'-BGSDGE	2.4	28	129
p,p'-BGMDGE	2.5	26	141
m,p'-BGMDGE	2.0	15	119
DGEBA	2.5	46	167

493

494 Koelewijn *et al.* worked on the synthesis method of bisguaiacol F isomers in order to obtain polycarbonates via  
 495 copolymerisation of BGF.<sup>77</sup> They also conducted in vitro experiments to assess the human oestrogen receptor  $\alpha$   
 496 activity of BGF, using two of the BGF isomers, namely 4,4'-BGF et 3-4'-BGF. Comparison was also made with 4-  
 497 4'-BPF and 4,4'-BPA, and the natural hormone oestradiol. It was shown that BPA and BPF fully activated hER $\alpha$  in  
 498 a dose-dependent manner, whereas the dose-response curves were only partial for the BGF isomers. The relative  
 499 oestrogenic efficacy (REE) is an indication of the efficacy of the receptor activation compared to the one of the  
 500 hormones (that has a REE of 100 %). REE for BPA and BPF were respectively 96 and 126 % showing a similar



501 interaction between the bisphenols and the oestrogen receptor, whereas it was only 48 and 37 % for BGF isomers.  
 502 The para-para orientation of 4,4'-BGF showed a higher activity compared to the 3,4' isomer, which confirmed that  
 503 the para-para orientation is an important criterion. The lower concentration needed for a given effect, called EC<sub>50</sub>  
 504 was 1.3·10<sup>-11</sup> M for the 17β-E2 compared to 6.6·10<sup>-7</sup> M for BPA and as high as 9.4 and 8.7·10<sup>-5</sup> M for 4,4' and 3,4'  
 505 isomers respectively. This means that a higher amount of BGF is required to activate the receptor. Overall, BGF  
 506 isomers showed 426-457 times lower affinity than BPA. These results are promising, as they are consistent with  
 507 previous reports using other evaluation methods.<sup>78</sup>  
 508 Peng *et al.* also performed in vitro testing on bisguaiacol F isomers.<sup>79</sup> Since the synthesis of bisguaiacol could  
 509 generate isomer mixtures, they determined the ratios of isomers that were obtained from the condensation of vanillyl  
 510 alcohol and guaiacol, and used these mixtures for the in vitro testing. The two in vitro assays chosen were MCF-7  
 511 cell proliferation assay and VM7Luc4E2 TA test. E2 and BPA were used as positive controls. Both assays gave  
 512 consistent results. Three mixtures testes contained ratios of 3,4-BGF and 4,4-BGF (4,4-BGF being the major one),  
 513 and one mixture contained the three isomers, with a majority of 2,4-BGF. The results showed that when the  
 514 mixtures contained a high proportion of 4,4-BGF, or when it contained 2,4-BGF, an increase in the proliferation rate  
 515 was observed in the MCF-7 assay, indicating an oestrogen affinity. However, the proliferation rate was lower than  
 516 that of BPA. The mixtures containing higher proportions of 3,4-BGF did not induce MCF-7 cell proliferation. The  
 517 VM7Luc4E2 test also showed that the high 3,4-BGF containing mixtures had non-detectable EA. The other BGF  
 518 mixtures did show some EA, but with lower EC<sub>50</sub> values. These results suggest that high 4,4-BGF concentration and  
 519 2,4-BGF containing mixtures are moderately active on the oestrogen receptor, but still less active than BPA.  
 520



521

522

Figure 14 - Bisphenols and bisguaiacols used in ERα affinity tests

523 in a different report, Peng *et al.* tried to determine the influence of methoxy groups on the oestrogen affinity of  
 524 bisphenols, especially at relevant environmental concentrations.<sup>80</sup> They synthesized a total of 9 bisphenols bearing  
 525 different numbers of methoxy moieties, with different phenol orientations (Figure 14). They also performed a  
 526 comparison of oestrogen activity with BPA and BPF. The assays conducted were first the determination of the  
 527 oestrogen affinity, especially the lower concentration at which an effect is observed. Secondly, they tried to assess  
 528 the effect of environmental concentrations of bisphenols on the viability of human cell lines (MCF-7 cells and  
 529 VM7Luc4E2). Their work showed that the presence of only one methoxy on the bisphenol, drastically reduced the  
 530 EA. No bisguaiacol had a detectable EA at concentrations lower than 10<sup>-7</sup> M. At relevant environmental  
 531 concentrations of bisphenols, the two in vitro assays of cell proliferation were consistent. At this concentration, for  
 532 all bisguaiacols, the % RME2 that illustrates the normalized EA was lower than for BPA or BPF, in at least one cell  
 533 line. The only exception was for one meta-para isomer which would require further investigations.  
 534 Amitrano *et al.* designed a study using molecular docking in order to study the influence of methoxy groups on the  
 535 calculated binding affinity of bisphenols with the ERα receptor.<sup>81</sup> The authors evaluated several structures that could  
 536 be derived from lignin, bisphenols bearing one or two methoxies on each aromatic ring. The influence of the  
 537 bridging unit between the phenols was also studied, and the orientation of methoxy substitution on the ring. Their  
 538 results suggest that methoxies do have an influence on the interaction between the bisphenols and the receptor via  
 539 steric hindrance. However, the effect was especially significant when at least two methoxies were attached to one of

540 the phenols, when there was no substitution on the bridging methylene. The authors also suggest that bulky  
 541 substituents on the bridging unit have also an influence on the affinity with the receptor, likely due to the steric  
 542 hindrance, especially when the phenols were substituted. Both methoxy substitution on the phenol and bulky groups  
 543 on the bridging unit are the key parameters to possibly prevent interaction with ER $\alpha$ . The substitution orientation  
 544 (*ortho*, *meta*, *para*) do not have a significant influence for bulky monomers, *i.e.* containing 2 methoxies on one  
 545 phenol ring. However, when containing one methoxy on each phenol ring, the results were consistent with the  
 546 reported *in vitro* tests by Peng and co-workers.<sup>79</sup>  
 547 Some guaiacyl and syringyl bisphenolic compounds were evaluated by Hong *et al.* with intention to predict the  
 548 oestrogen activity of a set of compounds using an *in silico* model, based on available data from the literature.<sup>82</sup> In  
 549 this work, p,p'-BGF, p,p'-BGS (from Figure 14), and another bisguaiacol having one methoxy group on one of the  
 550 ortho position, with a dimethyl-substituted bridging unit *i.e.* Bisguaiacol A (also reported in Amitrano *et al.*<sup>81</sup>) were  
 551 evaluated and their binding affinity predicted. From this three monomers, p,p'-BGS and bisguaiacol A were predicted  
 552 as non-binder to the receptor. Bisguaiacol F (p,p'-BGF) was predicted to be binder to the receptor, but with a  
 553 moderate confidence (probability to be binder is lower than 80 %). The quantitative binding affinity calculated for  
 554 this latter bisphenol was slightly lower than BPA. This result is in accordance with the reported *in vitro* data  
 555 described before. If bisguaiacol F do show an activity *in vitro*, as described *e.g.* in Koelewijn *et al.*, the real-life  
 556 concentration needed would be higher than for BPA, thus the ED potential would be lower.<sup>77</sup>

## 557 9. Cyclopentanone bisvanillin

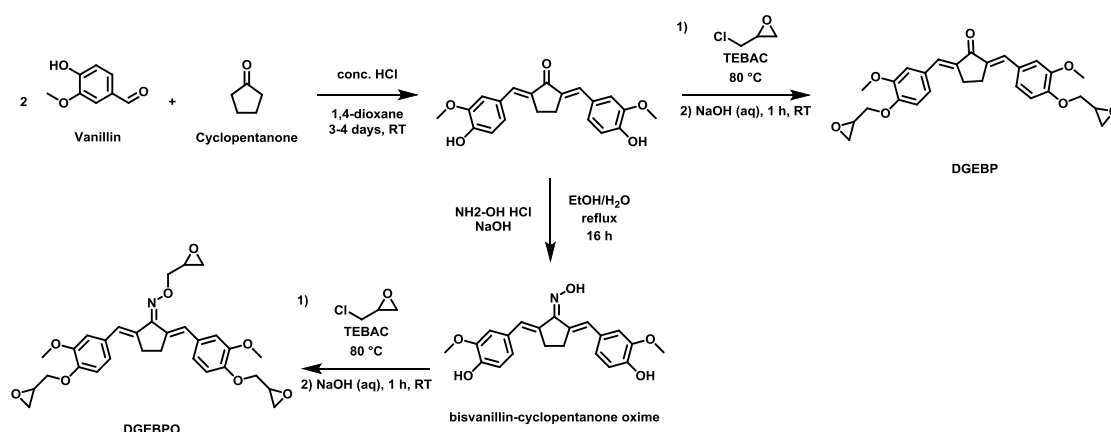
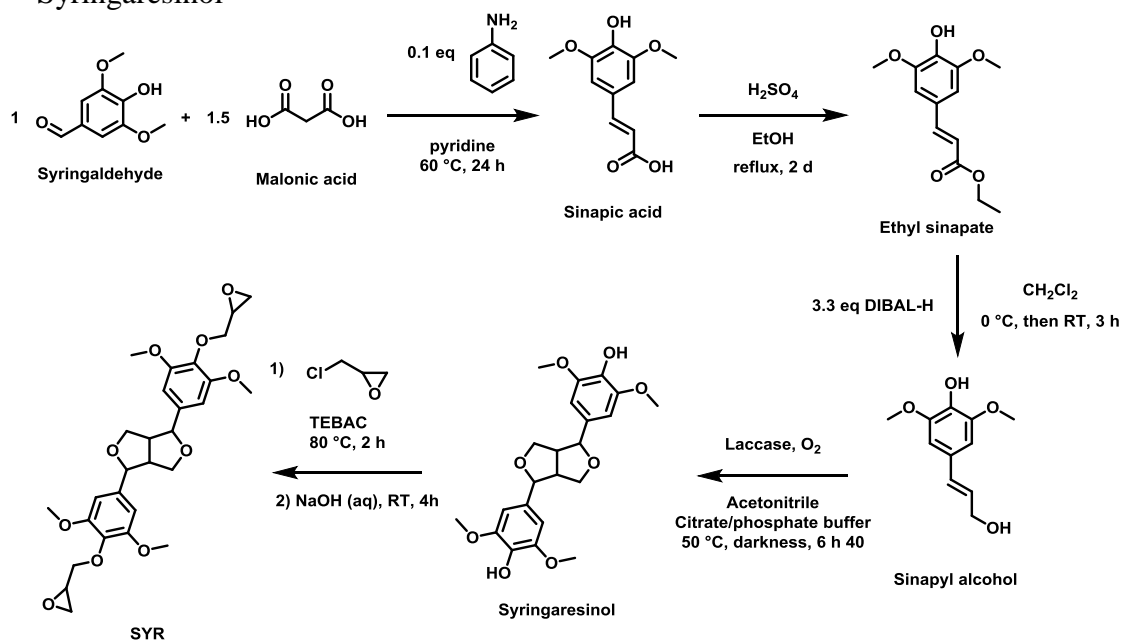


Figure 15 - Synthesis of DGEBO and DGEBP from vanillin, according to Mogheiseh *et al.*<sup>83</sup>

562 Shibata and Ohkita synthesized a divanillin-based monomer by an aldol condensation between two equivalents of  
 563 vanillin and cyclopentanone (Figure 15), and used phenolic hardeners in order to generate epoxy-phenol  
 564 thermosets.<sup>84</sup> More recently, Mogheiseh *et al.* used this divanillin-based monomer, and synthesized a slightly  
 565 modified epoxy-phenol.<sup>83</sup> They formed an oxime by the reaction of the ketone with hydroxylamine. The compound  
 566 containing two vanillin moieties and the oxime could be glycidylated, adding three glycidylether moieties. They  
 567 used several hardeners, some containing hydroxyls, among them the biobased decanediamine (DA10). The fully  
 568 cured material with the amine was characterized using infrared spectroscopy, gel content, mechanical and thermal  
 569 properties. The glass transition temperature of the system DGEBO/DA10 was 102 °C and the alpha transition  
 570 measured by DMA was 109 °C. For comparison, DGEBA/DA10 thermoset has a  $T_g$  of 98 °C and  $T_\alpha$  of 97 °C  
 571 according to Ménard.<sup>85</sup> The thermoset based on DGEBO displayed a storage modulus of 1.7 GPa compared to 1.0  
 572 GPa for DGEBA/DA10, due to the more rigid structure of DGEBO that is brought by the cyclopentenedione link  
 573 between the two aromatic rings, and the higher epoxy functionality. The same trend is observed at the rubbery state  
 574 with a modulus of 93.0 MPa for DGEBO based material, compared with 23.2 MPa for DGEBA/DA10. In terms of  
 575 thermal stability under inert atmosphere, the  $T_{d5\%}$  of DGEBO material was 313 °C, which is slightly lower than  
 576 DGEBA/DA10 (337 °C). This trend is often observed with methoxy-containing monomers such as vanillin-based  
 577 compounds. Char yield at 700 °C was determined for the cured materials and DGEBO, displaying 2.5 % compared  
 578 to 5.2 % for DGEBA/DA10. Usually, it was observed that vanillin-based epoxides give higher char yields, and this  
 579 result could be explained by a lower contribution to char formation of the cyclopentenedione link between the  
 580 aromatics, even if the higher functionality of the monomer could lead to a better stability as compared to the  
 581 difunctional DGEBA.  
 582

583  
584

## II. Syringaldehyde Syringaresinol



585

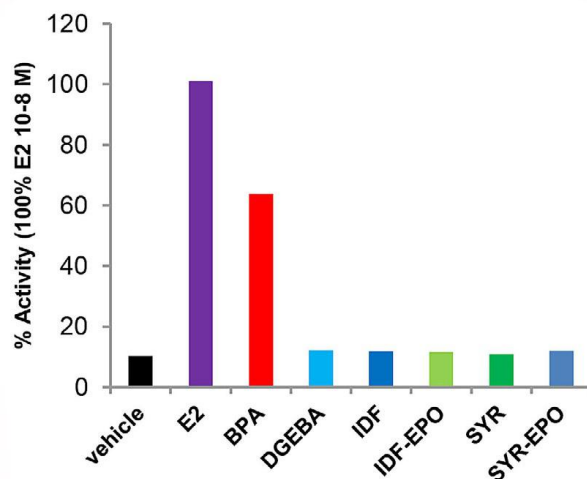
586 Figure 16 – Synthesis of epoxy monomer of Syringaresinol from Syringaldehyde according to Janvier *et*  
587 *al.*<sup>86</sup>

588 Syringaresinol is a natural polyphenol found in some plants, but in very low yields. However, researchers have  
589 developed several catalytic and biocatalytic processes to afford multigram scale of this antioxidant.<sup>87</sup> Access to large  
590 quantities of this natural molecule has led to its use as an epoxy precursor, after glycidylation (Figure 16). Janvier *et*  
591 *al.* performed the synthesis of this diepoxide, and then studied the network properties with different hardeners such  
592 as DA10, IPDA and DIFFA.<sup>86</sup> The IPDA/SYR network displayed a  $T_g$  of 126 °C, which is slightly lower than  
593 DGEBA. The  $\alpha$  transition temperature of the SYR network was 157 °C (as compared to 166 °C for DGEBA/IPDA.  
594 The glassy modulus (measured at 50 °C) of SYR/IPDA was 758 MPa while with DGEBA the value was 783 MPa.  
595 The moduli and transition temperatures were similar to each other, indicating that even if the crosslinking density  
596 was expected to be lower for the SYR network (due to a higher molecular weight between the crosslinks), the  
597 rigidity brought by the bicyclic linkage counterbalanced the effect on the network. At the rubbery plateau, the  
598 DGEBA network displayed a modulus of 16 MPa, compared to 12 MPa for the SYR network. The presence of a  
599 higher density of aromatics in DGEBA lead to a higher modulus.

600 When cured with DA10, the SYR network displayed a  $T_g$  of 73 °C, compared to the DGEBA network reported by  
601 Ménard *et al.* with a  $T_g$  of 98 °C.<sup>88</sup> However, regarding the  $\alpha$  transition, the reported DA10/DGEBA value was 97  
602 °C whereas for the SYR network, the  $T_\alpha$  was 102 °C. The similar values displayed under mechanical investigations  
603 lead to the conclusion that the SYR based networks display excellent mechanical properties compared with  
604 DGEBA. At the glassy plateau, the values were not comparable for DGEBA and SYR networks since the  
605 measurements were not performed at the same temperature (at 50 °C reported by Janvier *et al.* and at 0 °C reported  
606 by Ménard *et al.*). At the rubbery state, the SYR-DA10 material had a modulus of 14 MPa compared to the reported  
607 23.2 MPa for DGEBA. The lower value obtained is probably due to the lower crosslinking density.

608 Finally, the last hardener used is DIFFA, which lead to a  $T_g$  of 102 °C and a  $T_\alpha$  of 108 °C, whereas the  
609 DGEBA/DIFFA network had a  $T_g$  of 92 °C and a  $T_\alpha$  of 110 °C. These very similar values, show promising results  
610 for this epoxy monomer as a substitute for DGEBA. Regarding the rubbery modulus, the SYR network displayed a  
611 value of 10 MPa compared to 23.2 MPa for DGEBA. The rigidity brought by the bicyclic linkage does not prevent  
612 free rotation once the  $\alpha$  transition happened. The global thermal stability of the networks was lower for SYR  
613 compared with DGEBA (over 300 °C for DGEBA, and slightly under for SYR, with a difference of approximately  
614 30 °C). The char formation was higher for SYR networks, attaining 29.4 % for DIFFA/SYR at 700 °C.

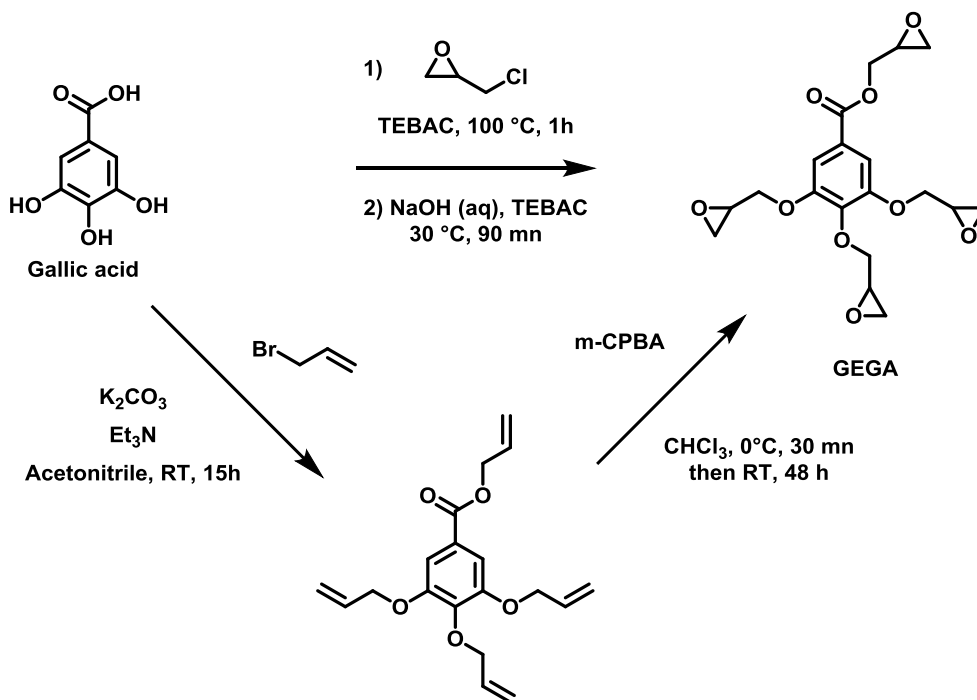
615 Syringaresinol and its glycidylated derivative were evaluated by Janvier *et al.* against ER $\alpha$  and compared with BPA,  
616 DGEBA, E2 and an isosorbide-based bisferulate described later in this review.<sup>86</sup> The activity relatively to the human  
617 hormone were plotted for all the compounds tested, at 10<sup>-8</sup> M. It was shown that the new epoxy monomers and the  
618 corresponding diols did not show any oestrogenic activity, since they display the activity corresponding to the  
619 vehicle (Figure 17). In addition, no dose-response was observed in the concentration range 10<sup>-13</sup> to 10<sup>-5</sup> M.



620

621 Figure 17 - In vitro evaluation of relative activity of syringaresinol diol (SYR) and diepoxy (SYR-EPO)  
 622 against HERα by Janvier *et al.*<sup>86</sup> Comparison were made with BPA, DGEBA. IDF and IDF-EPO are  
 623 isosorbide-based compounds.

624 III. Gallic acid



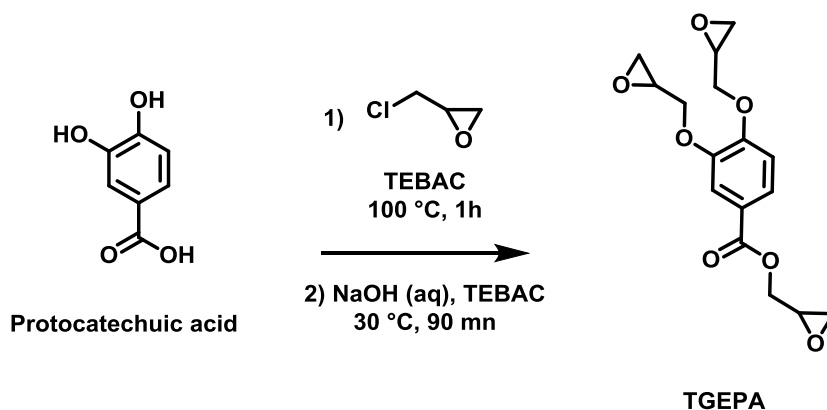
625

626 Figure 18 - Synthetic pathways for the synthesis of GEGA, from Tarzia *et al.* and Aouf *et al.*<sup>89,90</sup>

627 Glycidylether of gallic acid was prepared by allylation of the carboxylic acid and the subsequent epoxidation of the  
 628 allylic double bonds (Figure 18).<sup>90</sup> Aouf *et al.* performed the oxidation using two methods, the first using *m*CPBA  
 629 and the second one using Oxone in milder conditions. However, the Oxone method gave lower yield of the tetra-  
 630 epoxide compared with the *m*CPBA method. GEGA was cured with IPDA using a mixture of the trifunctional and  
 631 tetrafunctional monomers, with a mean of 3.8 epoxy per monomer. The thermoset properties were compared with  
 632 the DGEBA/IPDA system. Dynamic mechanical analysis showed a  $T_{\alpha}$  of 233 °C for GEGA, much higher than for  
 633 DGEBA (160 °C). This higher transition can be explained by the higher crosslinking density of GEGA, due to a  
 634 higher functionality and the lower molecular weight compared to DGEBA. The temperature of 5 % degradation of  
 635 the material under inert atmosphere ( $T_{d5\%}$ ) is 300 °C for GEGA and 350 °C for DGEBA. The lower thermal stability  
 636 of GEGA is probably due to the presence of the ester bond. However, the char yield at 600 °C was 23 % for GEGA

637 and 8 % for DGEBA. The higher crosslinking and aromatic density brought by GEGA lead to a higher stability and  
 638 char formation at high temperature, compared to DGEBA.  
 639 In the work of Tarzia *et al.*, curing of GEGA was performed using IPDA and Jeffamine D230, which is a  
 640 polypropylene-oxide based diamine.<sup>89</sup> They observed by DSC comparable curing exotherms with both amines  
 641 (488 J·g<sup>-1</sup> with Jeffamine and 531 J·g<sup>-1</sup> with IPDA). They also observed similar peak temperatures (respectively 94  
 642 and 90 °C). The glass transition temperature after curing at 150 °C was also measured by DSC. The IPDA system  
 643 displayed a  $T_g$  of 145 °C and the one with Jeffamine was 83 °C. In comparison, from Duchet and Pascault<sup>91</sup>, the  
 644 DGEBA/IPDA system displayed a  $T_g$  of 156 °C, and the DGEBA cured with Jeffamine D230 had a  $T_g$  of 80 °C. In  
 645 the work of Tarzia *et al.*, the glass transition temperatures of GEGA thermosets are very similar to DGEBA  
 646 thermosets. Compared with the work of Aouf *et al.* it can be observed that the reported values for IPDA/GEGA  
 647 were slightly different. Indeed, as a comparison with  $T_g$ , the alpha transition of IPDA/GEGA from Aouf *et al.* is 233  
 648 °C.<sup>89,92</sup> However, in the work of Tarzia *et al.*, the reporting curing procedure at 150 °C was different than the  
 649 procedure from Aouf *et al.* which was 30 minutes at 90 °C and then 2 hours at 200 °C. Due to the high functionality  
 650 of GEGA one could expect that with the same amine, GEGA would lead to higher glass transition temperatures or  
 651  $T_a$  than with DGEBA. It could be deduced that the differences were due to an incomplete curing process from  
 652 Tarzia *et al.* since the ratio between trifunctional and tetrafunctional GEGA was reported to be the same. This is also  
 653 confirmed by the fact that Tarzia *et al.* observed some residual enthalpy in the 2<sup>nd</sup> heating ramp in DSC. Thus,  
 654 thermosets obtained from GEGA could have similar transitions than with DGEBA only if the thermoset was not  
 655 fully cured. Regarding the degradation of the cured thermosets, in the work of Tarzia *et al.* the char yield reported  
 656 for IPDA/GEGA was 18 % at 600 °C, which was lower than the one reported by Aouf *et al.*, confirming the  
 657 incomplete curing process. Regarding tensile tests, DGEBA systems gave lower tensile modulus than GEGA  
 658 systems. The tensile strength for epoxides cured with IPDA was higher with GEGA than with DGEBA. The  
 659 opposite trend was observed for both epoxides cured with Jeffamine. It seems that the DGEBA systems can be  
 660 subjected to more plastic deformation than GEGA systems. This is confirmed by the global higher percentage of  
 661 elongation at break. The GEGA systems were more brittle due to the crosslinking density.  
 662 In a study screening 253 industrial chemicals, gallic acid was evaluated for its activity against androgen receptor.  
 663 The results indicated that this compound does not have any activity against the AR.<sup>93</sup> Unexpectedly, some studies  
 664 report a protective effect of gallic acid on the toxicity induced by BPA. For example, a recent study by Trivedi *et al.*  
 665 showed in vitro that the addition of gallic acid reduced the toxicity induced by BPA, especially on red blood  
 666 corpuscle.<sup>94</sup>

#### 667 IV. Protocatechuic acid



673 Figure 19 - Synthesis of TGEPA from protocatechuic acid, according to Aouf *et al.*<sup>90</sup>

674 Protocatechuic acid is a catechol bearing a carboxylic acid moiety. It is a natural polyphenol found in seeds such as  
 675 chia, canola or sunflower, or in fruits and berries such as mangosteen.<sup>95</sup> It has also been demonstrated that  
 676 protocatechuic acid can be obtained from glucose, via microbial fermentation.<sup>96,97</sup> The glycidylation reaction of  
 677 protocatechuic acid was first performed by Aouf *et al.* in a paper describing the effect of different substituents of  
 678 natural phenols on the reaction of glycidylation.<sup>90</sup> No thermosetting polymers were prepared from this study, but  
 679 recently, Chen *et al.* prepared crosslinked networks with DDM as the hardener.<sup>98</sup> It has to be noted that the  
 trifunctional epoxy monomer can also be obtained by allylation and subsequent oxidation of the double bonds.<sup>99</sup>

680 Chen *et al.* performed non-isothermal curing kinetics using Kissinger's method in order to assess the activation  
 681 energies of the TGEPA/DDM system. Using five different heating rates, the authors measured an  $E_a$  of  $54 \text{ kJ}\cdot\text{mol}^{-1}$   
 682 compared to  $57 \text{ kJ}\cdot\text{mol}^{-1}$  for DGEBA/DDM system, reported before with the same method.<sup>100</sup> The slightly more  
 683 favourable activation energy was attributed to the presence of the ester moiety that could activate one of the glycidyl  
 684 residue. The alpha transition determined by DMA for TGEPA/DDM was not observed by the  $\tan \delta$  peak before  
 685  $250 \text{ }^\circ\text{C}$ , which is quite higher than DGEBA/DDM, which  $T_\alpha$  was measured at  $189 \text{ }^\circ\text{C}$ . The storage modulus of the  
 686 TGEPA network was higher than DGEBA (respectively  $1.9 \text{ GPa}$  vs  $1.6 \text{ GPa}$ ) at room temperature, and it is  
 687 explained by the rigid structure of the monomer compared to DGEBA. It has also to be noted that the single  
 688 aromatic ring of the new monomer prepared by the authors could also lead to a higher aromatic density in the  
 689 network, and thus, a higher rigidity. The very high  $T_g$  was also confirmed by the measurement of coefficient of  
 690 thermal expansion, determined by thermal dilatometry. Using this method,  $T_g$  was measured to be  $176 \text{ }^\circ\text{C}$  for  
 691 DGEBA/DDM compared to  $221 \text{ }^\circ\text{C}$  for TGEPA/DDM, which is coherent with previous characterizations. Finally,  
 692 regarding thermal stability under nitrogen atmosphere, the  $T_{d5\%}$  of TGEPA network was  $321 \text{ }^\circ\text{C}$ , lower than for  
 693 DGEBA ( $364 \text{ }^\circ\text{C}$ ), as often observed with monomers containing esters. However, the char yield measured at  $1000$   
 694  $^\circ\text{C}$  was  $16 \%$  for the DGEBA network, compared to  $28 \%$  for TGEPA network, showing a better charring ability,  
 695 probably due to the high aromatic density of the network. 3,4-dihydroxybenzoic acid (protocatechuic acid) is  
 696 considered as a human metabolite resulting from the exposure to parabens.<sup>101</sup> Parabens are well known preservatives  
 697 that are also suspected of endocrine disruption. However, so far they have not been evaluated as endocrine  
 698 disruptors.

## 700 V. Ferulic acid

701

702 Ferulic acid is a phenolic compound that can be found in bagasse, wheat and rice brans or beetroot pulp. It is  
 703 composed of an aromatic phenolic ring bearing a methoxy moiety in ortho position, and an  $\alpha,\beta$ -unsaturated  
 704 carboxylic acid in para position. This compound that can be extracted from non-edible agricultural waste.<sup>88</sup>

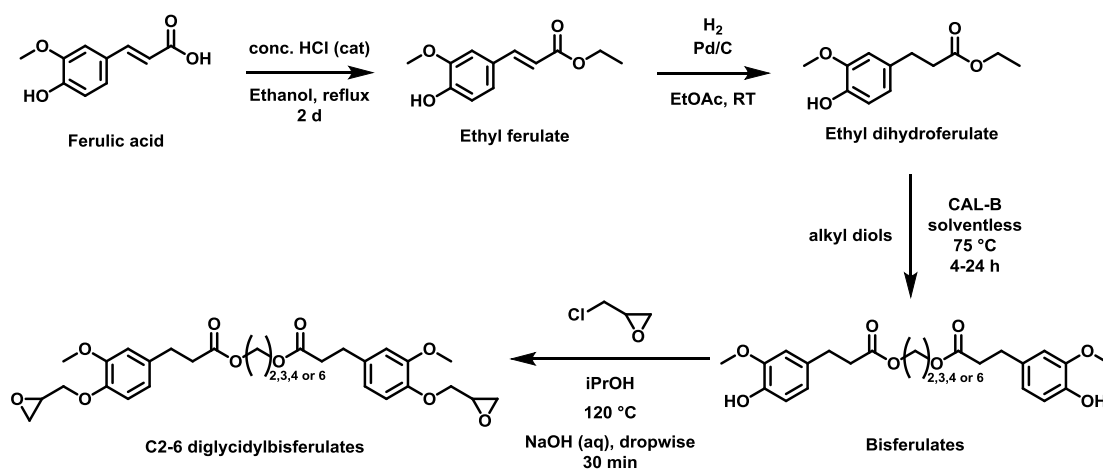
705

### 706 1. Bisferulates with alkyl ester linker

707

708 Maiorana *et al.* synthesized an ester of ferulic acid by an acidic esterification with ethanol. The obtained ester was  
 709 subsequently reduced in the same pot, using Pd/C and dihydrogen at ambient temperature and pressure. This ester  
 710 was then used as a starting material for transesterification reactions using a lipase in order to obtain di or  
 711 trifunctional derivatives with different linkages. The diols utilized were ethanediol, propanediol, butanediol and  
 712 hexanediol (all linear) as shown in Figure 20.<sup>102</sup> Ménard *et al.* used the same method using isosorbide, butanediol  
 713 and butanediamine to obtain bisferulates, and glycerol was used to obtain a trifunctional compound.<sup>88</sup> The  
 714 corresponding esters or amides were then subjected to glycidylation, in order to obtain the corresponding epoxy  
 715 monomers. Thermosets were prepared with different amines, and compared with DGEBA systems in each case.  
 716 Three amines were used as hardeners, namely IPDA (cycloaliphatic), DA10 (aliphatic) and difurfurylamine A  
 717 (DIFFA) obtained from the condensation of furfurylamine with acetone.

718

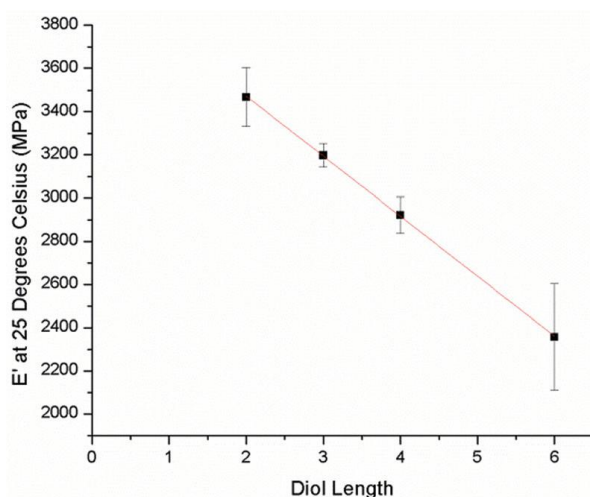


719

720 Figure 20 - Reaction scheme for the synthesis of alkyl bisferulates derived epoxy monomers according to  
 721 Maiorana *et al.*<sup>102</sup>

722

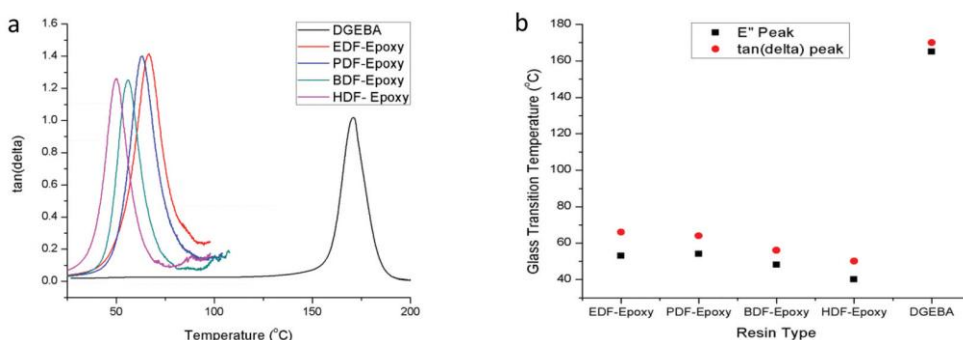
723 Regarding bisferulates synthesized from linear diols, Maiorana *et al.* used IPDA as the hardener. They were able to  
724 compare the epoxy-amine networks properties as a function of diol size, and with DGEBA also for comparison.  
725 They compared the viscosity of the epoxies at 25 °C, and calculated the flow activation energy. They showed that  
726 the temperature dependence of the viscosity for the bisferulates were similar to DGEBA. A linear correlation was  
727 observed for the storage moduli at 25 °C when it was plotted against the diol length. The storage moduli were  
728 reduced as the length of the linker increased. This is mainly due to the increased chain mobility in the thermoset.  
729 The glassy moduli of the bisferulates based networks were in the range 2300-3500 MPa, while the value for  
730 DGEBA network is 2640 MPa (close to the C4 bisferulate (Figure 21)).  
731



732

733 Figure 21 - Young's modulus of bisferulates/IPDA thermosets as a function of the diol spacer length, from  
734 Maiorana *et al.*<sup>102</sup>

735 Regarding the  $\alpha$  transition of the networks and the loss moduli peaks, a slight decrease was observed as the linker  
736 length increased (Figure 22). This is consistent with the increase in chain mobility as the number of carbons in the  
737 linker increased. However, for all the bisferulates diepoxides, the transitions were observed at lower temperatures, in  
738 the range 40-70 °C as compared to DGEBA (higher transition around 170 °C).  
739



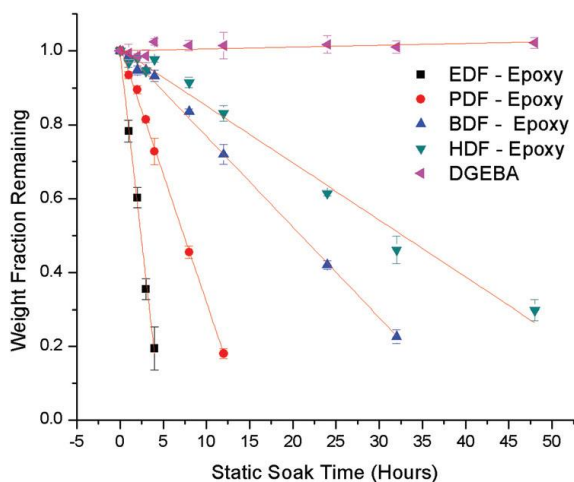
740

741 Figure 22 - a)  $\tan \delta$  peaks of alkyl bisferulates based thermosets with IPDA, b) E'' peaks and  $\tan \delta$  peak  
742 temperatures plotted against the different epoxy structures. EDF = C2, PDF = C3, BDF = C4 and HDF =  
743 C6, reproduced from Maiorana *et al.*<sup>102</sup>

744

745 The degradation behaviour of all the thermosets was also investigated under nitrogen. It was observed that longer  
746 linkers resulted in higher  $T_{d5\%}$  with an increase from 300 to 331 °C for C2 to C6 diols. The onset of degradation was  
747 slightly higher for DGEBA network, however in the same range of temperature. Similar thermal resistance indicates  
748 similar thermal stability and suitability of the thermoset for same type of applications. It can also be noted that the  
749 char yields were higher for bisferulates (shorter chains gave higher char yields). As mentioned previously, the

750 methoxy-containing monomers are more prone to increase the char formation. However, the increase in alkyl carbon  
 751 content decreases the char formation, mainly due to the lower density of the aromatics and the crosslinking.  
 752 The hydrolytic degradation of the networks was studied in alkaline conditions at 60 °C), providing interesting  
 753 information regarding the possible chemical recycling of the thermosets, and also the possible leaching of the  
 754 compounds. The cured samples were immersed in an alkaline media at 60 °C and their weight was monitored as a  
 755 function of time (Figure 23). This figure shows that the DGEBA does not degrade even after 50h, whereas the  
 756 degradation kinetics for ester containing materials have a linear correlation with the linker size. Shorter alkyl chains  
 757 degrade faster since the hydrophilicity of shorter chains are higher as confirmed by contact angle measurements.  
 758



759  
 760 Figure 23 - Solid fraction as a function of soaking time in alkaline medium for alkyl bisferulate based  
 761 thermosets, reproduced from Maiorana *et al.*<sup>102</sup>

762 The C4 linker containing epoxide was also cured with DA10 and DIFFA by Ménard and co-workers.<sup>88</sup> It could be  
 763 observed that the use of aliphatic hardeners with the C4 monomer gave a slightly less stable material with  $T_{d5\%}$  of  
 764 314 °C for IPDA and DA10, compared to the use of DGEBA as the epoxide (respectively 331 and 337 °C). With  
 765 DIFFA however, the thermal stabilities were comparable with DGEBA (306 °C for the bisferulate and 301 °C for  
 766 DGEBA). It seems that the crosslinking density of the DGEBA-DIFFA is responsible for the lower thermal stability.  
 767 Char yields were higher with all the hardeners with bisferulates, the highest values were obtained with DIFFA as the  
 768 hardener for all the networks. The glass transition temperatures for all networks based on the C4 bisferulates were  
 769 nearly one third of the ones obtained with DGEBA, for all hardeners (due to lower crosslinking densities). DMA  
 770 measurements showed that the alpha transitions followed a similar trend. The glassy modulus of C4 bisferulate was  
 771 the same as the DGEBA when DA10 was used as the hardener. The elastic modulus of bisferulate network with  
 772 DA10 however was half of the value obtained for DGEBA (10.8 MPa vs 23.2 MPa). It seems that the rigidity of the  
 773 monomers is comparable at  $T < T_g$ , whereas at  $T > T_g$ , the molecular motion is responsible (for bisferulate), probably  
 774 due to the lower crosslinking density, and the presence of a linear alkyl chain (inducing free rotations). For the  
 775 networks obtained with DIFFA, the glassy modulus is higher for DGEBA (2.1 GPa) than for the bisferulate  
 776 (1.75 GPa), probably due to the higher aromatic density with DGEBA. Over the glass transition temperature, similar  
 777 trends with DA10 was observed.  
 778 Maiorana *et al.* performed screening of the EA of the n-alkyl bisferulates before glycidylation. Comparison between  
 779 EA was performed using the natural oestrogen, BPA, BPS and DGEBA (Figure 24).<sup>102</sup> The assay conducted was a  
 780 measure of the activity of the ER $\alpha$ . While BPA and BPS showed 60 % activity compared to the hormone E2, the n-  
 781 alkyl bisferulates did not show a significant activity compared to DGEBA or the vehicle. No dose-response effect  
 782 was measured in the studied concentration range.



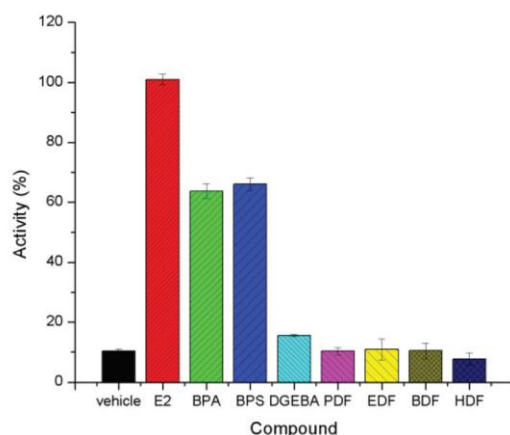


Figure 24 - In vitro activity comparison of alkyl bisferulates, from Maiorana *et al.*<sup>102</sup>

## 2. Bisferulate with amido linker

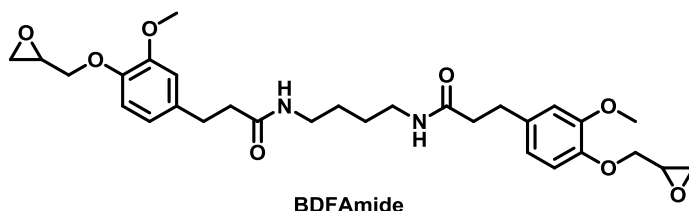
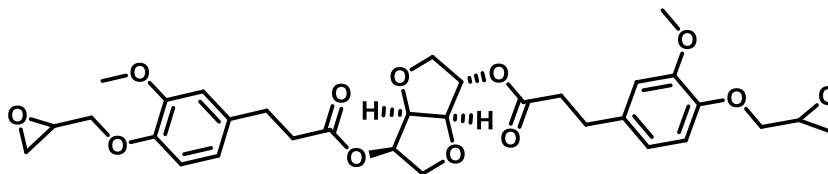


Figure 25 - Structure of the BDFAmide synthesized by Ménard *et al.*<sup>88</sup>

In the work of Ménard *et al.*, butanediamine was used as a linker for the synthesis of a bisferulate, which glycidylation affords a diepoxy monomer (Figure 25). After curing with DA10, IPDA and DIFFA, properties of the networks were evaluated against DGEBA systems. With DA10, the  $T_{d5\%}$  are respectively 297 °C for the bisferulate and 337 °C for DGEBA, which shows a better stability for the network that did not contain amide bonds. It was also observed that the stability of the ester-containing network was higher, which was unexpected since amide bond is considered thermally more stable. Char yield of the BDFAmide network was 18.2 % compared to 5.2 % for DGEBA. The  $T_g$  of the amide containing thermoset was 69 °C, which was lower than for DGEBA (98 °C). This can be due to a lower crosslinking density. It was also observed that the amide containing network has a higher  $T_g$  than the ester pendant (33 °C), probably due to the hydrogen-bonding ability of the amide moiety. Mechanical properties of the material were not evaluated due to the high melting point of the monomer. The measured  $T_g$  was 75 °C, half the value of DGEBA network. The IPDA/BDFAmide system lead to a  $T_{d5\%}$  of 282 °C (lower than DGEBA at 331 °C). The char yield was 18.2 %, higher than that of DGEBA (10.2 %). It can be noted that the char yield for IPDA-cured amide bisferulate was similar to DA10-cured network. The cycloaliphatic or linear aliphatic amine did not seem to have an influence on the char formation. The low thermal stability could most probably be due to incomplete curing.

Finally, the use of furfurylic diamine DIFFA led to a  $T_{d5\%}$  of 271 °C versus 301 °C for DGEBA, and a char yield of 23.7 % (14.8 % with DGEBA). The use of a furan-containing hardener increased the char yield globally, but it decreased the thermal stability as compared to the aliphatic amines (char formation is promoted by aromatic containing moieties, such as DIFFA). The  $T_g$  of 74 °C was similar to IPDA and DA10. The presence of furan rings should increase the rigidity; however, the crosslink density was decreased due to the structure of the DIFFA.

811 3. Bisferulate with isosorbide linker



812

813

Figure 26 - Structure of the isosorbide-based bisferulate epoxy monomer by Ménard *et al.*<sup>88</sup>

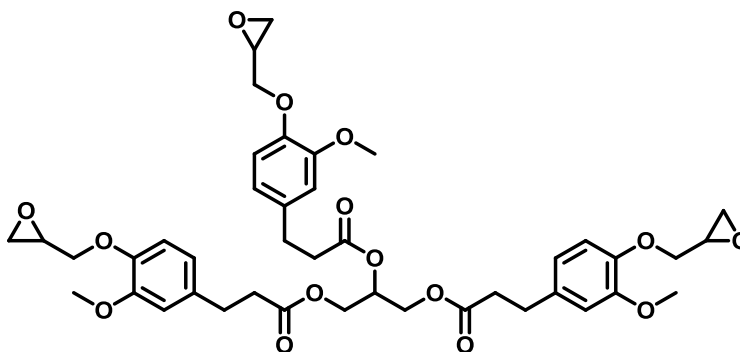
814

815 The bisferulate based on isosorbide linker synthesized by Ménard *et al.* also provided insight into the properties of  
816 bisferulate-based epoxides (Figure 26).<sup>88</sup> With all three hardeners, isosorbide-bisferulate networks had lower  
817 thermal stabilities (lower  $T_{d5\%}$ ) compared to DGEBA, but higher char yield due to the presence of the methoxy  
818 moiety. Glass transition temperature and alpha transition temperatures were also lower than DGEBA. Comparing  
819 with the other bisferulates, the  $T_g$  was lower than the amide linker, but higher than the linear ester linker (C4). But  
820 the glassy moduli with DA10 and IPDA were lower for DGEBA networks. The bicyclic linker provided significant  
821 higher rigidity to the networks, although the effect was counterbalanced by the crosslinking density when DIFFA  
822 was used, resulting in similar modulus (around 2.0 GPa). At  $T > T_g$ , the elastic modulus was lower for all the  
823 networks with the bisferulate than with DGEBA. Even if the bicyclic structure of isosorbide linker conferred an  
824 important rigidity, it seems that at high temperature, it does not impact the mobility of the chains in order to the  
825 elastic modulus high (also confirmed by the relatively low alpha transitions temperatures).  
826 The endocrine activity of the bisferulate and its glycidylether derivative was assessed.<sup>86</sup> The activity of the  
827 bisferulates at  $10^{-8}$  M was comparable to the one of the vehicle, meaning that the diol and the epoxy monomer did  
828 not show any specific activity. In addition, no dose-response activity was observed in a concentration range between  
829  $10^{-13}$  and  $10^{-5}$  M.

830

831 4. Trifunctional ferulic ester epoxy monomer

832



GTF

833

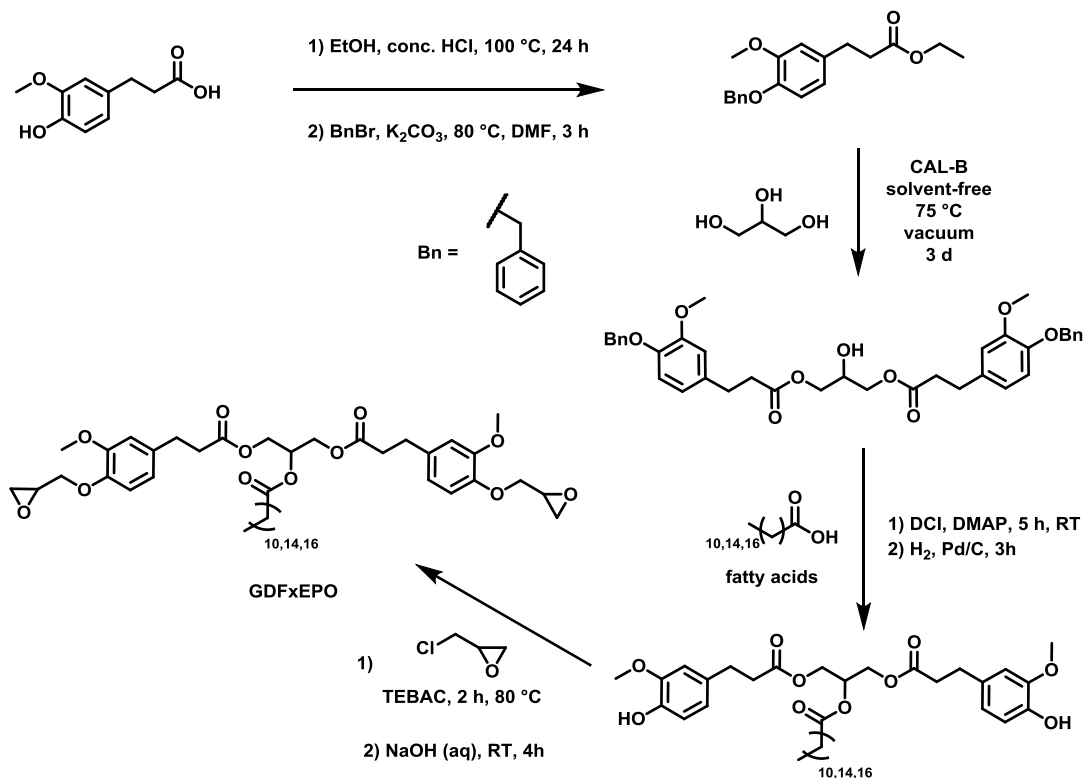
834 Figure 27 - Structure of the trifunctional ferulate ester (GTF) epoxy monomer synthesized by Ménard *et*  
835 *al.*<sup>88</sup>

836 Using glycerol as the linker between ferulate residues, Ménard *et al.* also provided data about the behaviour of a  
837 trifunctional monomer in different networks (Figure 27).<sup>88</sup> The glycerol-based triferulate GTF gave lower thermal  
838 stabilities than for DGEBA for all hardeners, but higher char yields. The higher crosslinking and aromatic density  
839 did not increase the thermal stability, mainly due to the presence of the fragile ester linkages, but as expected the  
840 higher aromatic density did improve the char formation. Glass transition and  $\alpha$  transitions were also lower with the  
841 glycerol-based monomer than with DGEBA with all the hardeners, namely 58 °C for DIFFA, 54 °C for DA10 and  
842 73 °C for IPDA (glass transition) compared with respectively 92, 98 and 150 °C for DGEBA. The same trend was  
843 observed for  $T_\alpha$ . Mechanical properties revealed different trends. With IPDA as the hardener, DGEBA and GTF had  
844 the same glassy modulus (1.7 GPa) and the elastic modulus was lower for GTF (16.4 MPa vs 21.0 MPa for  
845 DGEBA). With DA10, the glassy modulus was higher for GTF (2.4 GPa vs 1.0 GPa) whereas the elastic modulus  
846 was almost the same (around 23-24 MPa). With DIFFA, the glassy modulus was 1.7 GPa for GTF while with

847 DGEBA it was 2.1 GPa. The elastic modulus was very low for GTF (7.9 MPa), while it was 21.2 MPa for DGEBA.  
 848 It seems that in the case of DIFFA, increasing the crosslinking density improves the rigidity at the glassy plateau,  
 849 but not too beneficial for temperatures above  $T_g$ .

850  
 851  
 852

### 5. Bisferulate ester with side-chain containing linker



853

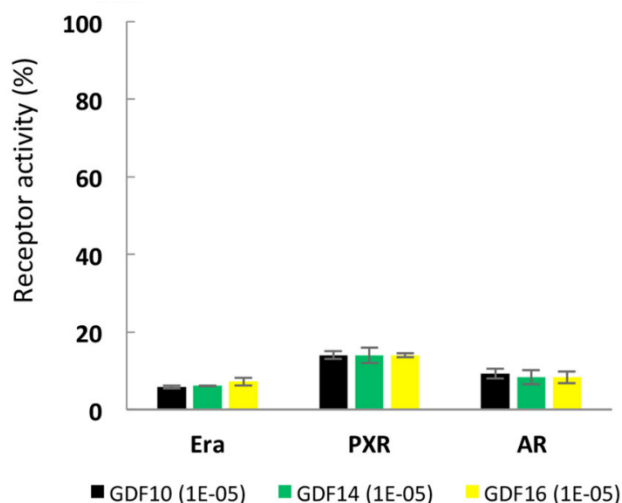
854

Figure 28 - Synthetic pathway for GDFxEPO monomers, by Hollande *et al.*<sup>103</sup>

855

856 Ferulic acid was also used to synthesize other diepoxides, based on a glycerol linker, but with the addition of a fatty  
 857 ester chain. The variation of the length of this fatty acid residue allowed Hollande *et al.* to study the influence of  
 858 hydrophobic properties on the degradation in acidic aqueous environment, and on the endocrine receptor activities  
 859 of the bisphenols (which is discussed later in this review).<sup>103</sup> All the monomers were denoted GDFxEPO with x  
 860 corresponding to the number of carbon of the fatty side chain (Figure 28). The monomers cured with DA10 led to  $T_g$   
 861 between 3 and 5 °C. As a comparison, the C4 bisferulate by Ménard *et al.* led to a  $T_g$  of 33 °C, and DGEBA/DA10  
 862 of 98 °C.<sup>88</sup> The addition of a fatty acid side-chain led to a dramatic decrease of the  $T_g$ , as the side-chain acts as a  
 863 plasticizer. The same trend was observed with the other hardeners: DIFFA cured GDFxEPOs led to  $T_g$  between 11  
 864 and 16 °C as compared to 32 °C for the C4 bisferulate and 92 °C for the DGEBA. For the IPDA-based networks, the  
 865  $T_g$  of the GDFxEPOs were between 18 and 23 °C, 51 °C for the C4 bisferulate and 150 °C for DGEBA. For all the  
 866 GDFxEPO, the char yields obtained range between 7 and 17 %, the highest obtained for DIFFA cured monomers.  
 867 These values were very close to the char yields obtained with DGEBA. Usually, the presence of the methoxy on  
 868 phenols tend to increase the char yields, but the presence of the fatty acid esters lower the aromatic density in the  
 869 networks, decreasing the char formation. Thus, the decrease in alkyl content increases the char in ferulic acid based  
 870 monomers with phenolic methoxy groups, it. The opposite phenomena is observed for DGEBA networks, since  
 871 there is no phenolic methoxy or long alkyl chains present in the structure. However, regarding degradation  
 872 temperatures (especially  $T_{d5\%}$ ), it was observed that for the GDFxEPOs, temperatures of 280 to 310 °C were  
 873 measured (300-330 °C for DGEBA). The fatty chains-containing bisferulates had slightly lower thermal stabilities  
 874 compared to the same networks with DGEBA. In overall, the plasticizing effect of the alkyl chains led to similar  
 875 thermal stabilities, with lower  $T_g$  values as compared to DGEBA networks.  
 876 Regarding the wettability and degradation in aqueous acidic conditions, all the thermosets were evaluated by  
 877 measuring the contact angle, and the weight loss during incubation in 3 M HCl aqueous solution at 60 °C, up to

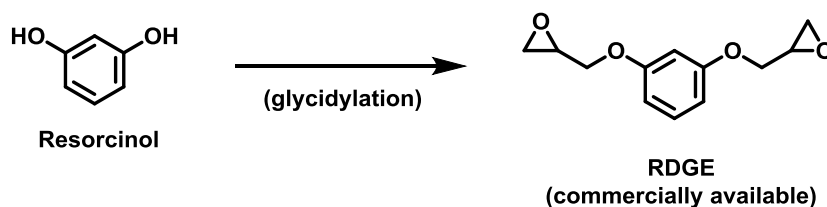
878 50 h. It was observed that, for all hardeners used, the water contact angle increased as the length of the fatty chain  
 879 increased. All the contact angles were measured between 60 and 90°, showing poor affinity with water. Hydrolytic  
 880 degradation was however faster for the shorter fatty acid chains. Complete degradation was observed for GDFxEPO  
 881 with x=10 after 50 h. No comparison with DGEBA was performed. And under alkaline conditions, barely any  
 882 degradation was observed for DGEBA/IPDA.<sup>102</sup>  
 883 The work of Hollande *et al.* also focused on the determination of oestrogenic affinity of the prepared bisferulates.<sup>103</sup>  
 884 Two other hormone receptors were also tested, namely PXR, a steroid receptor and AR, an androgen receptor. The  
 885 concentrations tested were in the range 10<sup>-14</sup> to 10<sup>-5</sup> M. At these concentrations, an oestrogen receptor activity was  
 886 recorded for the E2 hormone, and for BPA. No significant activity was observed for the GDFx (Figure 29). At  
 887 higher concentration, 10<sup>-5</sup> M, no abnormal receptor activity was measured for all the GDFx as well as other  
 888 receptors (PXR and AR). Also no antagonist activity of the GDFx was recorded for all the receptors.  
 889



890  
 891 Figure 29 – *In vitro* activity of the GDFxEPO diols against several hormone receptors by Hollande *et al.*<sup>103</sup>

892 VI. Resorcinol

893



894

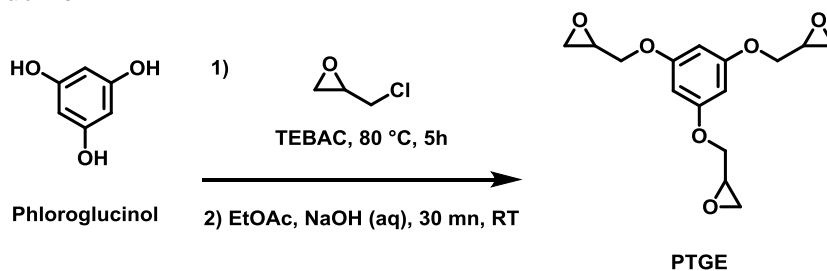
895 Figure 30 – Structures of Resorcinol and its diglycidylether derivative

896 Diglycidylether of resorcinol (RDGE, Figure 30) is a diepoxy monomer that has been widely reported in the  
 897 literature. It is composed of a monoaromatic phenolic compound, bearing two substituted phenolic hydroxyls,  
 898 leading to the diepoxide. This monomer has found a large range of applications, and appears in several patents. The  
 899 specific position of the two phenolic moieties of resorcinol gives high reactivity to the monomer. However,  
 900 resorcinol, that is the parent compound of the diglycidylether of resorcinol, has only been evaluated since 2016 as  
 901 regards to endocrinal disruption activity. It seems that resorcinol may have an effect on thyroid.<sup>104</sup> Recently, the  
 902 French health agency ANSES (Agence nationale de sécurité sanitaire alimentation, environnement, santé), has  
 903 recommended its classification as a SVHC for its endocrine disruption properties.<sup>105</sup> Since March 2022 the EU  
 904 regulation commission has added RDGE to the list of carcinogenic and mutagenic substances.<sup>106</sup>  
 905 Resorcinol based diepoxy monomer and its homopolymer, are used in all kinds of applications given the existence  
 906 of more than 1200 patents and 350 research journal articles. Among these articles, only a few of them give  
 907 qualitative data about thermosetting epoxy, cured with standard amine hardeners. For example, Mattar *et al.* used  
 908 HMDA and obtained thermosets with a  $T_g$  of 80 °C and a  $T_a$  of 110 °C.<sup>107</sup> The modulus at the glassy plateau was 2.5  
 909 GPa, and at the rubbery plateau, it was 20.52 MPa. The presence of the aromatic ring inside the network led to

910 relatively high transition temperatures. As a comparison, DGEBA/HMDA network showed an alpha transition at  
 911 118 °C and the E' at the rubbery state was 27.4 MPa.<sup>108</sup> The close values between DGEBA and resorcinol  
 912 diglycidylether showed that the higher crosslink density with the resorcinol gave close thermomechanical properties  
 913 to DGEBA thermoset, even if less aromatics were in the monomer structure. In a study evaluating the effect of the  
 914 geometry of the monomer in epoxy-amine networks, Riad *et al.* prepared several thermosets using resorcinol  
 915 diepoxy, cured with several aniline derivatives.<sup>109</sup> They obtained high  $T_g$  with monoaromatic diamines, between 129  
 916 and 148 °C. They also obtained a glass transition temperature of 175 °C with a diamine containing two benzene  
 917 rings in its structure. The rigidity of this latter hardener, and the higher aromatic density of the obtained network  
 918 leads to higher  $T_g$ . As mentioned earlier resorcinol and its derivatives are not recommended and are considered as  
 919 endocrine disruptor.

## 920 VII. Phloroglucinol

### 921



922

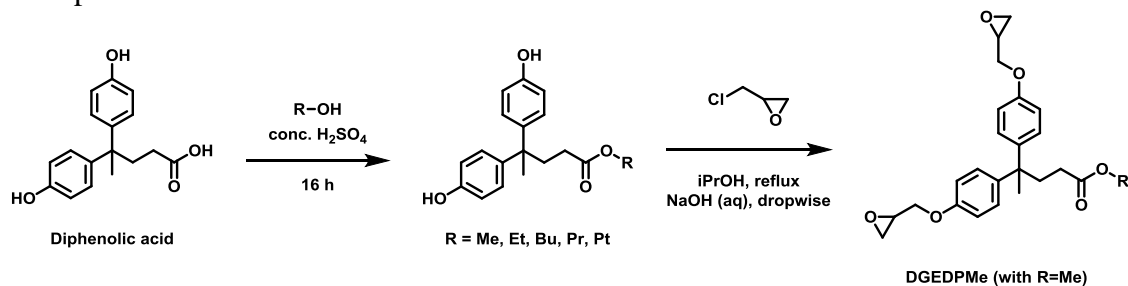
923 Figure 31 - Synthesis of PTGE according to Ménard *et al.*<sup>85</sup>

924 Phloroglucinol is a biobased phenolic compound bearing 3 phenolic hydroxyls. The structure of phloroglucinol can  
 925 be found in tannins.<sup>110</sup> This phenolic compound is also a widely used drug, especially for the symptomatic treatment  
 926 of abdominal pain.<sup>111</sup> The glycidylation reaction leads to a triepoxy monomer (Figure 31), containing generally  
 927 oligomers, due to the high reactivity of the phenol. More than 70 patents mention the use of PTGE (phloroglucinol  
 928 triglycidyletherin fiber-reinforced composites for medical prosthesis, binder for cork composites, anti-fouling  
 929 membranes and adhesives.

930 Ménard *et al.* used PTGE cured with several amine hardeners, and compared the thermomechanical properties with  
 931 and without the addition of a flame retardant.<sup>85</sup> The three curing agent used were DA10, DIFFA and IPDA. The  
 932 glass transition temperature of PTGE/IPDA network was 177 °C, compared to 157 °C for DGEBA/IPDA. This can  
 933 be explained by the higher functionality of the epoxy monomer, leading to higher  $T_g$  via limiting the chain mobility  
 934 in the network. Thus, despite the lower number of aromatic rings in the epoxy monomer compared to DGEBA, the  
 935  $T_g$  value is higher. Similar trend was observed when the two other curing agents were used. The PTGE/DIFFA  
 936 network has a  $T_g$  of 134 °C, whereas the DGEBA/DIFFA network has a  $T_g$  of 92 °C, and the PTGE/DA10 network  
 937 has a  $T_g$  of 137 °C, compared to 98 °C for DGEBA/DA10.<sup>88</sup> The thermal stability of PTGE/IPDA was however  
 938 lower under nitrogen, with a  $T_{d10\%}$  of 306 °C compared to 369 °C for DGEBA/IPDA. The lower aromatic content of  
 939 the monomer may explain the reported lower stability. Char formation was higher for PTGE networks compared to  
 940 DGEBA. The higher crosslinking density seems to be beneficial for the char formation using this epoxy monomer. It  
 941 can also be noted that without any fire-retardant additives, the PTGE networks display lower heat release rate.  
 942 However, the lower thermal stability of all the networks lead to fuel gas emissions at temperatures lower than for  
 943 DGEBA/IPDA thermoset (around 300 °C versus nearly 400 °C for DGEBA/IPDA). Phloroglucinol is known to  
 944 have an effect on human health since it is widely used as an anti-abdominal pain medication.<sup>111</sup> However, some  
 945 studies suggest the phloroglucinol to be potentially disruptor of thyroid receptors.<sup>112</sup> More studies are required to  
 946 verify the effect of this compound on the endocrine system.

947

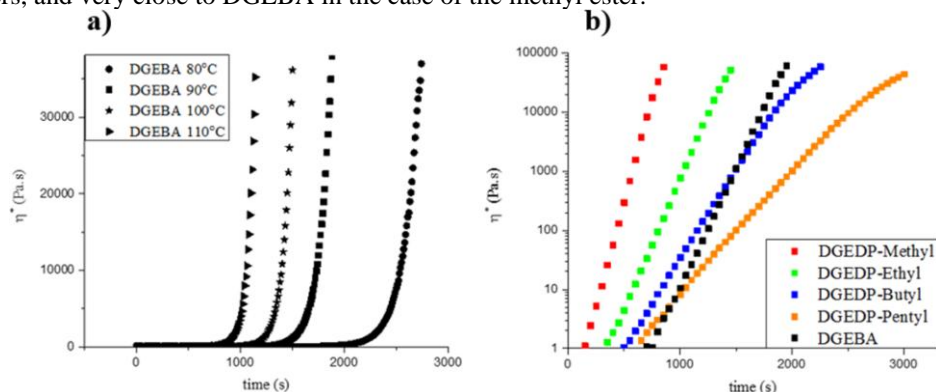
948 VIII. Diphenolic acid



949

950 Figure 32 – Synthesis of diphenolic acid ester based epoxy monomers according to Maiorana *et al.*<sup>113</sup>

951 Levulinic acid is a biobased compound that can be obtained from cellulose. It is a linear carboxylic acid containing a  
 952 methyl ester moiety. The condensation of two equivalents of phenol with the ester leads to a diphenolic compound  
 953 that is very similar to BPA, but instead of having two methyl moieties between the aromatic rings, the linker is  
 954 composed of a methyl and a carboxylic acid terminated alkyl chain. After esterification, Maiorana *et al.* obtained  
 955 several monomers with different length of side chain esters (Figure 32).<sup>113</sup> The glycidylation of these different  
 956 diphenols led to several monomers noted DGEDPMe for methyl, DGEDPEt for ethyl, and two others with butyl  
 957 (Bu) and pentyl (Pt) side chains. The viscosities of the pure monomers were measured and compared to DGEBA, at  
 958 25 °C. All the monomers displayed higher viscosities (12 to 792 Pa·s), compared to DGEBA (4 Pa·s). The methyl  
 959 ester monomer had the highest viscosity (792 Pa·s), with several orders of magnitude above all the other esters (12  
 960 to 63 Pa·s), probably due to a higher oligomerisation degree, evidenced by a higher deviation of the EEW compared  
 961 to the other esters. It was also mentioned that from ethyl ester, viscosity decreases with the increased chain length.  
 962 All the monomers were cured with IPDA and compared with DGEBA. The glass transition temperatures (from the  
 963 peak of loss modulus) decreased as the alkyl chain increased, from 158 °C (DGEDPMe) to 86 °C (DGEDPPt), and  
 964 were lower than for DGEBA (165 °C). Storage moduli were measured at 25 °C. For the methyl ester, this was  
 965 higher than for DGEBA (2640 MPa for DGEBA and 3278 MPa for DGEDPMe). For all the other monomers, the  
 966 storage moduli were lower, and decreased with the increase in the chain length. Tensile properties were also  
 967 measured. Higher tensile strength were measured for the esters between Me and Bu, and it was similar between Pt  
 968 and DGEBA thermosets. Strain at break was higher with Et and Pt (respectively 9.3 and 11 %), lower for Me (4.6  
 969 %) and similar with Bu (8.3 %), compared to DGEBA/IPDA (8.7 %). From these mechanical properties, it can be  
 970 seen that the presence of the methyl ester does not act as a plasticizer, contrary to longer alkyl chains, as it is shown  
 971 by storage moduli and  $T_g$  decreasing with the increase in the ester length. The different behaviour of the methyl ester  
 972 derivative was mainly due to the presence of triglycidylated products. During the synthesis of the monomer, the  
 973 formation of a carboxylate resulted in addition of some epichlorohydrin on the carboxylate residue in addition to the  
 974 phenols. The presence of trifunctional epoxide monomer, led to an increase of the mechanical properties. This can  
 975 also explain the lower elongation at break, due to a more tightly crosslinked network, hence the brittleness. The  
 976 thermal stabilities of the networks were also assessed. The  $T_{d10\%}$  were measured. These were similar for all the  
 977 esters, ranging from 361 to 363 °C, and slightly lower than for DGEBA (378 °C). Char yields were similar for all  
 978 the materials considered, between 10 and 13 %. These results show that the mechanical properties are very similar  
 979 for all the esters, and very close to DGEBA in the case of the methyl ester.



980

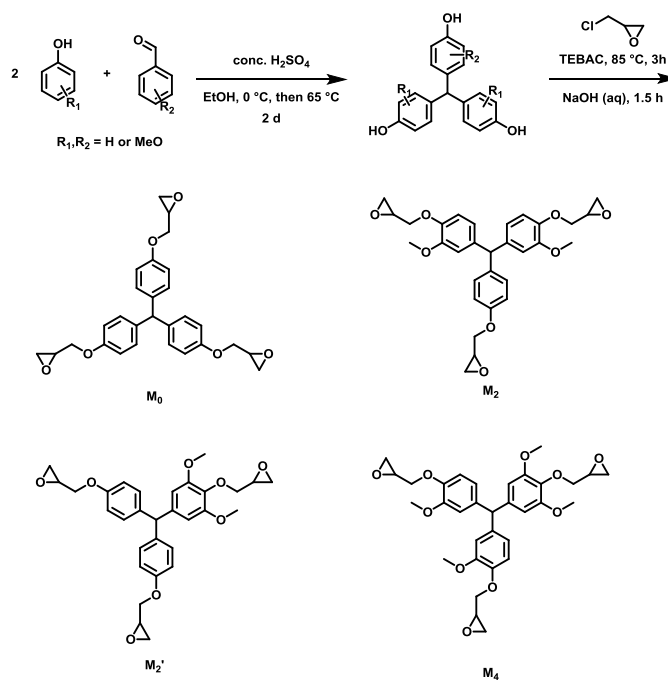
981 Figure 33 - Evolution of the complex viscosity as a function of cure time for (a) DGEBA at different  
 982 temperatures (y-axis linear scale). (b) DGEBA and DGEDP epoxies studied herein at 90 °C cure  
 983 temperature (y-axis log scale). Reproduced from Patel *et al.*<sup>114</sup>

984 Chemorheology of IPDA/DGEDP esters was also studied, and compared with DGEBA, in the work of Patel *et al.*,  
 985 as depicted in Figure 33.<sup>114</sup> Complex viscosities of formulations at 90 °C were determined, and it was shown that the  
 986 viscosity of the Me and Et esters increased faster than all the other formulations, including DGEBA. The induction  
 987 time in the rise of viscosity was longer for Bu and Pt, but lower than for DGEBA. However, once the viscosity  
 988 started to rise for DGEBA, the rate of the increase was faster for DGEBA than for the Pt and Bu esters. Moreover, a  
 989 slower rate of viscosity increase was observed for the pentyl ester. These data in addition with the kinetic studies,  
 990 lead to the conclusion that the pentyl ester monomer could be a good substitute for DGEBA for infusion moulding  
 991 applications, whereas the high reactivity of the methyl ester monomer (also containing trifunctional monomers)  
 992 could be interesting for adhesive applications, for which a fast reaction time is required. McMaster *et al.* cured these  
 993 monomers with IPDA, in addition to a propyl ester monomer, and evaluated their dielectric properties.<sup>115</sup>  
 994 Interestingly, they found that the propyl ester has a high dielectric constant (5.26 at 0.05 Hz), higher than the Bu and  
 995 Et esters, and especially higher than DGEBA. The DGEDPMe has higher dielectric constants, but as already  
 996 mentioned earlier, the thermomechanical properties are less consistent. The thermomechanical properties of the  
 997 DGEDPPr were also measured, with a  $T_g$  of 129 °C, strain at break of 8.3 % and tensile strength of 58 MPa. These  
 998 epoxy thermosets could be used as structural capacitors. Gao *et al.* studied the DGEDPMe cured with DDM.<sup>116</sup> They  
 999 measured a  $T_g$  of 153 °C for DGEDPMe/DDM, compared to 164 °C for DGEBA/DDM. The thermal stabilities of  
 1000 the thermosets were also quite similar under air, especially with the measure of the temperature at the onset of  
 1001 degradation which was 315 °C for DGEBA and 310 °C for DGEDPMe. The residual weight at 700 °C was slightly  
 1002 higher for DGEDPMe (2.7 % compared to 0.1 % for DGEBA). Impact strength, tensile strength and elongation at  
 1003 break were also very similar between both epoxy networks. Regarding flame retardant properties, the heat release  
 1004 rate peak was lower for DGEDPMe (520 kW·m<sup>-2</sup>) compared to DGEBA (711 kW·m<sup>-2</sup>), but the total heat release was  
 1005 similar, as well as smoke emission parameters (such as average smoke production rate, total smoke release or  
 1006 average CO production rate) were determined. Up to now the diphenolic acid based epoxy monomers have mainly  
 1007 been used in composites with different type of fillers such as cellulose nanocrystals.<sup>117</sup> Some reports have described  
 1008 the endocrine activity of the diphenolic acid derivatives, with R=H. Some research articles have concluded that  
 1009 diphenolic acid did not present any activity over several receptors, such as oestrogen receptor or androgen  
 1010 receptor.<sup>118</sup> However, some others *in silico* research suggest that diphenolic acid could be a weak ER $\alpha$  agonist.<sup>119</sup>  
 1011 More studies are required to assess the complete toxicological profile of this bisphenol. None of the ester derivatives  
 1012 have been evaluated for potential endocrine activity.

## 1013 IX. Triphenols

1014

1015



1017 Figure 34 - Synthetic scheme and structures for the obtention of triphenol epoxy monomers from Zhao *et*  
 1018 *al.*<sup>53</sup>

1019 Zhao *et al.* used the condensation of aromatic aldehydes on phenols in order to obtain several triphenols, bearing  
 1020 methoxies (Figure 34).<sup>53</sup> From all the synthesized triphenol, they used four of them for glycidylation reactions, and  
 1021 obtained triepoxy monomers. Curing was performed with DETA, and thermomechanical properties were measured.  
 1022 All the formulations presented low temperature reactivity, as monitored by DSC. For all the monomers, the curing  
 1023 exotherm started around 40 °C with a peak around 80 °C. The obtained networks were characterized using DMA  
 1024 and TGA (Table 3).

1026 Table 3 - Thermal and mechanical properties of thermosets studied by Zhao *et al.*<sup>53</sup>

Epoxy monomer	$T_{\alpha}$ (°C)	$E_{30}'$ (MPa)	$T_{d5\%}$ (°C)	Char yield (%)
M <sub>0</sub>	132	2745	257	20
M <sub>2</sub>	125	2598	206	17
M <sub>2'</sub>	120	2249	218	18
M <sub>4</sub>	118	2477	184	14
DGEBA	100	2042	305	8

1027

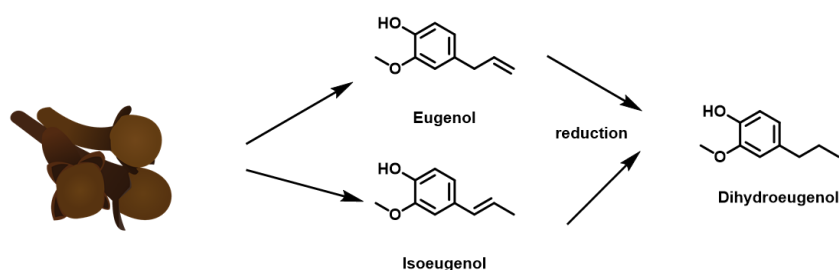
1028 All the results were compared to DGEBA thermoset, using the same amine hardener. As expected, alpha transitions  
 1029 temperatures were higher compared with DGEBA. Indeed, the higher rigidity of the monomers, due to their  
 1030 structures and aromatic densities, led to higher transition temperatures. Plus, the use of trifunctional monomers  
 1031 usually give higher transition temperatures and higher glassy moduli, due to a high crosslink density. The presence  
 1032 of methoxies lowered the values of transition and Young moduli. Thermal stability was also affected by the presence  
 1033 of the methoxy moieties. As expected, increasing the methoxy content, reduced the thermal stability. BPA-based  
 1034 thermoset in the absence of such methoxies, degrade at higher temperatures. Char yield however was higher for the  
 1035 triphenolic monomer based epoxides. The increase in char yields could be attributed to the increase in the aromatic  
 1036 density (compared to DGEBA). Surprisingly, the increase in methoxy functionality did not lead to an increase in  
 1037 char yield. In this case, the reduction of char yield with increasing methoxy content could be attributed to a lower  
 1038 crosslinking density. The steric hindrance brought by the methoxy groups may have a higher effect on the network  
 1039 structure, leading to reduced mechanical properties, compared to the doping effect on the char yield, as char  
 1040 formation is also highly dependent on the crosslinking density.

1041 Tensile tests of these thermosets, and all the triphenol-based networks displayed similar maximum stress  
 1042 (74.9–80.0 MPa), and elongation at break of 2.55–2.68 %. As a comparison, DGEBA/DETA network showed a  
 1043 maximum stress of 62.2 MPa and elongation at break of 3.56 %. The triphenol networks showed a higher rigidity  
 1044 and a higher brittleness, due to the crosslinking density. The only evaluated compound, M<sub>0</sub> (under commercial name  
 1045 of Tactix 742.<sup>120</sup>) did not show any strong activity on the receptor in competitive binding assay against ER $\alpha$ .<sup>121</sup>  
 1046 None of the other triphenol compounds have been evaluated so far. The work of Hong *et al.* predicts the binding  
 1047 affinity of a triphenol compound where the three phenols bear a methoxy group on the ortho position.<sup>82</sup> The  
 1048 compound has been predicted to be an ER $\alpha$  binder, with a moderate prediction confidence. However, the model  
 1049 could not calculate the quantitative affinity, since the monomer did not fit the receptor in the molecular docking  
 1050 calculations. The authors thus concluded that it is unlikely that this monomer would have a real affinity for the  
 1051 receptor.

1052

## 1053 X. Eugenol

1054



1055

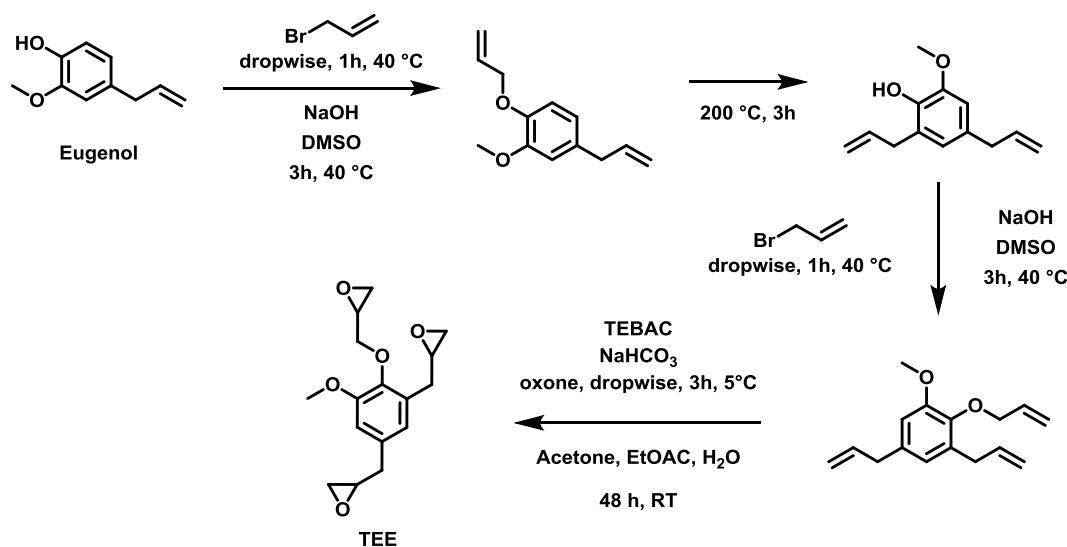
1056 Figure 35 - Structure of eugenol and isoeugenol from cloves, and their reduction to dihydroeugenol.  
 1057 These structures are epoxy monomer precursors.



1058 Eugenol is a natural phenol, one of the main constituents of clove oil. Its structure is a phenol bearing a methoxy  
 1059 moiety and an allyl moiety (Figure 35). It can also be obtained from the enzymatic hydrolysis of lignocellulose. It is  
 1060 used in perfumes, as food additive as well as in pharmaceuticals.<sup>122</sup> Eugenol can be easily modified to obtain diepoxy  
 1061 monomers, and its derivatives have been used as a starting compound, for the synthesis of thermoset polymers.  
 1062 Endocrine activity of eugenol has been assessed especially in the context of the use of essential oils that have gained  
 1063 a growing interest in the past years. Howes *et al.* looked at the activity of eugenol on the oestrogen and androgen  
 1064 receptors, using enzymatic tests( modified enzymes expressing the human receptors).<sup>123</sup> In this work, eugenol did  
 1065 not show any activity against the androgen receptor. However, it did show an activity on the oestrogen receptor, but  
 1066 at high concentration compared to the E2 hormone. It also showed an activity towards a competitive displacement  
 1067 bioassay, at high concentration ( $10^4$  to  $10^5$  higher than 17  $\beta$ -oestradiol). Overall, eugenol showed an anti-oestrogenic  
 1068 activity.

### 1069 1. Tri-epoxy-eugenol

1070  
1071



1072

1073

Figure 36 - Synthesis of TEE from Guzman *et al.*<sup>124</sup> and Yoshimura *et al.*<sup>125</sup>

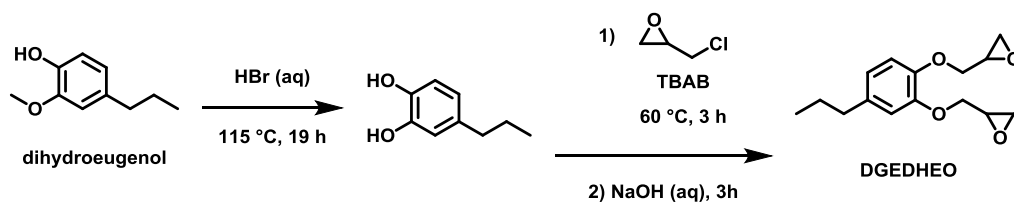
1074 A triepoxy can be obtained from eugenol, by a multi-step process, as depicted in Figure 36.<sup>124,125</sup> First, eugenol is  
 1075 reacted with allyl bromide, leading to the alkylation of the phenol moiety. Then, a Claisen rearrangement can be  
 1076 performed via a thermal activation. The allyl moiety grafted onto the phenol is rearranged into an allyl moiety, but  
 1077 on the ortho position of the aromatic ring. The further allylation of the now free phenolic moiety leads to a triallyl  
 1078 monomer, since eugenol is naturally bearing an allyl moiety on para position. The oxidation of the three allyl  
 1079 moieties leads to a triepoxy monomer (triepoxy eugenol (TEE)). Santiago *et al.* used this trifunctional monomer in  
 1080 order to make thermosets, with IPDA and Jeffamine D400 as the hardeners.<sup>126</sup> The results were also compared with  
 1081 the corresponding DGEBA networks.

1082 With Jeffamine as hardener, the TEE displayed a  $T_g$  of 59 °C, which is slightly higher than with DGEBA ( $T_g$  = 50  
 1083 °C). With IPDA, a more rigid hardener, the  $T_g$  of TEE was 174 °C. These high  $T_g$  values are mainly because the  
 1084 trifunctional TEE monomer, leading to highly crosslinked networks. This effect is favoured with the rigid diamine  
 1085 IPDA, compared to the use of the polypropylene-based Jeffamine. Dynamic mechanical analysis showed a similar  
 1086 trend. The Young's modulus at the rubbery state were 12 MPa for DGEBA/Jeffamine, 35 MPa for TEE/Jeffamine,  
 1087 45 MPa for DGEBA and 214 MPa for IPDA. Tensile tests showed that the elongation at break was lower for the  
 1088 TEE networks as compared to DGEBA. The higher crosslinking density resulted in brittle material as the elasticity  
 1089 was reduced.

1090 As observed with methoxy-containing monomers, degradation temperatures of TEE networks were lower than for  
 1091 DGEBA networks, under nitrogen. Using Jeffamine as the hardener, DGEBA network had a  $T_{d5\%}$  of 354 °C,  
 1092 whereas the value for the TEE network was 314 °C. The same trend was observed with IPDA, with 348 °C for  
 1093 DGEBA, and 317 °C for TEE. However, the char yield was higher with TEE, thanks to the higher crosslinking  
 1094 density, and the contribution of the methoxy groups to the char formation. The obtained char yield were 7.6 % for  
 1095 DGEBA/Jeffamine and 15.4 % for TEE/Jeffamine, while with IPDA, the DGEBA had a char yield of 9.6 % as  
 1096 compared to 23.5 % when using TEE.

1097  
1098  
1099

## 2. Dihydroeugenol diepoxy



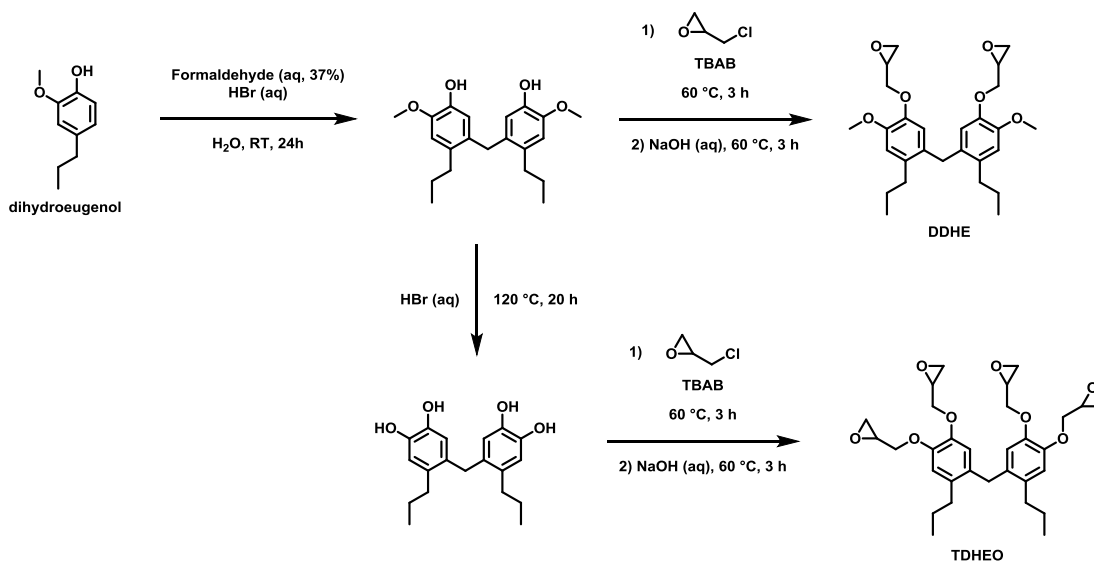
1100  
1101

Figure 37 - Synthesis of DGEDHEO from Zhao and Abu-Omar<sup>127</sup>

1102 Dihydroeugenol can be obtained from the hydrogenation of the double bond of eugenol, or *via* a catalytic  
1103 depolymerisation of lignin, over a Zn/Pd/C catalyst. Zhao *et al.* used dihydroeugenol, and performed an ortho  
1104 demethylation, in order to generate another phenolic hydroxyl, from the methoxy moiety.<sup>127</sup> The glycidylation of  
1105 this catechol derivative leads to a diepoxy monomer (Figure 37). The authors studied the curing reaction of the  
1106 diepoxy monomer with DETA, used dihydroeugenol or the catechol derivative as catalysts, and prepared composites  
1107 using nanoclay. They obtained low temperature curing, with fast kinetics, with a full conversion observed by DSC.  
1108 For example, 100 % conversion was obtained in less than 60 minutes. Post curing at 95 °C was however performed  
1109 to ensure complete curing. DMA performed on the cured networks revealed a  $T_g$  of 40 °C, which is much lower than  
1110 the reported data for DGEBA (100 °C). The Young's modulus of the DGEDHEO/DETA was 175 MPa, which is  
1111 quite low, compared to the value reported for DGEBA/DETA (2 GPa). The lower transition temperature and lower  
1112 modulus could be due to the low aromatic density with a mono-phenolic compound, where the propyl moiety act as  
1113 a plasticizer in the network, but also causes steric hindrance. Thermal properties were evaluated by TGA, with a  
1114  $T_{d5\%}$  of 190 °C, and a char yield of 3 % at 500 °C under nitrogen. These low values can be explained by the use of an  
1115 aliphatic amine, leading to a low aromatic content in the network. As a comparison, DGEBA-DETA thermosets  
1116 gave  $T_{d5\%}$  of 305 °C and a char yield of 8 %.<sup>53</sup> The epoxy-amine network with DGEDHEO has been used as a  
1117 matrix forming material in composites containing nanoclay as filler.<sup>127</sup>

1118  
1119  
1120

## 3. Bis-eugenyls with a methylene linker



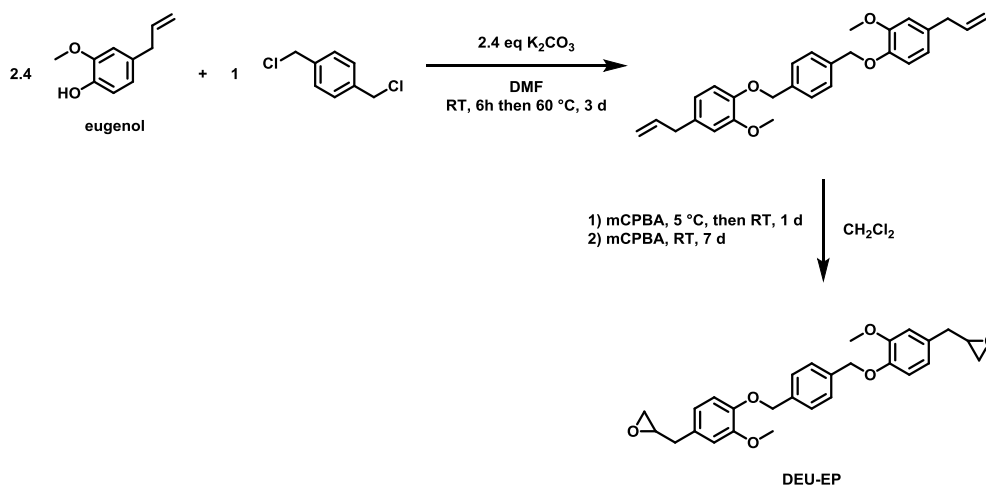
1121  
1122  
1123

Figure 38 - Synthetic pathway for the synthesis of DDHE and TDHEO monomers from Zhao and Abu-Omar<sup>128</sup>

1124 In a study, Zhao and Abu-Omar used two dimers obtained from dihydroeugenol.<sup>128</sup> First, dimerization of  
1125 dihydroeugenol leads to a bisphenol, which glycidylation results in a diepoxy monomer (DDHE, Figure 388). The  
1126 product from *o*-demethylation of dihydroeugenol, after dimerization, leads to a biscatechol compound, which after  
1127 glycidylation results in a tetraepoxy monomer (TDHEO, Figure 38).

1128 showed a  $T_{\alpha}$  of 70 °C for the DDHE/DETA network, and of 84 °C for the TDHEO/DETA network. The difference  
 1129 between the alpha transitions of both thermoset can mainly be explained by the higher functionality of the TDHEO  
 1130 network. Compared to DGEBA/DETA ( $T_{\alpha} = 100$  °C) these transitions are lower.<sup>53</sup> This is explained especially by  
 1131 the effect of the propyl moiety, which can either induce a plasticizing effect, or a steric hindrance in the network. In  
 1132 addition, the Young's moduli at the glassy state were 551 MPa for DDHE compared to 1441 MPa for TDHEO,  
 1133 indicating the important effect of the crosslinking density on the mechanical properties. The calculated crosslinking  
 1134 densities were 1.39 mol·dm<sup>-3</sup> for DDHE and 3.28 mol·dm<sup>-3</sup> for TDHEO (2 GPa for the DGEBA/DETA network)  
 1135 which are higher than for both of the eugenol-derived networks. Regarding thermal stability under inert atmosphere,  
 1136 both TDHEO and DDHE thermosets had comparable  $T_{d5\%}$ , respectively 245 and 235 °C, and between 10 and 11 %  
 1137 char yields. DGEBA/DETA network had a better thermal stability, with a  $T_{d5\%}$  of 305 °C and a char yield of 8 %. As  
 1138 evidenced often, the presence of the methoxy moieties lowers the degradation temperatures, but increases the char  
 1139 formation. Koelewijn *et al.* synthesized different bisphenols from lignin derivatives, in order to further synthesize  
 1140 polycarbonates and cyanate ester resins.<sup>129</sup> These bisphenols were mainly guaiacol derivatives, which were coupled  
 1141 in *meta* position. Among all monomers investigated in their work, the m-m'-4-n-propylguaiacol corresponded to the  
 1142 bisphenol based on dihydroeugenol reported by Zhao and Abu-Omar.<sup>128</sup> The different bisphenols were evaluated in  
 1143 vitro, and compared with BPA and the E2 hormone. Results using E2 as the reference showed that the synthesized  
 1144 bisphenol has a lower induction potential (maximum 0.67 relative to E2), and at higher concentrations (around 10<sup>-6</sup>  
 1145 M compared to 10<sup>-11</sup> M for E2). These preliminary results should be confirmed by more type of bioassays, as well as  
 1146 in vivo experiments.

#### 1147 4. Bis-eugenyl with aromatic ether spacer



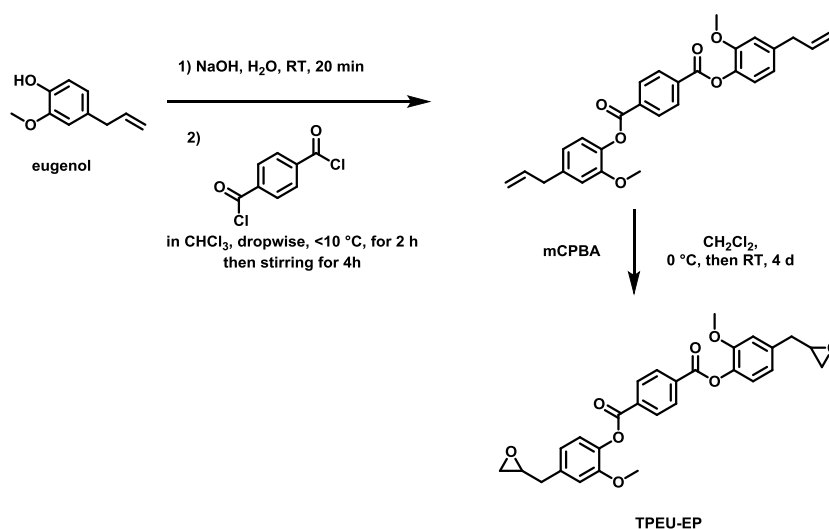
1152 Figure 39 - Synthesis of dieuogenyl monomer DEU-EP from Wan *et al.*<sup>48</sup>

1153 A diepoxy monomer was synthesized by Wan *et al.* using a dichloroxylylene, reacted with the phenol.<sup>48</sup> This led to  
 1154 an etherified dieuogenyl, containing an additional aromatic cycle. The epoxidation of the allyl bond of eugenol  
 1155 residues was then performed using *m*CPBA, in order to afford the diepoxidized monomer DEU-EP (Figure 39).  
 1156 Curing was performed using diaminodiphenylmethane hardener (DDM) and was compared with the DGEBA/DDM  
 1157 system. The curing was followed by DSC, and the crosslinking took place after successive melting of the hardener,  
 1158 and the diepoxy monomer. The peak maxima of the heat flux rate was nearly at the same temperature, *i.e.* 161 °C  
 1159 with DGEBA and 164 °C with DEU-EP. Isothermal curing kinetics revealed that, even if the total enthalpy of the  
 1160 curing reaction was close in both systems, a longer curing time was necessary to obtain 100 % conversion at 140 °C  
 1161 for eugenol-based monomer. This can be explained by a higher steric hindrance due to the presence of the methoxy  
 1162 moieties from eugenol residues. The mechanical properties were also investigated and compared, with a  $\tan \delta$  peak  
 1163 at 154 °C with DGEBA/DDM, and 114 °C with DEU-EP network. Even if the eugenol-based monomer had a higher  
 1164 aromatic density, the crosslink density of the material was lower, as the ether bond of the linker between eugenyls  
 1165 allowed a better motility of the chains, compared to DGEBA network. The crosslinking density was calculated to be  
 1166 2285 mol·m<sup>-3</sup> for DGEBA and 1346 mol·m<sup>-3</sup> for DEU-EP, confirming the hypothesis. However, the storage moduli  
 1167 at the glassy plateau revealed that the dieuogenyl epoxy network was more rigid and stiff at 30 °C, with values of 362  
 1168 MPa for DEU-EP/DDM, and 257 MPa for DGEBA/DDM. At temperatures lower than the  $T_{\alpha}$  the interaction  
 between the polymer chains in the network seem to have a stronger effect, accompanied by the aromatic density.

1169 Regarding the thermal stabilities, a slightly lower thermal stability was observed for the dieugenyl-based network.  
 1170 For the eugenol-based network, the  $T_{d5\%}$  under nitrogen was 341 °C (compared to 379 °C for DGEBA). The char  
 1171 yield was higher than with DGEBA (38 % as compared to 18 %). Flammability tests were also performed using a  
 1172 microscale combustion calorimeter, with a total heat release of 16 kJ·g<sup>-1</sup> for dieugenyl network and 27 kJ·g<sup>-1</sup> for  
 1173 DGEBA/DDM. The peak temperature of heat release rate was similar, attained at 410 °C for DGEBA, compared to  
 1174 406 °C for eugenol containing network. However, the peak heat release rate was 447 W·g<sup>-1</sup> for DGEBA network,  
 1175 compared to 201 W·g<sup>-1</sup> for the DEU-EP thermoset. In general, the eugenol-based diepoxy network had lower  
 1176 flammability, even if degradation happens at slightly lower temperature. Horizontal burning tests of the eugenol-  
 1177 based network showed that they were able to self-extinguish after burning for 10 seconds. This value for the  
 1178 DGEBA network was above 60 seconds.

## 1180 5. Bis-eugenyl with aromatic ester spacer

1181



1182

1183 Figure 40 - Synthesis of dieugenyl monomer with aromatic ester spacer from Wan *et al.*<sup>130</sup>

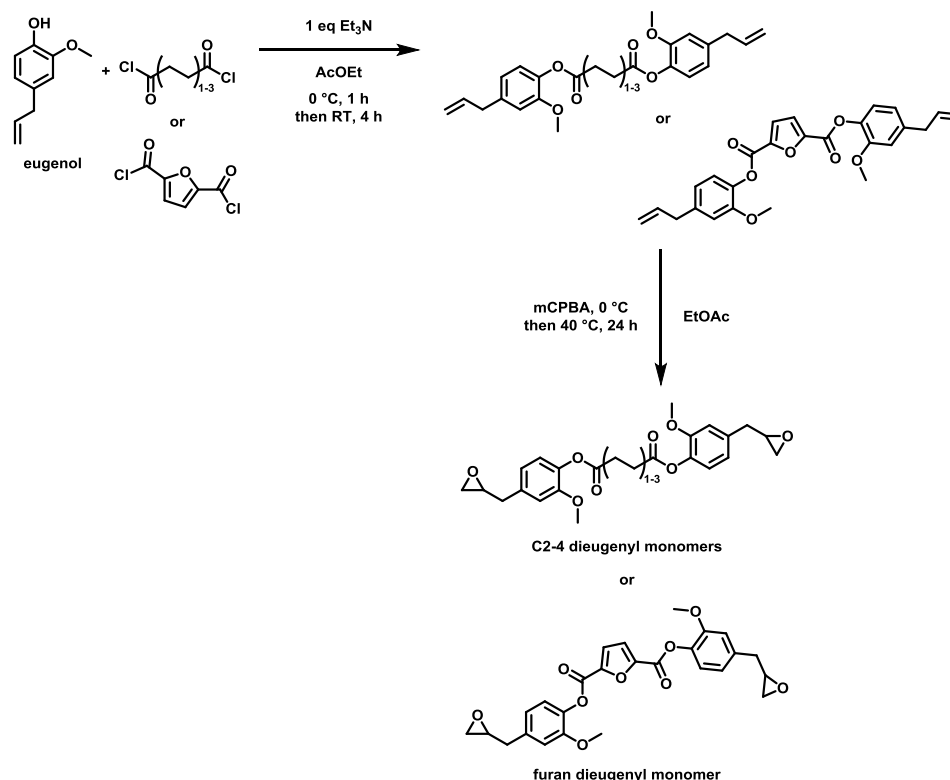
1184 Wan *et al.* used a biseugenyl with an aromatic linker, based on the terephthalic acyl chloride (Figure 40).<sup>130</sup> They  
 1185 used 33DDS in order to obtain epoxy-amine thermosets and compared the results with the DGEBA network with the  
 1186 same hardener. They measured an alpha transition temperature of 168 °C with the dieugenyl monomer, and 174 °C  
 1187 with DGEBA. The storage moduli at 30 °C were 3.5 GPa for TPEU-EP and 2.7 GPa for DGEBA. The higher  
 1188 rigidity of the eugenyl monomer increased the storage modulus, due to the higher aromatic density and the rigidity  
 1189 of the ester bonds. The rubbery modulus however was lower for the dieugenyl (10.59 MPa) compared to DGEBA  
 1190 network (19.53 MPa). This could be due to the influence of the crosslinking density, since it was 900 mol·m<sup>-3</sup> for  
 1191 TPEU-EP and 1640 mol·m<sup>-3</sup> for DGEBA. The rigidity brought by the aromatic rings and the ester bonds of the  
 1192 eugenyl monomer had more influence at low temperatures, especially because of the intermolecular interactions,  
 1193 that could be broken at higher temperatures. At the rubbery state, the lower crosslinking density and the breaking of  
 1194 the intermolecular interactions between chains allowed a better molecular motility. Regarding the thermal stability,  
 1195 it was observed that under nitrogen and under air, the eugenyl-based thermoset degraded at lower temperatures  
 1196 compared to DGEBA ( $T_{d5\%}$  under nitrogen were respectively 338 °C and 394 °C, and 337 and 387 °C under air).  
 1197 This lower degradation temperature is probably due to the presence of methoxy groups on the eugenyl residues, as  
 1198 well as the thermally labile ester bonds. For the eugenyl-based network the char yield under nitrogen was 32 % (14  
 1199 % for DGEBA).

1200 Burning behaviors of the thermosets were also investigating, using microscale combustion calorimetry and limiting  
 1201 oxygen index evaluation. The LOI of the DGEBA thermoset was 23.5 compared to 26.8 for the TPEU-EP network,  
 1202 demonstrating a lower flammability with the eugenol. However, even if the total heat release was lower (14.9 kJ·g<sup>-1</sup>  
 1203 compared to 24.9 kJ·g<sup>-1</sup> for DGEBA), as well as lower peak heat release rate for eugenyl (123 W·g<sup>-1</sup> compared to  
 1204 383 W·g<sup>-1</sup> for DGEBA). The peak temperature of the heat release was 376 °C for the dieugenyl, compared to 415 °C  
 1205 for DGEBA network. The fact that the eugenyl thermoset degraded at lower temperature could explain the lower  
 1206 peak temperatures. The flammability and the thermal stability of the eugenol containing network were lower  
 1207 compared to DGEBA.

1208

1209  
1210  
1211

## 6. Bis-eugenyls with alkyl ester or furanic ester spacers



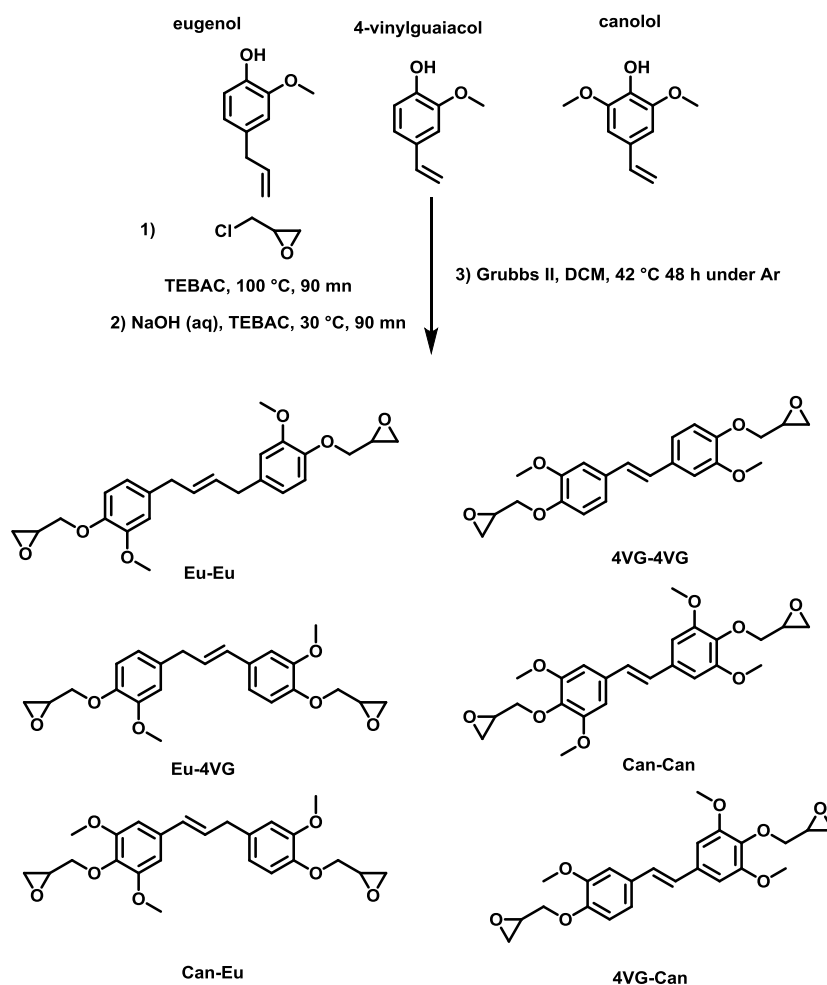
1212  
1213

Figure 41 - Structures of dieugenyl monomers by Chen *et al.*<sup>131</sup>

1214 Biseugenyls have been synthesized by Chen *et al.*<sup>131</sup> They synthesized four monomers by reacting two equivalents  
1215 of eugenol with diacyl chlorides, in order to obtain dieugenyls with different spacers. The obtained monomers  
1216 respectively contained ethyl ester, butyl ester and hexyl ester spacers, and finally a furfuryl ester spacer (Figure 41).  
1217 They performed a self-curing reaction, using catalyst, with DDM as the amine hardener. For the amine-cured  
1218 networks, they obtained  $T_g$  of 118 °C, 99 °C and 91 °C for the monomers containing the C2, C4 and C6 spacers, and  
1219 a higher  $T_g$  of 169 °C with the furfuryl ester spacer (higher than the 164 °C for DGEBA reported by Gao *et al.*<sup>116</sup>).  
1220 Both the furan rings and the ester bonds bring about rigidity to the network. On the contrary, the alkyl spacers  
1221 resulted in lower  $T_g$  values that were decreased with the increasing length of the alkyl chain. These results are in line  
1222 with the DMA results, where  $T_\alpha$  of 139 °C, 120 °C and 112 °C were obtained for the C2, C4 and C6 monomers  
1223 respectively. These values are lower compared to the values reported by Wan *et al.* for the DGEBA/DDM  
1224 system ( $T_\alpha = 154$  °C).<sup>48</sup> The furan-containing monomer had an alpha transition temperature of 181 °C, higher than  
1225 DGEBA, probably due to higher rigidity. The rubbery plateau was also measured for the networks. Values of 15 and  
1226 21 MPa were obtained for the alkyl containing thermosets, and 36 MPa for the furan-containing network. Regarding  
1227 the thermal stability, the  $T_{d5\%}$  of the different alkyl containing networks were in the range of 350-368 °C and 341 °C  
1228 for the furan containing system. The char yields varied in the range of 20-25 % for the alkyl-containing thermosets,  
1229 and 28 % when furan was used. The global thermal stability was thus slightly lower than DGEBA/DDM system,  
1230 reported by Wan.<sup>48</sup> Dielectric constants were also measured for all the thermosets, at ambient temperature at 1 GHz.  
1231 The results were similar for the alkyl containing networks (between 3.03 and 3.08) and 3.10 for the furan-containing  
1232 thermoset. Dissipation factors varied between 0.019 and 0.022 for all the evaluated thermosets. Comparing to the  
1233 self-cured epoxy networks with diamine cured networks, showed higher dissipation factors when amine hardeners  
1234 were used.

1235  
1236  
1237

## 7. Other vinylphenols



1238

1239 Figure 42 - Reaction pathway for the synthesis of diepoxy monomers from vinylphenols, according to  
 1240 Zago *et al.*<sup>132</sup> Nomenclature of the monomers corresponds to the different starting vinylphenols, eugenol  
 1241 (Eu), 4-vinylguaiacol (4VG) and canolol (Can).

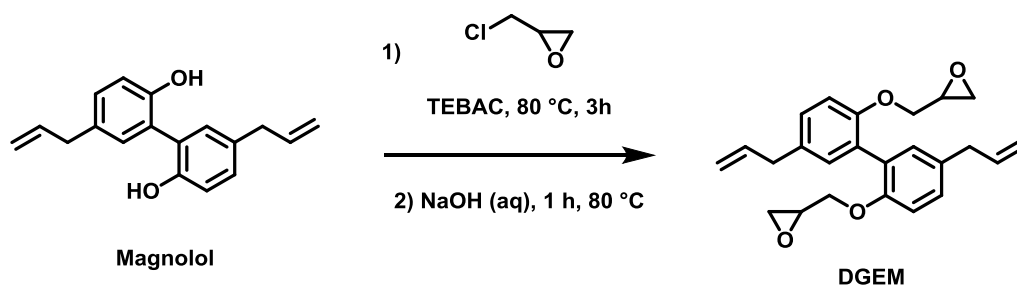
1242 Zago *et al.* designed several epoxy monomers derived from vinylphenols (Figure 42).<sup>132</sup> The first vinylphenol used  
 1243 was eugenol bearing a vinyl moiety, attached to the aromatic ring via a methylene. Two other vinyl phenols were  
 1244 obtained from vanillin and syringaldehyde, using the Knoevenagel–Doebner condensation reaction. The aldehyde  
 1245 was converted into a carbon-carbon double bond, leading to a vinyl moiety directly attached to the aromatic ring.  
 1246 The resulting vinyl phenols, namely 4-vinylguaiacol (from vanillin) and canolol (from syringaldehyde) were  
 1247 glycidylated and finally coupled, by using cross metathesis, in order to obtain diepoxy monomers. However, none of  
 1248 the resulting six diepoxy monomers have so far been used in thermosetting polymers.  
 1249 These interesting diepoxy monomers were evaluated by computational methods, for their potential ability to bind to  
 1250 the ER $\alpha$ .<sup>132</sup> All the starting monophenols, the glycidylated monophenols, and all the hydrolysed epoxies were  
 1251 evaluated. The molecular docking data revealed that some of the compounds could interact as agonist or antagonist  
 1252 of the receptor. However, when interaction was probable, the dissociation constant calculated, indicated that high  
 1253 concentrations (at least 7 times higher) would be needed to obtain an effective binding (with BPA as the reference).  
 1254 Thus, it is unlikely that these compounds would have an endocrine activity at relevant environmental concentrations.  
 1255 However, these data are only computational, and more investigation would be necessary. In addition, it could also  
 1256 be interesting to generate data for the non glycidylated bisphenols, as often considered regarding BPA and DGEBA.  
 1257 In the work of Hong *et al.*, two of the bisphenols synthesized by Zago *et al.* were included for prediction of the ER $\alpha$   
 1258 binding ability.<sup>82</sup> The bisphenol obtained from cross-coupling of eugenol (Eu-Eu), and the compound obtained from  
 1259 the cross-coupling of 4-vinylguaiacol (4VG-4VG) were evaluated. The 4VG-4VG bisphenol was predicted to be a  
 1260 non-binder to the ER $\alpha$ , with a low prediction confidence. The Eu-Eu bisphenol was predicted to be an oestrogen  
 1261 receptor binder. The quantitative affinity that was calculated indicated a higher binding affinity than BPA. These  
 1262 results are consistent with the work of Zago *et al.*, which showed a potential interaction of this compound both as  
 1263 agonist and antagonist of the receptor.<sup>132</sup> However, the prediction by Hong *et al.* had a low confidence. In vitro

1264 testing would provide more data to improve the predictions from *in silico* model. But these results suggest that such  
1265 monomer could not meet the criteria for substitution of BPA. When these results are evaluated regarding the work  
1266 on guaiacyls or syringyls discussed earlier in this paper, the results are rather consistent, especially regarding the  
1267 influence of methoxy moieties.<sup>81</sup> The presence of methoxies on the phenolic residues do not provide enough steric  
1268 hindrance to impede the binding to the receptor. The work of Hong et al. also provides prediction for bisphenols that  
1269 are similar, but which could be obtained from the double-bond reduction of Eu-Eu and 4VG-4VG. The results show  
1270 that these to hydrogenated bisphenols are predicted to be binder to the ER $\alpha$ . The absence of the double bond lead to  
1271 an increased affinity with the receptor. The hydrogenated Eu-Eu is predicted to have a higher affinity than BPA, and  
1272 the prediction to be binder have a high prediction confidence. The hydrogenated 4VG-4VG has a low prediction to  
1273 be binder, and the quantitative affinity would be lower than BPA. The authors suggest that this result indicates a  
1274 planar configuration required for the interaction with the receptor. The natural E2 has a planar configuration, and the  
1275 influence of the double bond would specifically modify the ability of the bisphenol to adopt the planar  
1276 configuration. Overall, the nature and the length of the bridging unit in bisphenols is also an important parameter, as  
1277 previously described.<sup>35,36</sup>

## 1278 XI. Magnolol

1279

1280



1282

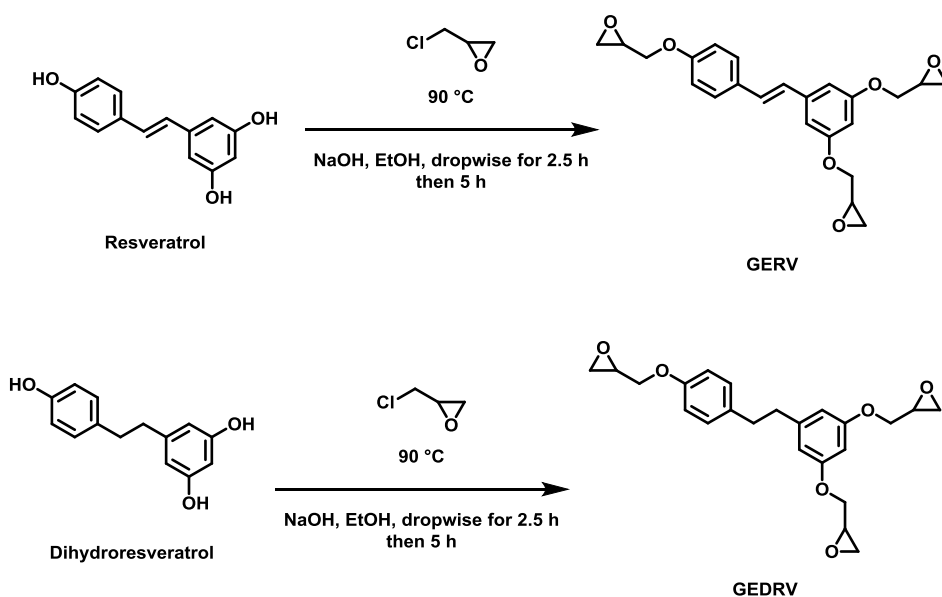
Figure 43 - Synthesis of DGEM according to Qi *et al.*<sup>133</sup>

1283 Magnolol is a natural diphenol, extracted from *Magnoliae officinalis*, bearing two allyl moieties. The glycidylation  
1284 of the phenolic moieties was performed by Qi *et al.* in order to obtain a diepoxy monomer (Figure 43), that was  
1285 subsequently cured with 44DDS.<sup>133</sup> The presence of the allyl moieties could provide the possibility of a second  
1286 crosslinking via thermal polymerization, within the same temperature range used for the epoxy amine polyaddition.  
1287 The DMA tests revealed an alpha transition at the peak of  $\tan \delta$  of 279 °C for DGEM compared to 231 °C for  
1288 DGEBA/DDS. The Young's modulus of the DGEM at ambient temperature was 3.7 GPa compared to 2.5 GPa for  
1289 DGEBA. This is mainly explained by a higher crosslinking density of DGEM, due to the further reaction of allyl  
1290 moieties. The calculated values of crosslinking densities were 3.2 kmol·m<sup>-3</sup> for DGEM compared to 2.3 kmol·m<sup>-3</sup>  
1291 for DGEBA/DDS. Flexural strength of both systems was quite similar, around 106-108 MPa, whereas the flexural  
1292 modulus of DGEM was 3.5 GPa, compared to 2.5 GPa for DGEBA. This reveals the higher rigidity of the DGEM,  
1293 resulting from the higher crosslinking density. The thermal stability under nitrogen atmosphere was similar for both  
1294 thermoset, with a  $T_{d5\%}$  of 402 °C for DGEM compared to 399 °C with DGEBA. This is an interesting result, since  
1295 usually DGEBA displays a higher thermal stability. The char yield was also higher for DGEM than for DGEBA,  
1296 with a value of 43 % compared to 15 %. These results show that the tetrafunctional monomer from magnolol give  
1297 outstanding properties to the epoxy networks. These thermosets also had high temperature resistance, with a lower  
1298 total heat release. DGEM could self-extinguish after 2.3 seconds, increasing to 4 seconds after a second application  
1299 of flame. Magnolol is a widely studied pharmacological compound. Generally, it has been used in traditional  
1300 Chinese and Japanese medicine and has been considered as a safe compound, with no reported adverse effects. It has  
1301 antibacterial, anti-inflammatory and antioxidant activities, among others.<sup>134,135</sup> To the best of our knowledge, no  
1302 endocrine activity has been reported for this compound.

1303

## 1304 XII. Resveratrol

1305



1306

1307

Figure 44 - Synthesis of resveratrol based epoxy monomers, according to Garrison *et al.*<sup>136</sup>

1308 Resveratrol is an interesting diphenolic compound that bears three phenolic hydroxyl groups. The glycidylation of  
 1309 those moieties lead to a trifunctional epoxy monomer. Resveratrol can be found in several vegetables, including  
 1310 grapes and more specifically, grape wastes.<sup>137</sup> Garrison *et al.* performed the synthesis of two resveratrol-based  
 1311 monomers, the first compound was made directly from the resveratrol (GERV), and the second from a hydrogenated  
 1312 form of the resveratrol (GEDRV), that originally bears a double bond between the aromatic rings (Figure 44).<sup>136</sup>  
 1313 They used two hardeners, a commercially available (DDM), and a compound prepared from resveratrol, leading to  
 1314 full resveratrol-based epoxy networks. The alpha transition temperature for GERV/DDM was 285 °C, whereas it  
 1315 was 178 °C for the GEDRV/DDM. For comparison, the DGEBA/DDM network displayed a lower  $T_g$  of 164 °C.<sup>116</sup>  
 1316 This is mainly explained by the higher crosslinked density from the trifunctional monomers based on resveratrol.  
 1317 Thermal stability was also evaluated, under nitrogen and under air. The  $T_{d5\%}$  of both resveratrol-based thermoset  
 1318 under nitrogen were in the range of 355-358 °C which showed no significant difference between saturated and  
 1319 unsaturated monomers. The DGEBA/DDM network under nitrogen displayed a  $T_{d5\%}$  of 376 °C, which is slightly  
 1320 higher.<sup>138</sup> The same range of  $T_{d5\%}$  was observed under air for DGEBA or resveratrol-based networks. The char yield  
 1321 was superior with the unsaturated epoxy resveratrol epoxy monomer (40.5 % vs 26.1 % for saturated), and  
 1322 significantly lower for DGEBA/DDM network (15 %). The higher crosslinking density in the case of resveratrol-  
 1323 based networks improved the char formation. More recently, Tian *et al.* prepared GERV and used PACM to obtain  
 1324 fully cured networks.<sup>139</sup> In their work, they were able to obtain the monomer with an EEW of 144 g·eq<sup>-1</sup> compared  
 1325 to 280 g·eq<sup>-1</sup> by Garrison *et al.*<sup>136</sup> Tian *et al.* performed DSC using several heating ramps, but did not fit the data  
 1326 with kinetic models in order to assess the activation energies of the curing reactions. Thermomechanical analysis  
 1327 was performed on cured samples, and the GERV/PACM system showed a  $T_\alpha$  of 302 °C compared with  
 1328 DGEBA/PACM with a  $T_\alpha$  of 149 °C. These results were also in agreement with the DMA analysis, giving a  $T_\alpha$  value  
 1329 of above 300 °C for GERV and 161 °C for DGEBA. The glassy moduli for DGEBA and GERV networks were  
 1330 respectively 2, 4 GPa and 1, 9 GPa at 25 °C, indicating a higher rigidity of DGEBA network. At the rubbery state,  
 1331 the  $E'$  for DGEBA was 41 MPa (at 200 °C).  $E'$  could not be measured for GERV network at 200 °C but at 300 °C  
 1332 the value was 363 MPa. Tensile properties were also evaluated, 78 MPa for GERV network, and 64 MPa for  
 1333 DGEBA. Tensile strain were respectively 4.5 % for GERV and 3.7 % for DGEBA (quite similar values given the  
 1334 standard error). The authors did not comment about the higher Young's modulus of DGEBA compared to GERV.  
 1335 The crosslinking density can be considered higher in GERV since it is a trifunctional monomer. However, it does  
 1336 not seem to imply a higher rigidity as it could have been expected. Thermal stability of the networks was assessed  
 1337 by TGA under nitrogen atmosphere. The reported  $T_{d5\%}$  for GERV/PACM was 320 °C and the  $T_{d5\%}$  for  
 1338 DGEBA/PACM was 348 °C. This result is in agreement with the work of Garrison *et al.* which showed that  
 1339 resveratrol-based epoxies have lower thermal stability.<sup>136</sup> The authors did not explain the earlier degradation of  
 1340 resveratrol based network, but it could be because of the carbon-carbon double bond between phenol rings, that may  
 1341 be less stable than the isopropylidene in DGEBA. Char yield at 800 °C was however higher in GERV network



1342 (12.4 %) compared to DGEBA (4.2 %), showing that high degrees of crosslinking leads to better thermal stability at  
1343 high temperature and a better ability to produce char. Non-isothermal degradation kinetics, using Kissinger's model,  
1344 gave activation energy of  $182 \text{ kJ}\cdot\text{mol}^{-1}$  for GERV and  $181 \text{ kJ}\cdot\text{mol}^{-1}$  for DGEBA networks. These results show that  
1345 there is probably no fundamental difference between the degradation mechanisms of the two thermosets.  
1346 Surprisingly, a mixture of DGEBA and GERV cured with PACM showed a significantly higher  $E_a$  of degradation  
1347 ( $222 \text{ kJ}\cdot\text{mol}^{-1}$ ). However, the authors did not discuss the reason for obtaining such elevated  $E_a$  value. Cone  
1348 calorimetry was used to determine the flame retardancy of the networks (LOI determination and SEM analysis of  
1349 the pyrolyzed material surfaces). Higher and sharper peak was observed for DGEBA network ( $2.1 \text{ MW}\cdot\text{m}^{-2}$   
1350 compared to  $1.5 \text{ MW}\cdot\text{m}^{-2}$  for GERV). LOI was also higher for DGEBA network (21 % compared to 15.7 % for  
1351 GERV). These results along with high char yield indicate a better fire resistance of resveratrol-based thermosets.  
1352 SEM images of the pyrolyzed materials showed homogeneous char layer in the case of GERV and an irregular  
1353 surface for the DGEBA.

1354 The evaluation of the dielectric permittivity showed that the DGEBA network had a higher permittivity as compared  
1355 to GERV. At the range of  $10 - 10^7 \text{ Hz}$ , DGEBA/PACM displayed a permittivity of 4.7-4.1 F/m while GERV/PACM  
1356 displayed 3.9-3.2 F/m. Generally, resveratrol-based epoxy monomers have very good thermomechanical properties  
1357 as well as a fair thermal stability, although lower than that of DGEBA. Resveratrol is a compound that is widely  
1358 studied for its pharmacological properties. It has been associated with protective cardiovascular effect *in vitro* and in  
1359 animals. It has also been studied in several clinical trials for its potential effect on cardiovascular diseases, cancer,  
1360 neurodegenerative or metabolic diseases. It is also sold as a dietary supplement, for its antioxidant activity.  
1361 However, a recent review warns that resveratrol is a phytoestrogen. The review collected evidence regarding the  
1362 activity of resveratrol on the  $\text{ER}\alpha$  in human.<sup>140</sup> In this work, Qasem concluded that the effect of resveratrol on the  
1363 oestrogen receptor is not always reported in studies, since its effect on the endocrine system may arise from repeated  
1364 exposure.

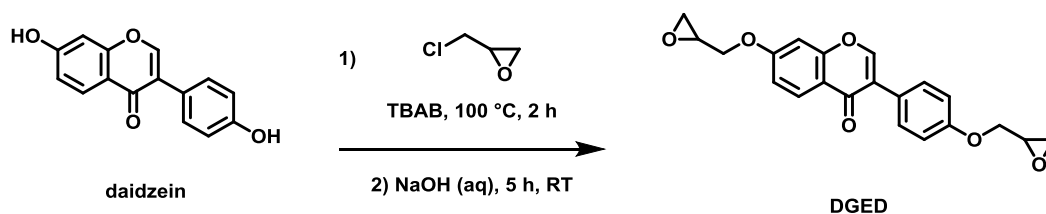
1365 In the work of Hong *et al.*, resveratrol and dihydroresveratrol were evaluated for their binding affinity with the  $\text{ER}\alpha$ ,  
1366 using *in silico* methods.<sup>82</sup> Resveratrol is considered to be a binder to the receptor, with a calculated affinity that is  
1367 lower than BPA, but slightly higher than BPF. This is consistent with the fact that resveratrol is a phytoestrogen,  
1368 thus it shows affinity with the oestrogen receptor. However, the calculations for dihydroresveratrol revealed no  
1369 binding affinity underlining the effect of the bridging unit between the phenol rings.  
1370

### 1371 XIII. Flavonoids

#### 1372 1. Daidzein

1373

1374

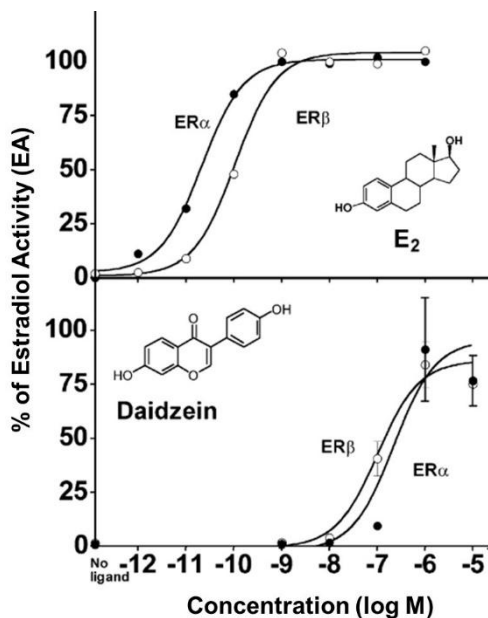


1376

1377 Figure 45 - Synthesis of DGED, according to Dai *et al.*<sup>141</sup>

1377 Daidzein is an isoflavone found in soybean biomass.<sup>142</sup> It is used in the food and pharmaceutical industry. The  
1378 bisphenolic nature of this compound led to its use as a building block for the synthesis of a diglycidylether. Dai *et al.*  
1379 *et al.* performed the synthesis of the monomer (Figure 45), and studied the properties with DDM as the curing agent,  
1380 and compared it with DGEBA network.<sup>141</sup> Among the different properties studied, it was found that the DGED had  
1381 an alpha transition of  $205 \text{ }^\circ\text{C}$  with DDM, which was higher than the measured for DGEBA/DDM network ( $172 \text{ }^\circ\text{C}$ ).  
1382 The Young's modulus at  $25 \text{ }^\circ\text{C}$  was  $2.8 \text{ GPa}$  ( $2.4 \text{ GPa}$  for DGEBA). These properties are mainly due to the high  
1383 crosslinking density, which was found to be  $6.4 \text{ mol}\cdot\text{m}^{-3}$  for DGED as compared to 3.5 for DGEBA/DDM. Other  
1384 mechanical properties were also measured, such as tensile strength and moduli, and also flexural strength and  
1385 moduli. In all cases, the thermoset from DGED were superior to DGEBA. Thermal stability under inert atmosphere  
1386 was lower, since the  $T_{d5\%}$  for DGED was  $335 \text{ }^\circ\text{C}$ , compared with DGEBA network with a  $T_{d5\%}$  of  $384 \text{ }^\circ\text{C}$ . The same  
1387 trend was observed under oxidative atmosphere. This is mainly due to the presence of the heterocycle in the  
1388 structure of daidzein, which may degrade first. However, regarding the char yield at  $800 \text{ }^\circ\text{C}$ , the DGED had a  
1389 remarkable superior char formation, 43 % compared to 16 % for DGEBA. The DGED also had low flammability,  
1390 with a superior LOI of 31.6 % (compared to 24.5 % for DGEBA), and an ability to self-extinguish within 13

1391 seconds. Daidzein is a phytoestrogen, which means it may have the potential to be agonist or antagonist to the  
 1392 oestrogen receptor.<sup>143</sup> It is well known that the consumption of soybean products may interact with the endocrine  
 1393 system, and daidzein is one of the compounds such a kind of effect. More specifically, daidzein is metabolized into  
 1394 equol that has even more activity. But compared to the natural hormone E2, these activities are lower and happen at  
 1395 higher concentrations (Figure 46).<sup>144</sup> It is also important to note that the mode of exposition between the  
 1396 consumption of soy products and the exposition from the use of epoxy thermosets would be very different. The  
 1397 effect on human health of the ingestion of daidzein and other isoflavones were extensively reviewed by Křížová *et*  
 1398 *al.*<sup>143</sup>  
 1399  
 1400



1401

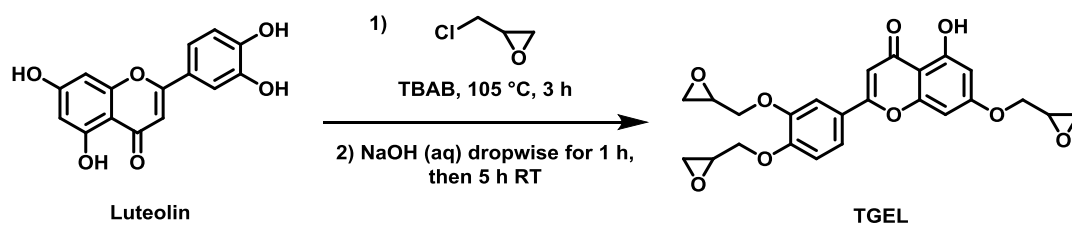
Figure 46 - *In vitro* activity of daidzein and E2, adapted from Muthyala *et al.*<sup>144</sup>

1402

## 2. Luteolin

1403

1404



1405

1406

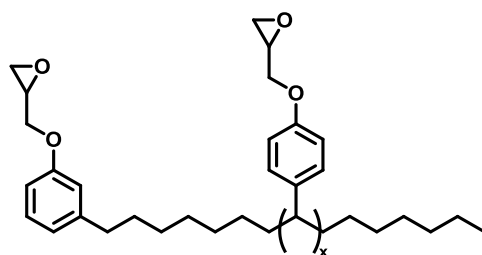
Figure 47 - Synthesis of TGEL from Luteolin according to Gao *et al.*<sup>145</sup>

1407 Luteolin is a natural flavonoid that can be found in herbs such as thyme, sage or oregano, in some types of celeries  
 1408 or radicchio, and in lower quantities in beets, Brussel sprouts and lemons.<sup>146</sup> It has shown some anti-microbial  
 1409 activity, anti-inflammatory properties and is considered to have a chemotherapeutic potential.<sup>146</sup> The chemical  
 1410 structure of luteolin is a polyphenol comprising a heterocycle, a resorcinol unit and a pyrocatechol unit. It leads to a  
 1411 compound bearing 4 phenolic hydroxyl moieties (Figure 47). However, only 3 are reactive towards glycidylation  
 1412 since one of the phenolic moieties is blocked by hydrogen-bonding with the carbonyl moiety, as shown by Gao *et*  
 1413 *al.*<sup>145</sup> The glycidylation reaction lead to a trifunctional epoxy monomer named diglycidylether of luteolin (DGEL)  
 1414 in the original publication, but that will be referred to as triglycidylether of luteolin (TGEL) in this article. The  
 1415 monomer was subsequently cured with DDS to afford epoxy thermosets. The curing reaction was first assessed by  
 1416 non-isothermal curing kinetics using Ozawa and Kissinger methods, and compared with DGEBA/DDS system.  
 1417 Good correlations were obtained with both methods, and DGEBA/DDS showed a lower activation energy than  
 1418 TGEL/DDS (60.7-65.5 kJ·mol<sup>-1</sup> for DGEBA/DDS vs 64.8-69.0 kJ·mol<sup>-1</sup> for TGEL/DDS). According to the authors,  
 1419 the lower activation energy was mainly due to the high functionality of the monomer. The thermal stabilities of the

1420 networks were evaluated by TGA under nitrogen and air. In both cases, DGEBA/DDS systems showed a higher  
1421  $T_{d5\%}$  (393 °C under N<sub>2</sub> and 374 °C under air), compared to TGEL/DDS (379 °C under N<sub>2</sub> and 346 °C under air), due  
1422 to an early decomposition of the heterocycle in TGEL. Both networks exhibit similar degradation pathways. Under  
1423 inert atmosphere, DGEBA/DDS and TGEL/DDS show a single main decomposition step. During this step, the  
1424 weight loss for DGEBA/DDS was higher than in TGEL/DDS, resulting in a low char yields for DGEBA/DDS, at  
1425 700 °C (12 % for DGEBA and 44 % for TGEL). Under oxidative atmosphere, the same trend was observed, with  
1426 two decomposition steps for all networks, but with a first weight loss at lower temperature for TGEL than for  
1427 DGEBA. The higher functionality and higher aromatic density of TGEL lead to more char yield under nitrogen, and  
1428 a delayed decomposition of the material. Several mechanical properties were assessed, such as dynamic mechanical  
1429 and tensile properties. DMA revealed an alpha transition of 314 °C for TGEL/DDS network, which is a high value,  
1430 compared to DGEBA/DDS with a  $T_{\alpha}$  of 217 °C. The Young's modulus at the glassy plateau at 30 °C were 3.8 GPa  
1431 for TGEL and 2.7 GPa for DGEBA networks. The high value for TGEL has to be balanced with the fact that a high  
1432 loss modulus was observed before 100 °C, with a value inferior to 3 GPa at this temperature. The same trend was  
1433 observed with DGEBA. The rubbery values of Young's modulus were 2.1 GPa for TGEL/DDS and 50 MPa for  
1434 DGEBA/DDS, illustrating high stiffness of the TGEL. This is in agreement with tensile tests giving lower  
1435 elongation at break for TGEL (9.5 %) compared to DGEBA (10.8 %), but a higher tensile strength with TGEL  
1436 compared to DGEBA networks (respectively 69.2 MPa and 57.2 MPa). Surprisingly the crosslinking density of  
1437 TGEL/DDS network was 1.5 kmol·m<sup>-3</sup> whereas it was 2.2 kmol·m<sup>-3</sup> for DGEBA/DDS network. This could be due  
1438 to the high molecular weight of the epoxy monomer, and to its non-symmetric structure, leading to a lower global  
1439 crosslinking density. Flame retardant properties were extensively evaluated by Gao *et al.*, using microscale  
1440 calorimetry, LOI tests, TGA-FTIR and Pyrolysis-GC/MS. MCC revealed a lower total heat release for TGEL/DDS  
1441 than for the DGEBA network (24.3 kJ·g<sup>-1</sup> for TGEL vs 29.1 kJ·g<sup>-1</sup> for DGEBA). The heat release capacity of  
1442 DGEBA network was four times higher than for TGEL (respectively 399 J·g<sup>-1</sup>·K<sup>-1</sup> and 101 J·g<sup>-1</sup>·K<sup>-1</sup>). The LOI value  
1443 of the TGEL network was 32.5 % whereas it was 27.0 % for DGEBA. Raman spectroscopy showed that TGEL  
1444 network displays a higher graphitization degree after pyrolysis, which is a desirable property when using char-  
1445 forming material. Decomposition studies showed that DGEBA/DDS could release more aromatic compounds than  
1446 TGEL/DDS network, indicating that most aromatic compounds stay in the condensed phase. Among all the  
1447 biological mechanisms of endocrine system, sulfonation of steroids by sulfotransferase enzymes is part of the  
1448 oestrogenic system. Indeed, the sulfonation of steroids lead to a change in their properties, for instance, oestrogen  
1449 sulfonates are no longer agonist to the oestrogen receptor.<sup>147</sup> Thus, any activity on these enzymes could affect the  
1450 endocrine system, and have indirect endocrine disruption potent.  
1451 Waring *et al.* evaluated several phytoestrogen or xenoestrogen as inhibitors to sulfotransferases.<sup>147</sup> The  
1452 inhibition potent of several flavonoids were tested on SULT 1A1, and luteolin enzymes showed an IC50 of only 3  
1453 nM, but did not show any inhibition activity for SULT 1A3 (a sulfotransferase), at submicromolar scale. It had also  
1454 no effect on the SULT 2A1 activity. These findings were in agreement with a previous study.<sup>148</sup> In the work of  
1455 Waring *et al.* it was shown that for some enzymes, the inhibition potent of flavonoids is several orders of magnitude  
1456 superior to the synthetic compounds such as alkylphenols or phthalates.<sup>147</sup> The authors noted that for example  
1457 supplementation with flavonoids may not be universally beneficial, since the addition of exposition to synthetic  
1458 endocrine disruptors, naturally occurring flavonoids in diet and supplementation may lead to increased risks of  
1459 cancer. In another work, Nordeen *et al.* also highlighted luteolin as a multi-functional endocrine disruptor, with a  
1460 potent progesterone antagonist and oestrogen agonist activity.<sup>149</sup> They assessed the effect of luteolin on the steroid  
1461 signalling, using T47D cell lines expressing oestrogen and progesterone receptors. The authors also signal out that  
1462 use of flavonoids supplements could be dangerous for patient with certain type of cancers. Surprisingly, a study  
1463 described the protective effect of luteolin against bisphenol A toxicity, in drosophila.<sup>150</sup> The protective effect has  
1464 been partly attributed to the antioxidant properties of luteolin.

#### 1465 XIV. Cardanol and Cardol

1466  
1467



NC-514

1468

1469 Figure 48 – Cardanol-based polyepoxide commercial monomer NC-514 idealized structure, according to  
1470 Jaillet *et al.*<sup>151</sup>

1471 Cardanol is an interesting natural phenolic compound, extracted from the cashew nutshell oil, which is a by-product  
1472 of cashew nut production. This vegetable oil has the advantage of providing biobased aromatics, with alkyl chain,  
1473 allowing the possibility to design new building blocks, especially for polymers.<sup>152</sup> Cardanol based epoxy resins from  
1474 Cardolite NC-514 (Figure 48), showed interesting properties. In a paper published by Jaillet *et al.*, its networks with  
1475 IPDA and Jeffamine were studied.<sup>151</sup> The structural characterization led to the conclusion that NC-514 was mainly  
1476 composed of diepoxy monomers, with a small percentage of unsaturated compounds. The epoxy structure with  
1477 cardanol was composed of a phenol ring, with a C15 alkyl chain attached on the *meta* position. Natural cardanol has  
1478 unsaturated bonds, which was reacted with phenol in NC-514. This leads to the attachment of another phenol, as a  
1479 side-group of the alkyl chain. The phenol substitution led to a low unsaturation degree in the formulation. Both  
1480 phenolic moieties from the natural cardanol, and the pending phenolic side-groups were then substituted by a  
1481 glycidyl moiety, leading to a difunctional epoxy resin. In this work the EEW was determined around 363 eq.g<sup>-1</sup>.  
1482 Jaillet *et al.*, studied the formulations of NC-514 with diamine hardeners with higher gel content. Network made  
1483 using NC-514 and IPDA had a  $T_g$  of 50 °C (with 90 % gel content). When NC-514/Jeffamine D400 was used the  $T_g$   
1484 was 15 °C (with 90 % gel content). As a comparison, the DGEBA/IPDA network had a  $T_g$  of 158 °C. Regarding the  
1485 mechanical properties, a  $T_a$  of 59 °C was obtained for NC-514/IPDA, and 9 °C for Jeffamine D400/NC-514.  
1486 DGEBA/IPDA network had a  $T_a$  of 158 °C and DGEBA/Jeffamine network had a  $T_a$  of around 50 °C as reported by  
1487 Soares.<sup>153</sup> The presence of long alkyl chain, especially the pending end chain from cardanol after crosslinking,  
1488 endows plastifying properties that lead to a low glass transition temperatures to the epoxy network. At the glassy  
1489 state, a Young modulus of 1.2 GPa for NC514/IPDA and 7 MPa with Jeffamine were recorded (compared to 1.4  
1490 GPa for DGEBA/IPDA). The use of polyether-based hardener, Jeffamine, led to a sharp decrease in Young's  
1491 modulus at the glassy state as compared to when cardanol was used. However, at the rubbery state, the difference of  
1492 Young's modulus was more pronounced for IPDA based networks, with  $E'$  of 19.6 MPa for DGEBA and 3.2 for  
1493 NC-514 (close to the value of NC-514/Jeffamine, of 2.6 MPa). It could be presumed that at the glassy state, the  
1494 global network is more affected by the presence of rigid moieties (aromatic rings), and the hardener (for IPDA  
1495 networks). While at the rubbery state, the presence of alkyl chain results in increased mobility and low crosslinking  
1496 density.  
1497

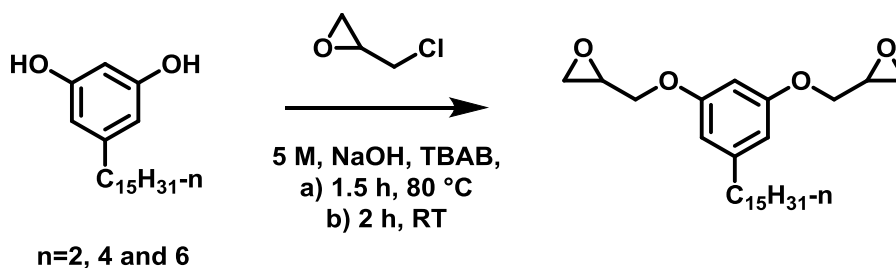


Figure 49 - Synthesis of diglycidylether of cardol by Makwana *et al.* [Cite 10.1016/j.eurpolymj.2022.111029]

1498

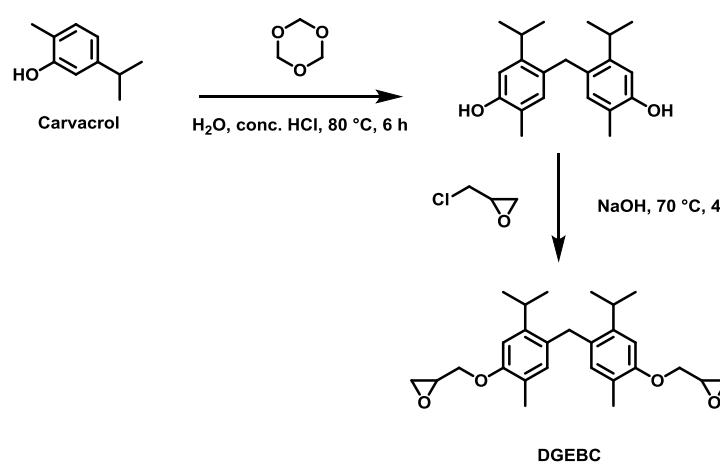
1499 Besides cardanol, cashew nutshell liquid also contains cardol, which differs from cardanol mainly by bearing an  
1500 additional phenolic hydroxyl moiety. Makwana *et al.* took advantage of this difunctionality by preparing a diepoxy  
1501 monomer by direct glycidylation of cardol, as shown in Figure 49. [Cite 10.1016/j.eurpolymj.2022.111029] The

1502 diepoxy monomer was used with two amine hardeners, namely DETA and IPDA. Several formulations based on the  
1503 DGEC (diglycidylether of cardol) in mixture with DGEBA were also performed and cured with IPDA. Pure  
1504 DGEBA resins were also prepared with both hardeners. Focusing on materials containing pure DGEC as the epoxy  
1505 monomer, the authors reported an EEW of 215 g·mmol<sup>-1</sup>, and a multi-step curing procedure was adopted. Using  
1506 non-isothermal DSC, the monitoring of curing reactions revealed that DGEC displayed lower curing exotherms than  
1507 DGEBA, when cured with both amines. After curing, the crosslinked materials also revealed lower  $T_{g,s}$ , respectively  
1508 63 °C for DGEC-IPDA and 45 °C for DGEC-DETA, compared to 155 and 145 °C for the corresponding  
1509 formulations using DGEBA. The plastifying effect of the C15 alkyl chain drastically decreases the glass transition  
1510 temperatures of cardol-based materials. Thermal stability under inert atmosphere of DGEC resins displayed very  
1511 similar values compared to the DGEBA pendent. Indeed, while DGEC-IPDA and DGEC-DETA show Td5% of 359  
1512 and 348 °C, the corresponding DGEBA networks displayed respectively Td5% of 349 and 350 °C. However, char  
1513 formation of DGEC was significantly lower, respectively 3.4 and 4.8 % with IPDA and DETA, whereas for  
1514 DGEBA it is 9.3 % and 9.8 % with IPDA and DETA. This again can be explained by the presence of long alkyl  
1515 chain in cardol, that greatly decreases the aromatic density in the materials compared to DGEBA. Besides the  
1516 plastifying effect of these alkyl chains revealed by DSC, mechanical properties also confirmed the trend, when  
1517 determined by DMA and tensile testing. Cardol-based materials prepared with IPDA displayed a  $T_{\alpha}$  of 74 °C (154  
1518 °C with DGEBA), a Young's modulus of 0.75 GPa (compared to 2.4 GPa with DGEBA). The tensile strength  
1519 measured was 23 MPa and the elongation at break was 9.7 % at 1 mm·min<sup>-1</sup>. The same formulation with DGEBA  
1520 had a tensile strength of 75 MPa and an elongation at break of 3.1 %. Regarding materials prepared with IPDA, the  
1521 same trend is observed. DGEC materials displayed a  $T_{\alpha}$  of 67 °C (132 °C with DGEBA), a Young's modulus of 0.52  
1522 GPa (2.24 GPa with DGEBA). Again, tensile testing revealed a tensile strength of 11.82 MPa (65 MPa with  
1523 DGEBA) and an elongation at break of 5.1 % (compared with 2.8 % for DGEBA). All those mechanical properties  
1524 indicate that DGEBA based materials are stiffer than DGEC based one, that display a more elastic behaviour. The  
1525 authors also analysed the cryo-fracture of samples by scanning electron microscopy, assessing that all materials  
1526 appear homogenous, indicating that no phase separation occurs during processing.  
1527

1528 While phenolic compounds extracted from cashew nutshell liquid have a very different structure compared to  
1529 bisphenol A, it is still interesting to survey literature about endocrine activity. Interestingly, some cardanol  
1530 derivative has been tested in YES and YAS agonist and antagonist assays. [Cite  
1531 <https://dx.doi.org/10.1016/j.indcrop.2018.12.060>] These assays were performed in comparison with phthalates, that  
1532 are also endocrine disruptors, and widely used as plasticizers. Contrary to the phthalates, epoxidized cardanol  
1533 derivatives did not show any activity, or non-significant activity. While these tested structures are relatively  
1534 different than the monomers studied for epoxy amine networks, it is worth mentioning.  
1535

## 1536 XV. Carvacrol

1537



1538

1539

Figure 50 - Synthesis of DGEBC from carvacrol

1540 Carvacrol is a terpenoid phenolic compound that is found in oregano oil, or synthesized from cyclic monoterpenes  
1541 such as *p*-cymene. In 2016, Harvey *et al.* synthesized a bisphenol from carvacrol and a formaldehyde source,  
1542 trioxane.<sup>154</sup> Garrison and Harvey then used this bisphenol in order to synthesize a diepoxy monomer (diglycidylether  
1543 of bis(3,5-dimethyl-4-hydroxyphenyl)methane (DGEBC), Figure 50), and also a diamine.<sup>138</sup> The use of diamine and DDM as hardener with the new

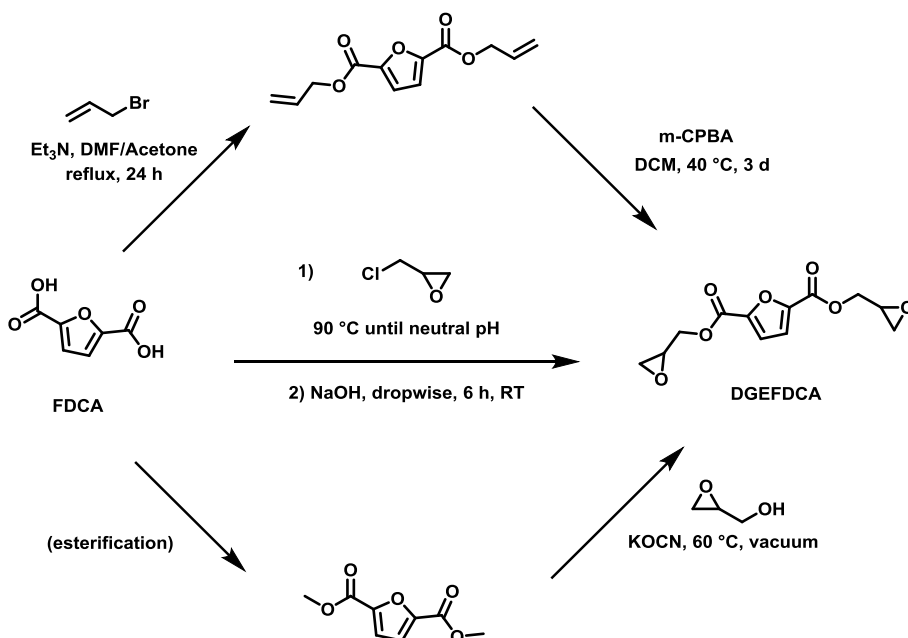
1544 epoxy monomer was studied. For DGEBA/DDM network,  $T_g$  was 179 °C whereas it was 161 °C for DGEBC/DDM,  
 1545 as evaluated using DSC measurements. These similar values and the lower values of DGEBC may be due to modest  
 1546 plasticizing effect of the isopropyls. Thermal stability of the cured networks was assessed using TGA both under air  
 1547 and nitrogen. Under nitrogen,  $T_{d5\%}$  were 367 and 376 °C for DGEBC and DGEBA cured with DDM. Similar values  
 1548 were obtained when analysis was performed under air. Char yield under nitrogen for DGEBC and DGEBA cured  
 1549 with DDM was 10 - 20 % for DGEBA and less than 10 % with DGEBC. It should be noted that, bis(4-vinylphenyl)acetylene  
 1550 contains two isopropyl and two methyl groups on the aromatic rings that degrade at lower temperature thus do not  
 1551 contribute towards char formation.

1552  
 1553 As discussed earlier Hong *et al.*, evaluated a wide set of potential substitutes of BPA for their binding affinity with  
 1554 ERα using an *in silico* method.<sup>82</sup> This method allowed for the qualitative and quantitative prediction of the binding  
 1555 ability of each compound, as well as the quantitative affinity if considered a binder. The bis(4-vinylphenyl)acetylene was part of this  
 1556 set, and it was predicted to be binder. The calculated affinity was 100 times higher than BPA, indicating a strong  
 1557 receptor binder. However, the certitude of the prediction was very low.

## 1558 Furanics

### 1559 I. Furan dicarboxylic acid

1560  
 1561



1562

1563

Figure 51 – Several synthesis pathways of DGEFDCA from furandicarboxylic acid

1564 A diepoxy monomer can easily be obtained from furandicarboxylic acid (FDCA). Several synthesis pathways have  
 1565 been reported to date (Figure 50). The first path involves the alkylation of both carboxylic acid moieties. The diallyl  
 1566 is then epoxidized with meta-chloroperbenzoic acid to afford the diepoxy monomer.<sup>155</sup> Two other pathways are also  
 1567 available, as reported by Marotta and co-workers.<sup>156</sup> First, the direct glycidylation of the dicarboxylic acid, reacted  
 1568 with epichlorohydrin. Second, transesterification can be performed on the dimethyl ester of the FDCA, with  
 1569 glycidol, using potassium cyanate as a low toxicity catalyst. Several research articles described the properties of  
 1570 networks with DGEFDCA, using different hardeners. Deng *et al.* used two hardeners, an anhydride, and a polyether  
 1571 diamine (commercially known as D230 or Jeffamine D230). This amine is a polypropylene based oligomer of  
 1572 approx. 230 g·mol<sup>-1</sup>.<sup>155</sup> DGEFDCA cured with D230 led to a  $T_g$  of 101 °C, as compared with a DGEBA/D230  
 1573 network with  $T_g$  of 98 °C as determined by Ma and co-workers.<sup>157</sup> When using aromatic amines, such as 33DDS and  
 1574 44DDS, higher  $T_g$  values of 176 °C and 215 °C were obtained. DGEBA/33DDS had a  $T_g$  of 184 °C and  
 1575 DGEBA/44DDS of 238 °C.<sup>55</sup> Comparing curing with aromatic amines and polyether amines, the obtained  $T_g$  values  
 1576 were very similar to the DGEBA networks. In the recent work of Liu *et al.* the curing of DGEFDCA with DDM  
 1577 showed a higher  $T_g$  than the equivalent DGEBA, namely 156 °C for the furan-based network, compared to 124  
 1578 °C.<sup>158</sup> Indeed, higher crosslink densities were obtained with DGEFDCA (1.9 mol·dm<sup>-3</sup>) compared to DGEBA/DDM  
 1579 with 0.3 mol·dm<sup>-3</sup>. The higher molecular weight between crosslinks in the DGEBA thermoset led to a higher chain

1580 mobility in the network. In addition, hydrogen bonding with the furanic ring, increases the rigidity of the network at  
 1581 low temperatures. Higher crosslinking densities with 33DDS and 44DDS were also measured. Mechanical  
 1582 properties of DGEFDCA cured with DDM were also higher than for DGEBA network, with a storage modulus at  
 1583 the rubbery state (22.3 MPa compared to 2.69 MPa for DGEBA). The networks with 33DDS and 44DDS gave  
 1584 similar results both at glassy and rubbery states. Elongation at break, tensile strength and the shore hardness were  
 1585 slightly better for the furanic based network compared to the DGEBA/DDS systems. The rigidity that is brought by  
 1586 the furan moiety seems to be beneficial for the mechanical properties of the cured thermosets. Mechanical properties  
 1587 for networks with D230 were also investigated. The obtained flexural strength was lower for DGEFDCA thermoset,  
 1588 with a strength of 75 MPa, compared with 121 for DGEBA. The flexural moduli was 2.5 GPa for DGEFDCA/D230  
 1589 and 2.95 GPa for DGEBA/D230.<sup>155</sup> The flexural tests performed on networks with different hardeners demonstrate  
 1590 that DGEFDCA networks are stiffer and more brittle compared to DGEBA networks. The thermal stabilities of the  
 1591 networks were also evaluated under inert atmosphere. For the D230 networks, the  $T_{d5\%}$  of DGEFDCA was 267 °C  
 1592 and the char yield 6.8 %, compared to DGEBA/D230 with  $T_{d5\%}$  of 366 °C and char yield of 4.4 %. The DDM  
 1593 network led to  $T_{d5\%}$  of 326 °C and char yield of 28.1 % for DGEFDCA. Finally, for DDS cured materials, the  $T_{d5\%}$   
 1594 was 324 °C for both 33DDS and 44DDS with DGEFDCA, and respectively 27 and 18 % char yields, compared to  
 1595 405 and 397 °C for DGEBA/33DDS and DGEBA/44DDS with 20 and 14 % char yields. As discussed earlier, the  
 1596 furan-based thermosets have lower degradation temperatures, but higher char yields. The work of Meng *et al.* also  
 1597 focused on fire resistance behaviour of the thermosets. They reported that the total heat release of DGEFDCA based  
 1598 networks was lower than DGEBA networks. They also showed that the heat release capacities were lower with the  
 1599 furanic epoxide, namely 132 J·g<sup>-1</sup>·K<sup>-1</sup> and 222 J·g<sup>-1</sup>·K<sup>-1</sup> for DGEFDCA/33DDS and DGEFDCA/44DDS  
 1600 respectively (compared to DGEBA/33DDS HRC of 601 J·g<sup>-1</sup>·K<sup>-1</sup> and DGEBA/44DDS HRC of 516 J·g<sup>-1</sup>·K<sup>-1</sup>). These  
 1601 results show that furanic based networks have lower flammability, even if they degrade at lower temperature. The  
 1602 work of Sutton *et al.* assessed several endocrine activities of furanic compounds. FDCA was thus evaluated in  
 1603 CALUX bioassays, for the determination of endocrine activity on ER $\alpha$ , an androgen receptor, and also a thyroid  
 1604 receptor.<sup>159</sup> FDCA did not show any activity on sexual hormone receptors, but it did show a repression activity on  
 1605 the thyroid TR $\beta$  receptor. The activity obtained with 1 gram of nonylphenol was equivalent to the activity of 1700  
 1606 grams of FDCA, meaning that the compound could have an activity at a high exposure. However, these in vitro tests  
 1607 are not enough to assess the activity of the compound and more studies are required to get reliable results.

## 1609 II. 2,5-furfuryldiol

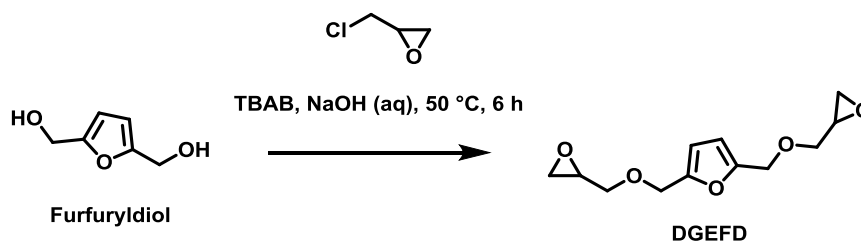


Figure 52 - Synthesis of DGEFD according to Meng *et al.*<sup>160</sup>

1613 Diglycidylether of 2,5-furfuryldiol is a monofuranic diepoxy that has been extensively studied (Figure 52), as a  
 1614 substitute for DGEBA. Several articles reported properties of thermoset with different diamine hardeners, such as  
 1615 PACM<sup>161,162</sup>, 4,4'-DDS and 3,3'-DDS<sup>163</sup>, polyethers diamines (commercially known as EDR-148 and EDR-192)<sup>160</sup>,  
 1616 DDM<sup>164</sup> and some furfurylamine derivatives.<sup>161</sup> These studies suggest that the use of DGEFD give lower  $T_g$  values  
 1617 than DGEBA, but with superior mechanical properties such as higher Young's moduli, higher tensile and flexural  
 1618 strength, lower flammability, higher char yield and lower degradation temperatures. The dynamic mechanical  
 1619 properties of these compounds are summarized in Table 4. As can be de-ducted from these data, the higher glass  
 1620 transition temperatures (or alpha transition) from DGEBA thermoset are probably due to the higher aromatic density  
 1621 brought by the bisphenolic moiety. The rigidity of the network (due to aromatics) is not counterbalanced with higher  
 1622 crosslinking density from DGEFD, due to the lower molecular weight of the monomer. Intermolecular interactions  
 1623 such as pi-stacking may also explain the higher  $T_g$  with DGEBA, contrary to DGEFD. However, at the glassy state,  
 1624 the Young's moduli were higher for DGEFD, which may be due to the dense packing of the network (crosslinking  
 1625 density) and the intermolecular interactions such as hydrogen bonding brought about by the oxygen of the furan. At  
 1626 the rubbery state, the networks with DDS and DGEFD had higher Young's moduli, most likely due to the packing  
 1627 density of the network, as hydrogen bonding should become very weak at higher temperatures.<sup>163</sup>

1628

1629  
1630

Table 4 - Mechanical and thermal properties of DGEFD cured with different amines, and compared with DGEBA

Amine Hardener	$T_g$ or $T_\alpha$ (°C)		$E'_{\text{glassy}}$ (GPa)		$E'_{\text{rubbery}}$ (MPa)	
	DGEBA	DGEFD	DGEBA	DGEFD	DGEBA	DGEFD
33DDS	184	102	1.9	2.4	17.56	36.15
44DDS	238	114	1.9	2.7	16.02	24.53
DEGA	-	13.5	-	-	-	-
EDR-148	98 / 108 <sup>122</sup>	13	1.34 <sup>122</sup>	-	13.2 <sup>122</sup>	-
EDR-192	-	7.6	-	-	-	-
PACM	176	80	2.37	approx. 2.5	-	-
Epikure W	198	94	-	-	-	-
DFDA	121	62	approx. 2.5	approx. 3.5	-	-
DFDA-Me	128	69	approx. 2.5	approx. 3.5	-	-
DDM	164 <sup>116</sup>	126 / 149	-	2.4	-	17

1631

1632 Regarding the thermal stability of DGEFD thermosets under inert atmosphere, as shown in Table 5 it is clear that the  
1633 stability of the resins is lower than DGEBA. This is probably due to the presence of the methylene moieties in  
1634 DGEFD, compared to DGEBA, where the glycidylether is directly attached to the phenol moiety. However, as often  
1635 observed for thermosets containing furan rings, the char yield is higher in the DGEFD thermosets.  
1636

1637 Table 5 - Thermal stability of DGEFD thermosets cured with different amines, and compared with DGEBA

Amine Hardener	$T_{d5\%}$ (°C)		Char yield (%)	
	DGEBA	DGEFD	DGEBA	DGEFD
33DDS	402	302	20.5	44.1
44DDS	398	255	13.8	42.3
DEGA	-	308	-	21
EDR-148	300 <sup>122</sup>	314	12 <sup>122</sup>	19
EDR-192	-	326	-	15.8
PACM	336	303	0	6
Epikure W	-	-	-	-
DFDA	301	272	<25	40
DFDA-Me	315	303 / 296*	<25	39 / 2*
DDM	376 <sup>138</sup>	296*	15 <sup>138</sup>	4*

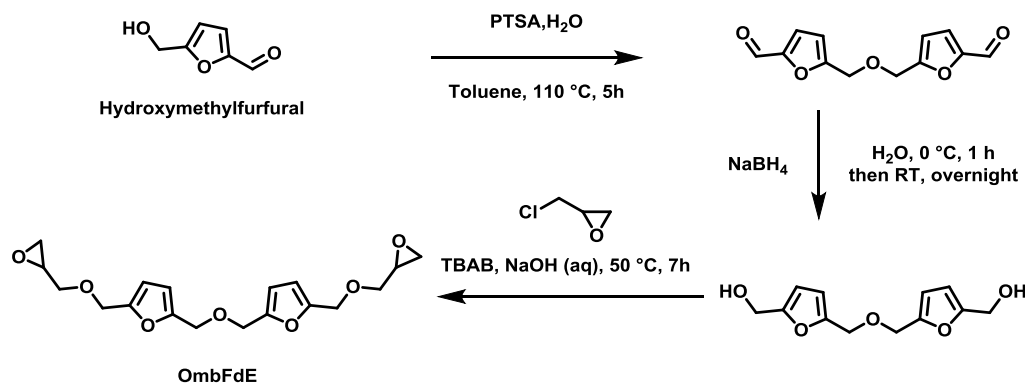
1638 \* under air

1639 Additional properties were also evaluated. Meng *et al.* characterized mechanical properties via measuring the  
1640 flexural and tensile strength.<sup>163</sup> They have shown that the DGEFD-based epoxy networks had superior mechanical  
1641 properties. Both the tensile and flexural strengths were higher for DGEFD than for DGEBA. The shore hardness  
1642 was also higher in the case of the furan-based epoxy. They reported that the tensile strength of DGEFD cured with  
1643 44DDS was comparable to that of polyoxymethylene and Nylon-6. These enhanced mechanical properties were  
1644 mainly attributed to the hydrogen bonds formed thanks to the heterocycle of DGEFD. The fire resistance of the  
1645 cured material was also investigated. For example, it was shown that DGEFD cured with both DDS and amine  
1646 could self-extinguish in 7 seconds. DGEBA-based networks burnt for longer times, where the flame spreading  
1647 reached 10.2 mm·min<sup>-1</sup> for DGEBA/44DDS and 8.5 mm·min<sup>-1</sup> for DGEBA/33DDS. The self-extinction of DGEFD  
1648 thermoset could be explained by the higher char formation due to the presence of the furan rings. The influence of  
1649 the amine is also very important. In a different work, using polyetheramines as the curing agents (EDR-148 and  
1650 EDR-192), it shown that DGEFD thermoset could stay ignited for longer times (> 60 s).<sup>160</sup> The flammability was  
1651 lowered by using the same curing agent with a monomer bearing 2 furan rings. The ability to self-extinguish may  
1652 probably be influenced by a ratio of furan rings to the alkylether with better resistance to fire with higher loadings of  
1653 furan rings. In the case of DGEFD/DDS system, the synergy between aromatic and furanic rings led to low  
1654 flammability. These results were also confirmed by microscale combustion calorimetry. The DGEFD/DDS systems



1655 showed lower heat release capacities ( $121 \text{ J}\cdot\text{g}^{-1}\cdot\text{K}^{-1}$  for 33DDS and  $179 \text{ J}\cdot\text{g}^{-1}\cdot\text{K}^{-1}$  for 44DDS), than for DGEBA  
 1656 (respectively 601 and  $516 \text{ J}\cdot\text{g}^{-1}\cdot\text{K}^{-1}$ ). The total heat release of the networks with DGEFD were also lower than with  
 1657 DGEBA, precisely  $14.9$  and  $23.6 \text{ kJ}\cdot\text{g}^{-1}$  for 33DDS and 44DDS cured materials, compared to  $32.3$  and  $36.4 \text{ kJ}\cdot\text{g}^{-1}$   
 1658 for DGEBA/33DDS and DGEBA/44DDS networks. In the work of Hong *et al.*,<sup>82</sup> one furan-containing molecule  
 1659 was considered. The furfuryldiol was predicted to be non-binder to the oestrogenic receptor  $\alpha$  with a good reliability.  
 1660 In a recent paper by Sutton *et al.*, several new furfuryldiols were synthesized and their toxicity was assessed.<sup>159</sup>  
 1661 Especially, endocrine activity for several receptor such as human oestrogen receptor  $\alpha$ , androgen receptor and a  
 1662 thyroid receptor, were evaluated. In all the trials, the CALUX bioassays did not show any activity. For ER $\alpha$   
 1663 activity, no dose-dependent response was seen. Furfuryldiol did not show any potential *in vitro* endocrine activity.

### 1664 III. Bisfuran with ether linker



1667  
1668 Figure 53 - Synthesis of OmbFdE according to Meng *et al.* from hydroxymethylfurfural<sup>160</sup>

1669 The bisfuranic diepoxide monomer, OmbFdE, was prepared by dimerization of hydroxymethylfurfural (HMF), via a  
 1670 dehydration reaction.<sup>160</sup> The obtained dialdehyde was then reduced with sodium borohydride to afford the  
 1671 corresponding diol. The glycidylation of the diol led to the formation of the diepoxide monomer (Figure 53). This  
 1672 diepoxide monomer was then cured with different alkylether amines, containing respectively 1 ether linkage (DEGA),  
 1673 2 ether moieties (also known as EDR-148) and 3 ether moieties (*aka* EDR-192). Thermomechanical properties were  
 1674 measured, and also fire resistancy was investigated. Comparison with DGEBA was not performed, but data of the  
 1675 network with EDR-148 hardener can be found in the article of Faye *et al.*<sup>122</sup> Glass transition temperatures of EDR-  
 1676 148 network with OmbdFdE was  $20.6 \text{ }^\circ\text{C}$  whereas with DGEBA it was  $98 \text{ }^\circ\text{C}$  as obtained by DSC. The presence of  
 1677 numerous alkyl ether linkages in OmbFdE led to higher segmental mobility inside the networks. This is confirmed  
 1678 by the fact that curing OmbFdE with amine containing increasing number of alkylethers, lowers the  $T_g$  (from  $25$  to  $7$   
 1679  $^\circ\text{C}$ ). The comparison with the above mentioned DGEFD containing two furan rings showed that the higher content  
 1680 of furan rings results in higher  $T_g$  values. It seems that even though the use of OmbFdE leads to lower molecular  
 1681 weight between the crosslinks, the  $T_g$  would still be higher when two furan rings are present as compared to one in  
 1682 the case of DGEFD.

1683 Examination of the thermal stability and fire resistance, showed that,  $T_{d5\%}$  of the cured materials were in the range of  
 1684  $265\text{-}291 \text{ }^\circ\text{C}$ , with the obtained lower temperature for EDR-148 cured monomer. Compared with DGEBA/EDR-148,  
 1685 with a  $T_{d5\%}$  of  $300 \text{ }^\circ\text{C}$ , the furanic based monomer showed a lower degradation temperature, as often observed.  
 1686 However, a higher char yield was obtained with OmbFdE, in the range of  $18\text{-}25 \%$ . This is higher than the case of  
 1687 DGEBA/EDR-148 network with  $12 \%$ , and DGEFD with  $15\text{-}21 \%$ . The presence of heterocycles is known to  
 1688 improve the char formation, as evidenced in the case of OmbFdE with 2 furan rings ( ) (compared to one in  
 1689 DGEFD). The presence of these two rings also had an effect on the behaviour of the material in fire. Faster self-  
 1690 extinction was obtained with OmbFdE compared to DGEFD. In addition, the total heat release of OmbFdE/EDR-  
 1691 148 was lower compared to DGEFD ( $13.7 \text{ kJ}\cdot\text{g}^{-1}$  vs  $15.6$ ), showing improvement due to the furan loading. In the  
 1692 work of Sutton *et al.*, the endocrine activity of the OmbFdE diol derivative was assessed *in vitro*, using CALUX  
 1693 testing methods.<sup>159</sup> Several parameters were evaluated such as activity on the ER $\alpha$ , the androgen receptor, and also a  
 1694 thyroid receptor. The diol did not show any activity against the oestrogen  $\alpha$  receptor, nor the thyroid receptor.  
 1695 However, a repression effect on the androgen receptor was observed, but at higher concentrations than the  
 1696 corresponding reference, Flutamide (an androgen repressor drug). These *in vitro* results are not sufficient to assess  
 1697 the global impact on human health.

1698

## 1699 Conclusion and perspectives

1700

1701 As shown in this review, a lot of epoxy monomer precursors could be derived from biomass feedstock, with a wide  
1702 range of properties. Some of these new materials show promising results for specific applications, and depending on  
1703 the targeted properties, some may be suitable to replace DGEBA. However, for some, the starting materials have  
1704 shown some serious toxicity issues, such as resorcinol. Some others are already known to mimic oestradiol (the  
1705 natural oestrogen hormone). When selecting a potential BPA substituent, one should be aware of the existing tested  
1706 precursors for their health hazard. Biobased compounds are seen as promising alternative to replace epoxy monomer  
1707 precursors. Indeed, the wide range of functionalities available in nature is an infinite source of innovation for  
1708 polymer chemists. The findings gathered here show that many of structures lead to thermoset properties that are  
1709 close to DGEBA based systems. A balance in material properties have to be found between thermal or mechanical  
1710 properties, when trying to remove BPA in epoxy resins. It is unlikely that a universal substitute could be found to  
1711 replace DGEBA. Indeed, most of the time the potential alternatives to BPA lead to lower mechanical properties.  
1712 Hence, the entire formulation must be replaced, and new hardeners should be envisaged. For example, the use of  
1713 amido-amines instead of amines could allow to restore some mechanical properties. One of the main issues with  
1714 BPA is not only that it is harmful, but it is also because its constant presence our daily lives, multiplying the chances  
1715 of exposure to the substance. The diversity of structures offered by bioresources could help to tackle the challenge  
1716 of BPA elimination, but if for each application a new monomer is required, the profitability will be difficult to attain  
1717 for industry, however, biorefining is developing opening new routes to obtain bio-sourced compounds.<sup>165</sup>  
1718 Substitution of harmful chemicals should not focus only on a single side of the problem. Using biomass feedstock  
1719 does not truly guarantee a sustainable approach. Hence, the use of low environmental impact biomass should be  
1720 favoured, such as cardanol. Hence, this non-edible natural phenol is a side-products of the production of cashew nut  
1721 and is not used. Moreover, if left on the soil after cashew harvesting, it could entail adverse effect to the  
1722 environment. Its production should attain 1Mt/y in the coming years, making this compound a promising starting  
1723 substance for the replacement of BPA. This review underlines also that using natural compounds to replace  
1724 petroleum based BPA could also lead to regrettable substitutions.<sup>166,167</sup> For example of the use of phytoestrogens,  
1725 such as resveratrol or daidzein should be taken with caution when used for the substitution of BPA. To avoid such  
1726 issues, the development of easily affordable methods to assess the toxicity of compounds are highly desirable. Many  
1727 research groups are developing such tests.<sup>168</sup> It is also worth mentioning that bio-refining should be performed also  
1728 with the evaluation of greenhouse gas emissions, to ensure that fossil resources substitution is environmentally  
1729 viable. The use of life-cycle analysis or other green metrics is also encouraged to determine the environmental  
1730 performance of the substitution.<sup>169,170</sup> Collaboration between scientists in different fields, and the access to easy-to-  
1731 use tools will improve the impact of the research in this field.

1732

1733

## 1734 References

1735

- 1736 1 Polaris Market Research, *Epoxy Resins Market Share, Size, Trends, Industry Analysis Report*, 2020.
- 1737 2 M. A. Hillmyer, *Science* (80-. ), 2017, **358**, 868–870.
- 1738 3 D. J. C. Constable, *ACS Sustain. Chem. Eng.*, 2020, **8**, 14657–14667.
- 1739 4 G. John, S. Nagarajan, P. K. Vemula, J. R. Silverman and C. K. S. Pillai, *Prog. Polym. Sci.*, 2019, **92**, 158–  
1740 209.
- 1741 5 J. S. Terry and A. C. Taylor, *J. Appl. Polym. Sci.*, 2021, 50417.
- 1742 6 R. Auvergne, S. Caillol, G. David, B. Boutevin and J.-P. Pascault, *Chem. Rev.*, 2014, **114**, 1082–1115.
- 1743 7 S. Kumar, S. Krishnan, S. Mohanty and S. K. Nayak, *Polym. Int.*, 2018, **67**, 815–839.
- 1744 8 F. A. M. M. Gonçalves, M. Santos, T. Cernadas, P. Ferreira and P. Alves, *Int. Mater. Rev.*, 2021, **0**, 1–31.
- 1745 9 R. L. Quirino, K. Monroe, C. H. Fleischer, E. Biswas and M. R. Kessler, *Polym. Int.*, 2021, **70**, 167–180.
- 1746 10 J. Liu, S. Wang, Y. Peng, J. Zhu, W. Zhao and X. Liu, *Prog. Polym. Sci.*, 2021, **113**, 101353.
- 1747 11 J. Liu, L. Zhang, W. Shun, J. Dai, Y. Peng and X. Liu, *J. Polym. Sci.*, 2021, **59**, 1474–1490.
- 1748 12 E. Ramon, C. Sguazzo and P. M. G. P. Moreira, *Aerospace*, , DOI:10.3390/aerospace5040110.

- 1749 13 F. Ng, G. Couture, C. Philippe, B. Boutevin and S. Caillol, *Molecules*, 2017, **22**, 149.
- 1750 14 J. Wan, J. Zhao, X. Zhang, H. Fan, J. Zhang, D. Hu, P. Jin and D.-Y. Wang, *Prog. Polym. Sci.*, 2020, **108**,  
1751 101287.
- 1752 15 S. Caillol, B. Boutevin and R. Auvergne, *Polymer (Guildf)*, 2021, **223**, 123663.
- 1753 16 N. Eid, B. Ameduri and B. Boutevin, *ACS Sustain. Chem. Eng.*, 2021, **9**, 8018–8031.
- 1754 17 L. Trullemans, S.-F. Koelewijn, I. Scodeller, T. Hendrickx, P. Van Puyvelde and B. F. Sels, *Polym. Chem.*,  
1755 2021, **12**, 5870–5901.
- 1756 18 A. Llevot, E. Grau, S. Carlotti, S. Grelier and H. Cramail, *Macromol. Rapid Commun.*, 2016, **37**, 9–28.
- 1757 19 J. S. Mahajan, R. M. O’Dea, J. B. Norris, L. T. J. Korley and T. H. Epps, *ACS Sustain. Chem. Eng.*, 2020, **8**,  
1758 15072–15096.
- 1759 20 J. Sternberg, O. Sequerth and S. Pilla, *Prog. Polym. Sci.*, 2021, **113**, 101344.
- 1760 21 G. F. Bass and T. H. Epps, *Polym. Chem.*, 2021, 4130–4158.
- 1761 22 F. Liguori, C. Moreno-Marrodan and P. Barbaro, *Chem. Soc. Rev.*, 2020, **49**, 6329–6363.
- 1762 23 M. Decostanzi, R. Auvergne, B. Boutevin and S. Caillol, *Green Chem.*, 2019, **21**, 724–747.
- 1763 24 V. Froidevaux, C. Negrell, S. Caillol, J. P. Pascault and B. Boutevin, *Chem. Rev.*, 2016, **116**, 14181–14224.
- 1764 25 C. Ding and A. S. Matharu, *ACS Sustain. Chem. Eng.*, 2014, **2**, 2217–2236.
- 1765 26 F. Vilarinho, R. Sendón, A. van der Kellen, M. F. Vaz and A. S. Silva, *Trends Food Sci. Technol.*, 2019, **91**,  
1766 33–65.
- 1767 27 P. Mercea, *J. Appl. Polym. Sci.*, 2009, **112**, 579–593.
- 1768 28 A. Goodson, H. Robin, W. Summerfield and I. Cooper \*, *Food Addit. Contam.*, 2004, **21**, 1015–1026.
- 1769 29 S. Errico, M. Bianco, L. Mita, M. Migliaccio, S. Rossi, C. Nicolucci, C. Menale, M. Portaccio, P. Gallo, D.  
1770 G. Mita and N. Diano, *Food Chem.*, 2014, **160**, 157–164.
- 1771 30 S. Almeida, A. Raposo, M. Almeida-González and C. Carrascosa, *Compr. Rev. Food Sci. Food Saf.*, 2018,  
1772 **17**, 1503–1517.
- 1773 31 R. Joskow, D. B. Barr, J. R. Barr, A. M. Calafat, L. L. Needham and C. Rubin, *J. Am. Dent. Assoc.*, 2006,  
1774 **137**, 353–362.
- 1775 32 N. K. Wilson, J. C. Chuang, M. K. Morgan, R. A. Lordo and L. S. Sheldon, *Environ. Res.*, 2007, **103**, 9–20.
- 1776 33 L. Wang, Y. Zhang, Y. Liu, X. Gong, T. Zhang and H. Sun, *Environ. Sci. Technol.*, 2019, **53**, 7095–7102.
- 1777 34 A. M. Brzozowski, A. C. W. Pike, Z. Dauter, R. E. Hubbard, T. Bonn, O. Engström, L. Öhman, G. L.  
1778 Greene, J.-Å. Gustafsson and M. Carlquist, *Nature*, 1997, **389**, 753–758.
- 1779 35 H. Okada, T. Tokunaga, X. Liu, S. Takayanagi, A. Matsushima and Y. Shimohigashi, *Environ. Health  
1780 Perspect.*, 2008, **116**, 32–38.
- 1781 36 H. Fang, W. Tong, L. M. Shi, R. Blair, R. Perkins, W. Branham, B. S. Hass, Q. Xie, S. L. Dial, C. L.  
1782 Moland and D. M. Sheehan, *Chem. Res. Toxicol.*, 2001, **14**, 280–294.
- 1783 37 H. MacKay and A. Abizaid, *Horm. Behav.*, 2018, **101**, 59–67.
- 1784 38 R. Hampl, J. Kubátová and L. Stárka, *J. Steroid Biochem. Mol. Biol.*, 2016, **155**, 217–223.
- 1785 39 D. Chen, K. Kannan, H. Tan, Z. Zheng, Y.-L. Feng, Y. Wu and M. Widelka, *Environ. Sci. Technol.*, 2016,  
1786 **50**, 5438–5453.
- 1787 40 M. Fache, B. Boutevin and S. Caillol, *ACS Sustain. Chem. Eng.*, 2016, **4**, 35–46.
- 1788 41 M. Fache, E. Darroman, V. Besse, R. Auvergne, S. Caillol and B. Boutevin, *Green Chem.*, 2014, **16**, 1987.

- 1789 42 X. Ji, N. Li, S. Yuan, X. Zhou, F. Ding, K. Rao, M. Ma and Z. Wang, *Ecotoxicol. Environ. Saf.*, 2019, **175**,  
1790 208–214.
- 1791 43 S. Ramachandra Rao and G. Ravishankar, *J. Sci. Food Agric.*, 2000, **80**, 289–304.
- 1792 44 M. Fache, R. Auvergne, B. Boutevin and S. Caillol, *Eur. Polym. J.*, 2015, **67**, 527–538.
- 1793 45 E. D. Hernandez, A. W. Bassett, J. M. Sadler, J. J. La Scala and J. F. Stanzione, *ACS Sustain. Chem. Eng.*,  
1794 2016, **4**, 4328–4339.
- 1795 46 F. Ng, L. Bonnet, G. David and S. Caillol, *Prog. Org. Coatings*, 2017, **109**, 1–8.
- 1796 47 Y. Tian, Q. Wang, Y. Hu, H. Sun, Z. Cui, L. Kou, J. Cheng and J. Zhang, *Polymer (Guildf.)*, 2019, **178**,  
1797 121592.
- 1798 48 J. Wan, B. Gan, C. Li, J. Molina-Aldareguia, E. N. Kalali, X. Wang and D.-Y. Wang, *Chem. Eng. J.*, 2016,  
1799 **284**, 1080–1093.
- 1800 49 F. G. Garcia, B. G. Soares, V. J. R. R. Pita, R. Sánchez and J. Rieumont, *J. Appl. Polym. Sci.*, 2007, **106**,  
1801 2047–2055.
- 1802 50 L. F. C. Nascimento, F. S. da Luz, U. O. Costa, F. de O. Braga, É. P. Lima Júnior and S. N. Monteiro,  
1803 *Materials (Basel)*, 2019, **12**, 3939.
- 1804 51 S. K. Sahoo, S. Mohanty and S. K. Nayak, *Chinese J. Polym. Sci.*, 2015, **33**, 137–152.
- 1805 52 P. Gnanasekar, M. Feng and N. Yan, *ACS Sustain. Chem. Eng.*, 2020, **8**, 17417–17426.
- 1806 53 S. Zhao, X. Huang, A. J. Whelton and M. M. Abu-Omar, *ACS Sustain. Chem. Eng.*, 2018, **6**, 7600–7608.
- 1807 54 P. Gnanasekar, H. Chen, N. Tratnik, M. Feng and N. Yan, *Compos. Part B Eng.*, 2021, **207**, 108585.
- 1808 55 J. Meng, Y. Zeng, P. Chen, J. Zhang, C. Yao, Z. Fang and K. Guo, *Eur. Polym. J.*, 2019, **121**, 109292.
- 1809 56 J. R. Mauck, S. K. Yadav, J. M. Sadler, J. J. La Scala, G. R. Palmese, K. M. Schmalbach and J. F.  
1810 Stanzione, *Macromol. Chem. Phys.*, 2017, **218**, 1700013.
- 1811 57 A.-S. Mora, R. Tayouo, B. Boutevin, G. David and S. Caillol, *Molecules*, 2019, **24**, 3285.
- 1812 58 A.-S. Mora, R. Tayouo, B. Boutevin, G. David and S. Caillol, *Green Chem.*, 2018, **20**, 4075–4084.
- 1813 59 C. Noè, S. Malburet, A. Bouvet-Marchand, A. Graillet, C. Loubat and M. Sangermano, *Prog. Org.*  
1814 *Coatings*, 2019, **133**, 131–138.
- 1815 60 Z. Wang, P. Gnanasekar, S. Sudhakaran Nair, R. Farnood, S. Yi and N. Yan, *ACS Sustain. Chem. Eng.*,  
1816 2020, **8**, 11215–11223.
- 1817 61 C. Aouf, J. Lecomte, P. Villeneuve, E. Dubreucq and H. Fulcrand, *Green Chem.*, 2012, **14**, 2328.
- 1818 62 M. Shen, R. Almallahi, Z. Rizvi, E. Gonzalez-Martinez, G. Yang and M. L. Robertson, *Polym. Chem.*, 2019,  
1819 **10**, 3217–3229.
- 1820 63 M. Shen and M. L. Robertson, *ACS Sustain. Chem. Eng.*, 2021, **9**, 438–447.
- 1821 64 Z. Fang, M. C. Weisenberger and M. S. Meier, *ACS Appl. Bio Mater.*, 2020, **3**, 881–890.
- 1822 65 M. Fache, C. Montéremal, B. Boutevin and S. Caillol, *Eur. Polym. J.*, 2015, **73**, 344–362.
- 1823 66 M. Fache, A. Viola, R. Auvergne, B. Boutevin and S. Caillol, *Eur. Polym. J.*, 2015, **68**, 526–535.
- 1824 67 Y. Liu and G. Huang, *J. Chromatogr. Sci.*, 2018, **56**, 65–67.
- 1825 68 A. Fic, B. Žegura, D. Gramec and L. P. Mašič, *Chemosphere*, 2014, **112**, 362–369.
- 1826 69 E. Savonnet, E. Grau, S. Grelier, B. Defoort and H. Cramail, *ACS Sustain. Chem. Eng.*, 2018, **6**, 11008–  
1827 11017.
- 1828 70 A. Llevot, E. Grau, S. Carlotti, S. Grelier and H. Cramail, *Polym. Chem.*, 2015, **6**, 6058–6066.

- 1829 71 E. Savonnet, C. Le Coz, E. Grau, S. Grelier, B. Defoort and H. Cramail, *Front. Chem.*, 2019, **7**, 1–6.
- 1830 72 S. V. Mankar, M. N. Garcia Gonzalez, N. Warlin, N. G. Valsange, N. Rehnberg, S. Lundmark, P. Jannasch  
1831 and B. Zhang, *ACS Sustain. Chem. Eng.*, 2019, **7**, 19090–19103.
- 1832 73 M. Ochi, M. Shimbo, M. Saga and N. Takashima, *J. Polym. Sci. Part B Polym. Phys.*, 1986, **24**, 2185–2195.
- 1833 74 M. Ochi, M. Yoshizumi and M. Shimbo, *J. Polym. Sci. Part B Polym. Phys.*, 1987, **25**, 1817–1827.
- 1834 75 W. Yuan, S. Ma, S. Wang, Q. Li, B. Wang, X. Xu, K. Huang, J. Chen, S. You and J. Zhu, *Eur. Polym. J.*,  
1835 2019, **117**, 200–207.
- 1836 76 K. H. Nicastro, C. J. Kloxin and T. H. Epps, *ACS Sustain. Chem. Eng.*, 2018, **6**, 14812–14819.
- 1837 77 S.-F. Koelewijn, D. Ruijten, L. Trullemans, T. Renders, P. Van Puyvelde, H. Witters and B. F. Sels, *Green  
1838 Chem.*, 2019, **21**, 6622–6633.
- 1839 78 A. T. Szafran, F. Stossi, M. G. Mancini, C. L. Walker and M. A. Mancini, *PLoS One*, 2017, **12**, e0180141.
- 1840 79 Y. Peng, K. H. Nicastro, T. H. Epps and C. Wu, *J. Agric. Food Chem.*, 2018, **66**, 11775–11783.
- 1841 80 Y. Peng, K. H. Nicastro, T. H. Epps and C. Wu, *Food Chem.*, 2021, **338**, 127656.
- 1842 81 A. Amitrano, J. S. Mahajan, L. T. J. Korley and T. H. Epps, *RSC Adv.*, 2021, **11**, 22149–22158.
- 1843 82 H. Hong, B. Harvey, G. Palmese, J. Stanzone, H. Ng, S. Sakkiyah, W. Tong and J. Sadler, *Int. J. Environ.  
1844 Res. Public Health*, 2016, **13**, 705.
- 1845 83 M. Mogheiseh, R. Karimian and M. Khoshsefat, *Chem. Pap.*, 2020, **74**, 3347–3358.
- 1846 84 M. Shibata and T. Ohkita, *Eur. Polym. J.*, 2017, **92**, 165–173.
- 1847 85 R. Ménard, C. Negrell, M. Fache, L. Ferry, R. Sonnier and G. David, *RSC Adv.*, 2015, **5**, 70856–70867.
- 1848 86 M. Janvier, L. Hollande, A. S. Jaufurally, M. Pernes, R. Ménard, M. Grimaldi, J. Beaugrand, P. Balaguer,  
1849 P.-H. Ducrot and F. Allais, *ChemSusChem*, 2017, **10**, 738–746.
- 1850 87 A. S. Jaufurally, A. R. S. Teixeira, L. Hollande, F. Allais and P.-H. Ducrot, *ChemistrySelect*, 2016, **1**, 5165–  
1851 5171.
- 1852 88 R. Ménard, S. Caillol and F. Allais, *Ind. Crops Prod.*, 2017, **95**, 83–95.
- 1853 89 A. Tarzia, J. Montanaro, M. Casiello, C. Annese, A. Nacci and A. Maffezzoli, *BioResources*, 2017, **13**, 632–  
1854 645.
- 1855 90 C. Aouf, C. Le Guernevé, S. Caillol and H. Fulcrand, *Tetrahedron*, 2013, **69**, 1345–1353.
- 1856 91 J. Duchet and J. P. Pascault, *J. Polym. Sci. Part B Polym. Phys.*, 2003, **41**, 2422–2432.
- 1857 92 C. Aouf, H. Nouailhas, M. Fache, S. Caillol, B. Boutevin and H. Fulcrand, *Eur. Polym. J.*, 2013, **49**, 1185–  
1858 1195.
- 1859 93 N. Araki, K. Ohno, M. Nakai, M. Takeyoshi and M. Iida, *Toxicol. Vitro.*, 2005, **19**, 831–842.
- 1860 94 M. Trivedi, D. Vaidya, C. Patel, S. Prajapati and J. Bhatt, *Chemosphere*, 2020, **241**, 125076.
- 1861 95 E. Valanciene, I. Jonuskiene, M. Syrpas, E. Augustiniene, P. Matulis, A. Simonavicius and N. Malys,  
1862 *Biomolecules*, 2020, **10**, 874.
- 1863 96 W. Li, D. Xie and J. W. Frost, *J. Am. Chem. Soc.*, 2005, **127**, 2874–2882.
- 1864 97 O. E. Örn, S. Sacchetto, E. W. J. van Niel and R. Hatti-Kaul, *Front. Bioeng. Biotechnol.*, 2021, **9**, 1–10.
- 1865 98 X. Chen, J. Hou, Q. Gu, Q. Wang, J. Gao, J. Sun and Q. Fang, *Polymer (Guildf.)*, 2020, **195**, 122443.
- 1866 99 Y. Tao, L. Fang, M. Dai, C. Wang, J. Sun and Q. Fang, *Polym. Chem.*, 2020, **11**, 4500–4506.
- 1867 100 J. Qin, G. Zhang, R. Sun and C. Wong, *J. Therm. Anal. Calorim.*, 2014, **117**, 831–843.
- 1868 101 L. Wang and K. Kannan, *Environ. Int.*, 2013, **59**, 27–32.

- 1869 102 A. Maiorana, A. F. Reano, R. Centore, M. Grimaldi, P. Balaguer, F. Allais and R. A. Gross, *Green Chem.*,  
1870 2016, **18**, 4961–4973.
- 1871 103 L. Hollande, I. Do Marcolino, P. Balaguer, S. Domenek, R. A. Gross and F. Allais, *Front. Chem.*, 2019, **7**,  
1872 1–11.
- 1873 104 F. Welsch, M. D. Nemeč and W. B. Lawrence, *Int. J. Toxicol.*, 2008, **27**, 43–57.
- 1874 105 ANSES, *Avis relatif à l'identification en tant que substance extrêmement préoccupante (SHVC) du*  
1875 *bisphénol A pour son caractère de perturbateur endocrinien*, 2020.
- 1876 106
- 1877 107 N. Mattar, A. R. de Anda, H. Vahabi, E. Renard and V. Langlois, *ACS Sustain. Chem. Eng.*, 2020, **8**,  
1878 13064–13075.
- 1879 108 J. F. Gerard, J. Galy, J. P. Pascault, S. Cukierman and J. L. Halary, *Polym. Eng. Sci.*, 1991, **31**, 615–621.
- 1880 109 K. B. Riad, R. Schmidt, A. A. Arnold, R. Wuthrich and P. M. Wood-Adams, *Polymer (Guildf.)*, 2016, **104**,  
1881 83–90.
- 1882 110 I. Pal Singh and S. B. Bharate, *Nat. Prod. Rep.*, 2006, **23**, 558.
- 1883 111 C. Blanchard, D. Pouchain, P. Vanderkam, M.-C. Perault-Pochat, R. Boussageon and H. Vaillant-Roussel,  
1884 *Eur. J. Clin. Pharmacol.*, 2018, **74**, 541–548.
- 1885 112 B. Thienpont, A. Tingaud-Sequeira, E. Prats, C. Barata, P. J. Babin and D. Raldúa, *Environ. Sci. Technol.*,  
1886 2011, **45**, 7525–7532.
- 1887 113 A. Maiorana, S. Spinella and R. A. Gross, *Biomacromolecules*, 2015, **16**, 1021–1031.
- 1888 114 A. Patel, A. Maiorana, L. Yue, R. A. Gross and I. Manas-Zloczower, *Macromolecules*, 2016, **49**, 5315–  
1889 5324.
- 1890 115 M. S. McMaster, T. E. Yilmaz, A. Patel, A. Maiorana, I. Manas-Zloczower, R. Gross and K. D. Singer, *ACS*  
1891 *Appl. Mater. Interfaces*, 2018, **10**, 13924–13930.
- 1892 116 L. Gao, G. Zheng, X. Nie and Y. Wang, *J. Therm. Anal. Calorim.*, 2017, **127**, 1419–1430.
- 1893 117 A. Patel, S. Mekala, O. G. Kravchenko, T. Yilmaz, D. Yuan, L. Yue, R. A. Gross and I. Manas-Zloczower,  
1894 *ACS Sustain. Chem. Eng.*, 2019, **7**, 16382–16391.
- 1895 118 O. Keminer, M. Teigeler, M. Kohler, A. Wenzel, J. Arning, F. Kaßner, B. Windshügel and E. Eilebrecht,  
1896 *Sci. Total Environ.*, 2020, **717**, 134743.
- 1897 119 F. M. McRobb, I. Kufareva and R. Abagyan, *Toxicol. Sci.*, 2014, **141**, 188–197.
- 1898 120 X. Colin, F. Essatbi, J. Delozanne and G. Moreau, *Polym. Degrad. Stab.*, ,  
1899 DOI:10.1016/j.polymdegradstab.2020.109314.
- 1900 121 T. Masuya, M. Iwamoto, X. Liu and A. Matsushima, *Sci. Rep.*, 2019, **9**, 9954.
- 1901 122 I. Faye, M. Decostanzi, Y. Ecochard and S. Caillol, *Green Chem.*, 2017, **19**, 5236–5242.
- 1902 123 M.-J. R. Howes, P. J. Houghton, D. J. Barlow, V. J. Pocock and S. R. Milligan, *J. Pharm. Pharmacol.*,  
1903 2002, **54**, 1521–1528.
- 1904 124 D. Guzmán, X. Ramis, X. Fernández-Francos, S. De la Flor and A. Serra, *Prog. Org. Coatings*, 2018, **114**,  
1905 259–267.
- 1906 125 T. Yoshimura, T. Shimasaki, N. Teramoto and M. Shibata, *Eur. Polym. J.*, 2015, **67**, 397–408.
- 1907 126 D. Santiago, D. Guzmán, X. Ramis, F. Ferrando and A. Serra, *Polymers (Basel)*, 2019, **12**, 44.
- 1908 127 S. Zhao and M. M. Abu-Omar, *Biomacromolecules*, 2015, **16**, 2025–2031.
- 1909 128 S. Zhao and M. M. Abu-Omar, *ACS Sustain. Chem. Eng.*, 2016, **4**, 6082–6089.
- 1910 129 S. F. Koelewijn, S. Van Den Bosch, T. Renders, W. Schutyser, B. Lagrain, M. Smet, J. Thomas, W. Dehaen,

- 1911 P. Van Puyvelde, H. Witters and B. F. Sels, *Green Chem.*, 2017, **19**, 2561–2570.
- 1912 130 J. Wan, B. Gan, C. Li, J. Molina-Aldareguia, Z. Li, X. Wang and D. Y. Wang, *J. Mater. Chem. A*, 2015, **3**,  
1913 21907–21921.
- 1914 131 C.-H. Chen, S.-H. Tung, R.-J. Jeng, M. M. Abu-Omar and C.-H. Lin, *Green Chem.*, 2019, **21**, 4475–4488.
- 1915 132 E. Zago, E. Dubreucq, J. Lecomte, P. Villeneuve, F. Fine, H. Fulcrand and C. Aouf, *New J. Chem.*, 2016,  
1916 **40**, 7701–7710.
- 1917 133 Y. Qi, Z. Weng, K. Zhang, J. Wang, S. Zhang, C. Liu and X. Jian, *Chem. Eng. J.*, 2020, **387**, 124115.
- 1918 134 Y. Lin, Y. Li, Y. Zeng, B. Tian, X. Qu, Q. Yuan and Y. Song, *Front. Pharmacol.*, ,  
1919 DOI:10.3389/fphar.2021.632767.
- 1920 135 A. Sarrica, N. Kirika, M. Romeo, M. Salmona and L. Diomede, *Planta Med.*, 2018, **84**, 1151–1164.
- 1921 136 M. D. Garrison, M. A. Savolainen, A. P. Chafin, J. E. Baca, A. M. Bons and B. G. Harvey, *ACS Sustain.*  
1922 *Chem. Eng.*, 2020, **8**, 14137–14149.
- 1923 137 M. Zwingelstein, M. Draye, J.-L. Besombes, C. Piot and G. Chatel, *Waste Manag.*, 2020, **102**, 782–794.
- 1924 138 M. D. Garrison and B. G. Harvey, *J. Appl. Polym. Sci.*, , DOI:10.1002/app.43621.
- 1925 139 Y. Tian, M. Ke, X. Wang, G. Wu, J. Zhang and J. Cheng, *Eur. Polym. J.*, 2021, **147**, 110282.
- 1926 140 R. J. Qasem, *Crit. Rev. Toxicol.*, 2020, **50**, 439–462.
- 1927 141 J. Dai, Y. Peng, N. Teng, Y. Liu, C. Liu, X. Shen, S. Mahmud, J. Zhu and X. Liu, *ACS Sustain. Chem. Eng.*,  
1928 2018, **6**, 7589–7599.
- 1929 142 Y.-S. Choi, B.-H. Lee, J.-H. Kim and N.-S. Kim, *J. Sci. Food Agric.*, 2000, **80**, 1709–1712.
- 1930 143 L. Křížová, K. Dadáková, J. Kašparovská and T. Kašparovský, *Molecules*, 2019, **24**, 1076.
- 1931 144 R. S. Muthyala, Y. H. Ju, S. Sheng, L. D. Williams, D. R. Doerge, B. S. Katzenellenbogen, W. G. Helferich  
1932 and J. A. Katzenellenbogen, *Bioorg. Med. Chem.*, 2004, **12**, 1559–1567.
- 1933 145 T. Gao, F. Wang, Y. Xu, C. Wei, S. Zhu, W. Yang and H.-D. Lu, *Chem. Eng. J.*, 2022, **428**, 131173.
- 1934 146 M. F. Manzoor, N. Ahmad, Z. Ahmed, R. Siddique, X. Zeng, A. Rahaman, R. Muhammad Aadil and A.  
1935 Wahab, *J. Food Biochem.*, 2019, **43**, 1–19.
- 1936 147 R. H. Waring, S. Ayers, A. J. Gescher, H.-R. Glatt, W. Meinel, P. Jarratt, C. J. Kirk, T. Pettitt, D. Rea and R.  
1937 M. Harris, *J. Steroid Biochem. Mol. Biol.*, 2008, **108**, 213–220.
- 1938 148 R. M. Harris, D. M. Wood, L. Bottomley, S. Blagg, K. Owen, P. J. Hughes, R. H. Waring and C. J. Kirk, *J.*  
1939 *Clin. Endocrinol. Metab.*, 2004, **89**, 1779–1787.
- 1940 149 S. K. Nordeen, B. J. Bona, D. N. Jones, J. R. Lambert and T. A. Jackson, *Horm. Cancer*, 2013, **4**, 293–300.
- 1941 150 O. A. Adesanoye, A. O. Abolaji, T. R. Faloye, H. O. Olaoye and A. O. Adedara, *Food Chem. Toxicol.*,  
1942 2020, **142**, 111478.
- 1943 151 F. Jaillet, E. Darroman, A. Ratsimihety, R. Auvergne, B. Boutevin and S. Caillol, *Eur. J. Lipid Sci.*  
1944 *Technol.*, 2014, **116**, 63–73.
- 1945 152 S. Caillol, *Curr. Opin. Green Sustain. Chem.*, 2018, **14**, 26–32.
- 1946 153 B. G. Soares, A. A. Silva, S. Livi, J. Duchet-Rumeau and J.-F. Gerard, *J. Appl. Polym. Sci.*, 2014, **131**, n/a-  
1947 n/a.
- 1948 154 B. G. Harvey, A. J. Guenther, T. A. Koontz, P. J. Storch, J. T. Reams and T. J. Groshens, *Green Chem.*,  
1949 2016, **18**, 2416–2423.
- 1950 155 J. Deng, X. Liu, C. Li, Y. Jiang and J. Zhu, *RSC Adv.*, 2015, **5**, 15930–15939.
- 1951 156 A. Marotta, V. Ambrogi, P. Cerruti and A. Mija, *RSC Adv.*, 2018, **8**, 16330–16335.

- 1952 157 S. Ma, X. Liu, L. Fan, Y. Jiang, L. Cao, Z. Tang and J. Zhu, *ChemSusChem*, 2014, **7**, 555–562.
- 1953 158 Y. Liu, J. Zhao, Y. Peng, J. Luo, L. Cao and X. Liu, *Ind. Eng. Chem. Res.*, 2020, **59**, 1914–1924.
- 1954 159 C. A. Sutton, A. Polykarpov, K. Jan van den Berg, A. Yahkind, L. J. Lea, D. C. Webster and M. P. Sibi,  
1955 *ACS Sustain. Chem. Eng.*, 2020, **8**, 18824–18829.
- 1956 160 J. Meng, Y. Zeng, G. Zhu, J. Zhang, P. Chen, Y. Cheng, Z. Fang and K. Guo, *Polym. Chem.*, 2019, **10**,  
1957 2370–2375.
- 1958 161 F. Hu, S. K. Yadav, J. J. La Scala, J. M. Sadler and G. R. Palmese, *Macromol. Chem. Phys.*, 2015, **216**,  
1959 1441–1446.
- 1960 162 F. Hu, J. J. La Scala, J. M. Sadler and G. R. Palmese, *Macromolecules*, 2014, **47**, 3332–3342.
- 1961 163 J. Meng, Y. Zeng, P. Chen, J. Zhang, C. Yao, Z. Fang, P. Ouyang and K. Guo, *Macromol. Mater. Eng.*,  
1962 **305**, 1900587.
- 1963 164 X. Shen, X. Liu, J. Dai, Y. Liu, Y. Zhang and J. Zhu, *Ind. Eng. Chem. Res.*, 2017, **56**, 10929–10938.
- 1964 165 F. Chemat, M. A. Vian and H. K. Ravi, *Curr. Opin. Green Sustain. Chem.*, 2021, **28**, 100450.
- 1965 166 A. Maertens, E. Golden and T. Hartung, *ACS Sustain. Chem. Eng.*, 2021, **9**, 7749–7758.
- 1966 167 P. Fantke, R. Weber and M. Scheringer, *Sustain. Chem. Pharm.*, 2015, **1**, 1–8.
- 1967 168 S. D. Dimitrov, R. Diderich, T. Sobanski, T. S. Pavlov, G. V. Chankov, A. S. Chapkanov, Y. H. Karakolev,  
1968 S. G. Temelkov, R. A. Vasilev, K. D. Gerova, C. D. Kuseva, N. D. Todorova, A. M. Mehmed, M.  
1969 Rasenberg and O. G. Mekenyan, *SAR QSAR Environ. Res.*, 2016, **27**, 203–219.
- 1970 169 D. E. Fagnani, J. L. Tami, G. Copley, M. N. Clemons, Y. D. Y. L. Getzler and A. J. McNeil, *ACS Macro*  
1971 *Lett.*, 2021, **10**, 41–53.
- 1972 170 S. Fadlallah, P. Sinha Roy, G. Garnier, K. Saito and F. Allais, *Green Chem.*, 2021, **23**, 1495–1535.
- 1973